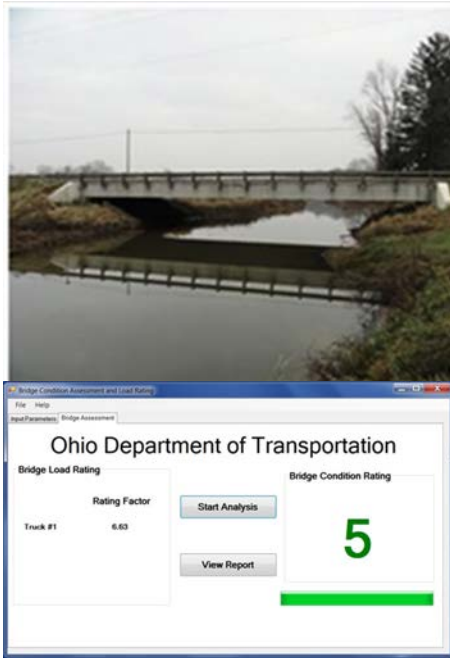


Bridge Condition Assessment and Load Rating using Dynamic Response



Prepared by:
AKM Anwarul Islam, PhD, PE
Frank Li, PhD
Hiwa Hamid, MS
Amer Jaroo, MS
Youngstown State University

Prepared for:
The Ohio Department of Transportation,
Office of Statewide Planning & Research

State Job Number 134695

July 2014



Technical Report Documentation Page

1. Report No.	2. Government Accession No.	3. Recipient's Catalog No.	
FHWA/OH-2014/7			
4. Title and Subtitle		5. Report Date	
Bridge Condition Assessment and Load Rating using Dynamic Response		July 2014	
		6. Performing Organization Code	
7. Author(s)		8. Performing Organization Report No.	
AKM Anwarul Islam, PhD, PE Frank Li, PhD Hiwa Hamid, MS & Amer Jaroo, MS			
9. Performing Organization Name and Address		10. Work Unit No. (TRAVIS)	
Youngstown State University One University Plaza Youngstown, Ohio 44555			
		11. Contract or Grant No.	
		SJN 134695	
12. Sponsoring Agency Name and Address		13. Type of Report and Period Covered	
Ohio Department of Transportation 1980 West Broad Street, MS 2380 Columbus, Ohio 43223		Final Report	
		14. Sponsoring Agency Code	
15. Supplementary Notes			
16. Abstract			
<p>This report describes a method for the overall condition assessment and load rating of prestressed box beam (PSBB) bridges based on their dynamic response collected through wireless sensor networks (WSNs). Due to a large inventory of deficient and aging bridges in the United States, the health monitoring of bridges can be very expensive; therefore, new tools for quick, efficient and response-based condition assessment and load rating of bridges will be helpful. The hypothesis is based on the assumption that the health of a bridge is associated with its vibration signatures under vehicular loads. Two WSNs were deployed on a 25-year old PSBB bridge under trucks with variable loads and speeds, and its dynamic response was collected at the current condition. The acceleration response of the bridge at its newest condition was collected from dynamic simulations of its full-scale finite element analysis (FEA) models mimicking field conditions. The FEA bridge model was validated by the field testing and numerical analysis. The acceleration data in time domain were transformed into frequency domain using Fast Fourier Transform to determine peak amplitudes and corresponding fundamental frequencies for the newest and current conditions. The analyses and comparisons of the bridge dynamic response between the newest and the current bridge interestingly indicate a 37% reduction in its fundamental frequency over 25 years of service life. This frequency reduction is linked to the reduction in condition rating of the current bridge. The analysis data, bridge structural dynamics and bridge geometric parameters have been used to calculate the in-service stiffness of the bridge to estimate its load bearing capacity. Using the results and algorithms from this research, application software is developed to instantly estimate the overall condition rating and load bearing capacity of a PSBB bridge under vehicular loads. The research outcome and the software will help in performing quick and cost-effective condition assessment and load rating of PSBB bridges, and may provide a better ability to plan replacements and develop load ratings.</p>			
17. Keywords		18. Distribution Statement	
Prestressed box beam bridge, bridge condition rating, bridge load rating, rating software, health monitoring of bridges, wireless sensor network, bridge maintenance		No restrictions. This document is available to the public through the National Technical Information Service, Springfield, Virginia 22161	
19. Security Classification (of this report)	20. Security Classification (of this page)	21. No. of Pages	22. Price
Unclassified	Unclassified	128	

Bridge Condition Assessment and Load Rating using Dynamic Response

Prepared by:

AKM Anwarul Islam, PhD, PE
Associate Professor

Hiwa Hamid, MS
Amer Jaroo, MS
Graduate Students
Civil & Environmental Engineering

Frank Li, PhD
Associate Professor
Electrical & Computer Engineering

Youngstown State University
One University Plaza
Youngstown, OH 44555
Tel: (330) 941-1740
E-mail: aaislam@ysu.edu

Prepared in cooperation with
The Ohio Department of Transportation
and
The U.S. Department of Transportation,
Federal Highway Administration

DISCLAIMER:

The contents of this report reflect the views of the authors who are responsible for the facts and the accuracy of the data presented herein. The contents do not necessarily reflect the official views or policies of the Ohio Department of Transportation or the Federal Highway Administration. This report does not constitute a standard, specification, or regulation.

July 2014

ACKNOWLEDGEMENTS

The researchers would like to thank the Ohio Department of Transportation (ODOT) and the Federal Highway Administration (FHWA) for sponsoring this OPREP research. The authors specially thank and express sincere gratitude to ODOT Technical Liaison, Mr. John Picuri and Ms. Amal Goza from ODOT District 4, for their input, contacting County personnel and highway patrol for scheduling dump trucks, and continuous presence, support and encouragement during data collection. The technical experts Mr. Jack Noble, Mr. Russ Snow, Mr. Gery Noirod, and Mr. Brian Olson from ODOT District 4, and Ms. Cynthia Gerst, Ms. Jill Martindale and Ms. Kelly Nye from the ODOT Central Office are greatly appreciated for their valuable contributions to this project. The researchers would also like to express sincere gratitude and thanks towards Mahoning, Ashtabula and Trumbull County personnel and Ohio Highway Patrol officers for their valuable support during data collection on bridges. Without the hard work, assistance and efforts of those involved, this project would not have been completed successfully. This research was partially supported by the YSU Center for Transportation and Materials Engineering (CTME). The support from the YSU CTME and its Executive Director, Ms. Joann Esenwein, is acknowledged and greatly appreciated.

ABSTRACT

This report describes a method for the overall condition assessment and load rating of prestressed box beam (PSBB) bridges based on their dynamic response collected through wireless sensor networks (WSNs). Due to a large inventory of deficient and aging bridges in the United States, the health monitoring of bridges can be very expensive; therefore, new tools for quick, efficient and response-based condition assessment and load rating of bridges will be helpful. The hypothesis is based on the assumption that the health of a bridge is associated with its vibration signatures under vehicular loads. Two WSNs were deployed on a 25-year old PSBB bridge under trucks with variable loads and speeds, and its dynamic response was collected at the current condition. The acceleration response of the bridge at its newest condition was collected from dynamic simulations of its full-scale finite element analysis (FEA) models mimicking field conditions. The FEA bridge model was validated by the field testing and numerical analysis. The acceleration data in time domain were transformed into frequency domain using Fast Fourier Transform to determine peak amplitudes and corresponding fundamental frequencies for the newest and current conditions. The analyses and comparisons of the bridge dynamic response between the newest and the current bridge interestingly indicate a 37% reduction in its fundamental frequency over 25 years of service life. This frequency reduction is linked to the reduction in condition rating of the current bridge. The analysis data, bridge structural dynamics and bridge geometric parameters have been used to calculate the in-service stiffness of the bridge to estimate its load bearing capacity. Using the results and algorithms from this research, application software is developed to instantly estimate the overall condition rating and load bearing capacity of a PSBB bridge under vehicular loads. The research outcome and the software will help in performing quick and cost-effective condition assessment and load rating of PSBB bridges, and may provide a better ability to plan replacements and develop load ratings.

Keywords: Prestressed box beam bridge, bridge condition rating, bridge load rating, rating software, health monitoring of bridges, wireless sensor network, bridge maintenance.

TABLE OF CONTENTS

ACKNOWLEDGEMENTS	iii
ABSTRACT.....	iv
TABLE OF CONTENTS	v
LIST OF FIGURES	vii
LIST OF TABLES	viii
CHAPTER 1: Introduction and Literature Reviews.....	1
1.1 General Overview	1
1.2 Problem Statement	3
1.3 Research Goals and Objectives.....	6
1.4 Condition Assessment and Load Rating Procedures	7
1.5 Wireless Sensor Technology.....	8
1.6 Modal Assurance Criterion.....	9
1.7 Literature Reviews	10
CHAPTER 2: Field Investigations	15
2.1 Bridge Selection.....	15
2.2 Bridge Descriptions	16
2.3 SunSPOT Sensors and WSN	18
2.4 Moving Loads on Bridges.....	20
2.5 WSN Setup and Data Collection.....	20
2.5.1 WSN Setup.....	21
2.5.2 Sensors and Truck Locations.....	23
2.6 Acceleration Data Collection.....	24
CHAPTER 3: Modeling and Simulation	26
3.1 Finite Element Analysis	26
3.2 Bridge Descriptions	26
3.3 Modeling of FEA Bridge	28
3.3.1 Creating Model Parts	28
3.3.2 Defining Part Properties.....	29
3.3.3 Creating Model Assembly.....	30
3.4 Load Generation.....	31
3.5 Bridge Model Analysis	33
3.5.1 Static and Dynamic Analyses.....	33
3.5.2 Frequency Analysis.....	35
3.6 FEA Model Validation.....	36
3.6.1 Experimental Validation	36
3.6.2 Theoretical Validation	37
Chapter 4: Bridge Condition Assessment.....	39
4.1 Modal Analysis	39
4.2 Dynamic Analysis of Beam Systems	40
4.3 Fast Fourier Transform	41
4.4 Peak-Picking Method.....	43
4.5 MAC Analysis	47
4.6 Results.....	48

4.7	Application Software Algorithms	49
4.8	Discussions	55
CHAPTER 5: Bridge Load Rating.....		57
5.1	Equation of Motion and Natural Frequency	57
5.2	Bridge Response Analysis	58
5.3	Load Rating Method	61
5.4	FEA Bridge Fundamental Frequency	61
5.5	Idealized Bridge and Load Rating Equations	63
5.6	Load Rating of Ashtabula Bridge	65
5.7	Load Rating Flow Chart.....	67
CHAPTER 6: Field Testing and Software Validation		70
6.1	Application Software Validation	70
6.2	Recommendations for Implementation of Research Findings.....	73
CHAPTER 7: Conclusions and Recommendations		74
7.1	Conclusions.....	74
7.2	Recommendations.....	76
REFERENCES		77
APPENDICES		80
	Appendix A.....	80
	Appendix B.....	87
	Appendix C.....	90
	Appendix D.....	93
	Appendix E.....	97
	Appendix F.....	104
	Appendix G.....	108

LIST OF FIGURES

Figure 1-1: Behavior of a bridge as an elastic spring.	12
Figure 2-1: Elevation and plan of views Mahoning Bridge.....	17
Figure 2-2: Elevation and plan views of Ashtabula Bridge.....	18
Figure 2-3: SunSPOT hardware kit.....	19
Figure 2-4: Internal parts of SunSPOT sensor and base station.	19
Figure 2-5: Recording axle dimensions and weights of dump trucks.....	21
Figure 2-6: Configuration of two WSNs used on bridges.	22
Figure 2-7: SunSPOT sensors with external battery.....	22
Figure 2-8: Graphical representation of truck path and sensor locations.	23
Figure 2-9: Field data collection of Mahoning and Ashtabula Bridge.	24
Figure 2-10: Acceleration of Field Bridge in time domain.....	25
Figure 3-1: Cross-section of PSBB in FEA Bridge.	27
Figure 3-2: Cross-section of FEA Bridge.	27
Figure 3-3: PSBB layout plan of FEA Bridge.	28
Figure 3-4: Various parts of FEA Bridge.	29
Figure 3-5: Assembled model of FEA Bridge.	31
Figure 3-6: Sensor locations and boundary conditions in FEA Bridge model.	32
Figure 3-7: Prestressing effect on FEA Bridge model (exaggerated).....	33
Figure 3-8: Acceleration of FEA Bridge in time domain.	35
Figure 3-9: Vibration mode shapes of FEA Bridge.	36
Figure 3-10: FEA Bridge model validation by frequency analysis.	37
Figure 3-11: FE model validation: a) pressure, b) deflected shape (exaggerated view).....	38
Figure 4-1: Idealization of Field Bridge.	40
Figure 4-2: Representative acceleration of Field Bridge in time and frequency domain.	42
Figure 4-3: Representative acceleration of FEA Bridge in time and frequency domain.....	43
Figure 4-4: Peak amplitude and corresponding fundamental frequency of Field Bridge.	44
Figure 4-5: Peak amplitude and corresponding fundamental frequency of FEA Bridge.	44
Figure 4-6: Bridge condition assessment input page.	52
Figure 4-7: Bridge condition assessment flow chart.....	53
Figure 4-8: Bridge condition assessment flow chart (continued).	54
Figure 4-9: PSBB bridge geometric property.	55
Figure 5-1: SDOF spring-mass system.	58
Figure 5-2: Frequency-amplitude graphs of Field Bridge.	59
Figure 5-3: Frequency-amplitude graphs of FEA Bridge.	60
Figure 5-4: FEA Bridge mode shape under vehicular loads.....	62
Figure 5-5: Beam with fixed end supports.....	63
Figure 5-6: Load rating flow chart.....	68
Figure 5-7: Load rating flow chart (continued).	69
Figure 6-1: Input Parameters tab of ODOTApp with Ashtabula Bridge data.	70
Figure 6-2: Bridge Assessment output tab of ODOTApp after analysis.	71
Figure 6-3: Input tab of ODOTApp with Trumbull Bridge dynamic response.	72
Figure 6-4: Output tab of ODOTApp with Trumbull Bridge dynamic response.	73

LIST OF TABLES

Table 1-1: Deficient and obsolete bridges in rural and urban areas	5
Table 1-2: Bridge postings in the U.S. (2007 – 2012)	5
Table 2-1: List of bridges proposed to ODOT for data collection.....	16
Table 3-1: Material properties used in FEA Bridge.....	30
Table 3-2: Comparison of results from FEA and approximate calculations	38
Table 4-1: Fundamental frequencies of beams with different support systems.....	41
Table 4-2: Peak amplitude of Field Bridge.....	45
Table 4-3: Peak amplitude of FEA Bridge	45
Table 4-4: Fundamental frequency of Field Bridge.....	46
Table 4-5: Fundamental frequency of FEA Bridge	46
Table 4-6: Sensors with corresponding MAC values	47
Table 4-7: National Bridge Inventory general condition rating guidance	49
Table 5-1: FEA Bridge data for fully-loaded truck at 25 mph	62
Table 5-2: Ashtabula Bridge load rating for different trucks	65
Table 5-3: Ashtabula Bridge load rating using VIRTIS and BARS.....	66
Table 5-4: Ohio legal vehicle weights and load configurations.	67

CHAPTER 1: Introduction and Literature Reviews

1.1 General Overview

The number of bridges in the United States has been increasing; and bridges have become the lifeline of the nation's transportation infrastructure and commerce. The majority of bridges in the United States were built to last around fifty years; however, their current average age is 42 years (ASCE, 2013). During their service life, the performance of bridges is compromised due to various reasons including corrosion in reinforcement, reduction in concrete strength, fatigue cracks in steel, cracks in concrete, etc. Consequently, the health and load bearing capacity of bridges decrease over time. A bridge inspection is carried out periodically on every bridge to ensure its capacity and safety under current traffic; otherwise, posting, widening, maintenance, rehabilitation, or replacement might be needed to ensure public safety.

The health monitoring of bridges using dynamic response includes identifying the amount of deterioration in current conditions of a bridge based on its vibration signatures under vehicular loads. The characteristics of dynamic response data are very complex to analyze and very challenging to be used as diagnostic tools to relate to the structural health, which sometimes require engineers to take different approaches and methods. The choice of a method over others depends on various factors related to the performance of a structure, such as age, degree of importance, accessibility, volume of traffic, time, cost, environment, etc.

The current bridge condition assessment consists of visual inspections of bridge components to evaluate their performance and structural integrity. The visual inspection is the primary and the most common method of bridge condition assessment that has been used for quite a long time. The basics of this method depend on the noticeable signs of damage and/or distress, such as cracking, spalling, loose connections, deflections, etc. that the structure has experienced over its service life. An inspected bridge is rated from “0” (failed) to “9” (excellent) depending on the present physical conditions of its components. However, a visual inspection alone, which depends on an inspector’s engineering judgment and visible signs of distress, may not reveal the invisible actual structural deficiencies and/or internal damage the bridge might have experienced over the years. Therefore, the reliability of this method is not well-assured.

Also, the condition assessment based on visual inspection methods contains levels of subjectivity due to lack of accessibility to critical components of a bridge.

On the other hand, drilling and coring are among the advanced destructive techniques for bridge inspection, which are mostly performed by extracting material samples from bridge components. These samples are tested in a lab to determine their properties and to reveal defects or deteriorations. These techniques usually cause damage to a structure, which requires repair. Moreover, based on the complexity of a structure, a large number of samples might be needed to assess the health condition of a structure, which is costly and time-consuming.

Non-destructive evaluation techniques including ultrasonic acoustic inspection are local approaches to structural inspection that can be labor-intensive, time-consuming and quite expensive (Lynch, 2005). Moreover, traditional wired sensor networks for health monitoring of large civil structures require large amounts of coaxial cables that are expensive to install and maintain.

The load rating of a bridge is usually defined as the service live load that can be carried over safely, and is expressed as a rating factor (RF) for a particular vehicle. Load and resistance factor rating (LRFR) and load factor rating (LFR) are commonly used to perform load rating of bridges to ensure public safety. These methods are recommended by the American Association of State Highway and Transportation Officials (AASHTO), and used by the Ohio Department of Transportation (ODOT) and other state Departments of Transportation (DOTs). However, it has been found that bridges typically have higher capacity in comparison to their theoretical strength (Lichtenstein, 1993).

According to the current data of deficient bridges in the state and highway system, out of 27,045 bridges across the State of Ohio, 6,773 (25%) were categorized as deficient bridges (USDOT, 2012). ODOT has its own Manual of Bridge Inspection (MBI), which is used for bridge inspections in the State of Ohio. Different types of inspection with diverse scope, intensity and frequency have been suggested in the MBI. Five general types among those are: Initial Inspection, Routine Inspection, Damage Inspection, In-Depth Inspection, and Special Inspection (ODOT, 2010).

The bridge load rating is performed in two of these five inspection types. During the Routine Inspection, a load rating might be performed to determine the need for establishing or revising a weight restriction on the bridge (ODOT, 2010). An In-Depth Inspection might require

a structural analysis to estimate the load bearing capacity to ensure the safety of one or more members and to distinguish any deficiency not easily understood during Routine Inspection (ODOT, 2010). Procedures, guidelines and policies for determining the safe live load bearing capacity of highway bridges in the State of Ohio were mentioned in the ODOT Bridge Design Manual (ODOT, 2007).

The current theoretical load rating of bridges is a very conservative approach and sometimes proposes capacity well below the actual strength. Health and functionality of a bridge deteriorates over time due to factors, such as loss in material strength, changes in load distribution and traffic characteristics, and unaccounted non-structural components. These factors are also related to the dynamic structural response of a bridge. Therefore, a new method to estimate the load rating of bridges by collecting and analyzing their real-time dynamic structural response was studied herein. This method will estimate the load bearing capacity of a prestressed box beam (PSBB) bridge and may help avoid over-conservative evaluation.

As the volume of traffic and the use of bridges in transportation networks have been increasing, a comprehensive health monitoring system is necessary to ensure public safety. The wireless sensor network (WSN) technology may be useful to ensure public safety by estimating damage and assessing the health condition of a PSBB bridge at earlier stages. The WSN technology has attracted researchers in developing new tools for assessing the condition of bridges through advanced communication technology. The primary goal of this research is to develop an application tool that will help ODOT and other state Departments of Transportation (DOTs) to evaluate their single-span PSBB bridges in a quick and cost-effective way.

1.2 Problem Statement

According to the U.S. Department of Transportation (USDOT), 66,749 (11%) bridges were categorized as structurally deficient, and 84,748 (13.9%) as functionally obsolete, as shown in Table 1-1, which was adopted from the “Report Card for America’s Infrastructure” published by the American Society of Civil Engineers (ASCE, 2013). Our infrastructure received a ‘D+’ with bridges having a ‘C+’ rating (ASCE, 2013). A structurally deficient bridge may be closed or restricted to traffic in accordance with weight limits because of its limited structural capacity. In order to ensure public safety, limits for speed and weight on these bridges must be posted. According to the National Bridge Inventory Standards (NBIS), bridges are considered

structurally deficient if general condition rating of a bridge component is “4” or less according to the Federal Highway Administration (FHWA, 2004). Functionally obsolete bridges may have design features and geometrics that do not meet current bridge standards. Bridges with narrow lanes and shoulders, and inadequate vertical clearance are some examples of functionally obsolete bridges. These bridges are not unsafe, but cannot accommodate current traffic volumes, vehicle sizes, and weights. In order to keep these bridges functional, they need to be upgraded to the current standards.

From 2001 to 2011, the number of structurally deficient plus functionally obsolete bridges in rural areas declined by 24,722. However, in urban areas during the same time frame, the amount increased by 3,577. In 2008, approximately one in four rural bridges was deficient, while in urban areas, the ratio was one in three. Numbers of structurally deficient and functionally obsolete bridges in rural and urban areas from 2001 to 2011 are shown in Table 1-1 (USDOT, 2012). In addition to the overall reduction in the amount of deficient bridges, the percentage of postings on the nation’s bridges has also declined gradually over the past five years. On the other hand, the number of bridges closed to traffic has climbed from 2,816 in 2007 to 3,585 in 2012. During the same time frame, the number of bridges posted for load restrictions has decreased from 67,969 to 60,971, as shown in Table 1-2 (ASCE, 2013). Posted bridges do not necessarily threaten public safety, but they can create traffic congestion and force emergency vehicles to take lengthy detours, when a bridge is closed. It was estimated in 2008 that it would cost roughly \$140 billion to repair every deficient bridge in the country – about \$48 billion to repair structurally deficient bridges and \$92 billion to improve functionally obsolete bridges (AASHTO, 2008). According to the National Surface Transportation Policy (NSTP) report, it will cost approximately \$850 billion to eliminate all existing bridge deficiencies as they arise over the next 50 years. This equates to an average annual investment of \$17 billion (NSTP, 2007). Through the Federal-Aid Highway Act of 1968 and its subsequent revisions, the FHWA requires all publicly owned highway bridges longer than 20 ft located on public roads to be inspected and evaluated following NBIS (FHWA, 2004) to ensure public safety.

Table 1-1: Deficient and obsolete bridges in rural and urban areas

Year	2001	2003	2005	2007	2009	2011
All bridges	589,685	591,940	590,553	599,766	603,259	630,141
Urban	133,401	135,415	137,598	151,171	156,305	183,918
	22.62%	22.88%	23.30%	25.20%	25.91%	29.19%
Rural	456,284	456,525	452,955	448,595	446,954	446,223
	77.38%	77.12%	76.70%	74.80%	74.09%	70.81%
Structurally deficient bridges, total	83,595	79,775	75,923	72,520	71,177	67,522
	14.18%	13.48%	12.86%	12.09%	11.80%	10.72%
Urban	12,705	12,316	12,600	12,951	12,828	11,923
	15.20%	15.44%	16.60%	17.86%	18.02%	17.66%
Rural	70,890	67,459	63,323	59,569	58,349	55,599
	84.80%	84.56%	83.40%	82.14%	81.98%	82.34%
Functionally obsolete bridges, total	81,439	80,990	80,412	79,804	78,477	76,366
	13.81%	13.68%	13.62%	13.31%	13.01%	12.12%
Urban	29,383	29,886	31,391	33,139	33,743	33,742
	36.08%	36.90%	39.04%	41.53%	43.00%	44.18%
Rural	52,056	51,104	49,021	46,665	44,734	42,624
	63.92%	63.10%	60.96%	58.47%	57.00%	55.82%

Table 1-2: Bridge postings in the U.S. (2007 – 2012)

Year	2007	2008	2009	2010	2011	2012
Closed to all traffic	2,816	2,966	3,552	3,538	3,578	3,585
Posted for load	67,969	66,052	66,249	63,072	61,575	60,971
Posted for other load-capacity restriction	2,559	2,529	2,669	2,953	2,916	3,040
Total	73,344 (12.3%)	71,547 (11.9%)	72,470 (12.0%)	69,563 (11.5%)	68,069 (11.25%)	67,596 (11.1%)

The AASHTO Bridge Analysis and Rating System (BARS) software has been used since the early eighties for theoretical load rating of bridges. BARS software, which uses the LFR approach, appears to be inappropriate in rating bridges designed using the Load and Resistance Factor Design (LRFD) method. However, AASHTO has recently developed another load rating software called VIRTIS that uses the LRFR approach. Although there is an increased emphasis on using LRFR over LFR, neither method, in fact, reveals hidden structural damage and/or deteriorations. As a result, realistic bridge load ratings are not available from either of the AASHTO software.

Table 1-2 shows that a large amount of the nation's bridges is structurally deficient or functionally obsolete, and deterioration of bridges is a continuous process. In addition, Table 1-2 shows that 11.1 percent of the nation's bridges are closed to traffic or posted for load restrictions. Therefore, it is vital to develop response-based cost-effective methods and tools to estimate the overall condition and load rating of bridges in a more realistic way. The outcome of this research will be useful for ODOT and other state DOTs in quick load rating of PSBB bridges.

1.3 Research Goals and Objectives

PSBB bridges have been used since the middle of the last century (around 1950) in the United States (NCHRP, 2009). These bridges constitute about 17 percent of bridges built annually on public roads according to recent National Bridge Inventory (NBI) data (NCHRP, 2008). They also constitute about 26 percent of bridges in the state of Ohio according to NBI data (FHWA, 2012). The span limit for PSBB bridges usually ranges from 15 to 100 ft, but span lengths up to 120 ft have been designed and constructed as well. This type of bridge is not normally used for four-lane divided highways, or where the one way design average daily truck traffic (ADTT) exceeds 2,500 (ODOT, 2011).

The objectives of this research are to develop application tools for condition assessment and load rating of PSBB bridges under vehicular loads by analyzing their dynamic response collected through WSN. The approach to achieve the stated objectives is to collect the dynamic response of a PSBB bridge under a moving vehicle with known weight and speed, analyze the response data, and determine relationships between response data and vehicular loads to assess bridge condition and safe service load bearing capacity. The hypothesis is based on the assumption that the dynamic response is a sensitive and important indicator of the physical integrity and condition of a structure. It is also the perception of the researchers that the global response of a bridge to vehicular loads is directly related to its overall structural health. Therefore, the present condition and load bearing capacity of a PSBB bridge can be estimated with an acceptable accuracy from the analysis of its dynamic response, such as acceleration. Condition assessment of a bridge is currently done by visual inspection while load rating is performed theoretically using software, such as BARS and VIRTIS. Often times these methods are inadequate, or perhaps inefficient, from a global perspective of bridge deterioration over the years due to vehicular and environmental distresses. A novel approach of assessing global

structural integrity and load bearing capacity of a bridge is proposed herein, which can be very quick and cost-effective.

Many of the damage detection algorithms proposed by the structural engineering community consider changes in global structural vibration characteristics as indicators of damage and deterioration of a bridge. The goals of this research are condition assessment and load rating of a PSBB bridge using WSN. In pursuit of these goals, two single-span PSBB bridges in Ohio were equipped with two sets of WSN for collecting real-time acceleration data from each bridge at various speeds and weights of trucks.

The application software developed from this research will be able to quickly assess the condition and load rating of single-span PSBB bridges by collecting their real-time dynamic response. This novel technique may fundamentally change the current theoretical approach of bridge condition assessment and load rating.

1.4 Condition Assessment and Load Rating Procedures

The following steps were followed to accomplish this response-based condition assessment and load rating:

1. Develop wireless sensor networks to collect the real-time acceleration response of the bridge under moving trucks in the field.
2. Perform Fast Fourier Transform (FFT) of acceleration data in time domain, and determine the peak amplitudes and corresponding fundamental frequencies of the field bridge in the current condition (referred hereafter as the “Field Bridge”).
3. Build full-scale 3D finite element analysis (FEA) models of the bridge from its original construction drawings, which represents the bridge at the newest condition (referred hereafter as the “FEA Bridge”).
4. Run simulations of the bridge models under same truck loads mimicking field conditions in order to determine the peak amplitudes and corresponding fundamental frequencies of the FEA Bridge.
5. Identify differences between the dynamic response of the FEA Bridge and the Field Bridge, and relate them to the reduction in the general condition rating (GCR) of the bridge. The GCR has been established by the National Bridge Inventory (NBI) to assess the structural condition of a bridge.

6. Calculate bridge bending stiffness of the Field Bridge by applying the theory of structural dynamics along with analysis data and bridge geometric parameters.
7. Estimate load bearing capacity of the bridge using the load-displacement relationship and the calculated bending stiffness.

1.5 Wireless Sensor Technology

With advancement in the wireless communication technology and its capability of health monitoring of structures, the use of wireless sensors in SHM has become a cost-effective choice to ensure public safety and increase public convenience. The wireless sensor technology uses networks of sensors over a structure to collect its dynamic response. The sensors can be installed at locations that are difficult to access during other methods of health assessment. In this method, the installation and labor costs of wireless sensors are minimal, while an efficient and accurate condition assessment is achieved in a short period of time. The wireless sensor communication technology for health monitoring of structures was proposed by Straser and Kiremidjian (Straser, et al., 1998). Even though it is challenging to measure the true behavior of a structure using this approach (Doebbling, et al., 1996), Kim, et al. (2007) deployed a 64-node WSN, distributed over the 4,200 ft long main span of the Golden Gate Bridge in San Francisco with the goal of identifying initial issues with WSN in monitoring structural health and ambient vibrations. Gangone, et al. (2008) deployed a 20-node WSN on a bridge in Potsdam, New York, which also supported strain gages apart from accelerometers. Both efforts were able to capture important modes of dynamic bridge behavior that agreed with theoretical results.

The bridge condition assessment and load rating can be performed using various methods. The time, cost, and reliability of each method are different from others. The major concern or challenge for engineers is to find a method that is quick and cost-effective, and has acceptable accuracy in detecting deficiencies in bridges. The WSN technology provides such opportunities in overcoming these challenges. The use of WSN was simple and fast, but efficient in collecting real-time dynamic response of PSBB bridges. The sensors were placed at different locations on the bridge to capture the response of the entire bridge at various critical locations. The traffic was closed for a short period of time only during the sensor placement and data collection. This method caused no damage to the bridge, but a little inconvenience to the public during lane closures.

1.6 Modal Assurance Criterion

The modal assurance criterion (MAC) analysis is a modal analysis technique that estimates the degree of correlation between two mode shape vectors. Most often, it is used to check the correlation between mode shapes obtained from experiments and analytical models. It was proposed by Allemang and Brown (Allemang and Brown, 1982) with MAC values ranging from 0 to 1. A MAC value close to 1 indicates well-correlated modes, whereas a value close to zero shows little or no correlation between two modes. The MAC procedure can be mathematically expressed by Eq. 1.1 (Allemang and Brown, 1982):

$$MAC(\{\phi_A\}_m, \{\phi_B\}_n) = \frac{|\{\phi_A\}_m^T \{\phi_B\}_n|^2}{(\{\phi_A\}_m^T \{\phi_A\}_m \{\phi_B\}_n^T \{\phi_B\}_n)} \quad (1.1)$$

Where, $\{\phi_A\}_m$ = mode shape of model A, $\{\phi_A\}_m^T$ = transpose of mode shape of model A, $\{\phi_B\}_n$ = mode shape of model B, $\{\phi_B\}_n^T$ = transpose of mode shape of model B.

The MAC analysis has been widely used in research as an efficient tool. Allemang (2002) reviewed the use of MAC over a period of 20 years and reported its significant contribution in the modal analysis. Yuan, et al. (2009a) used MAC to optimally place sensors on a cable-stayed bridge, whereas Caponero, et al. (2002) used an interferometer and MAC for identification of component modes. Desforges, et al. (1996) used MAC for tracking modes during flutter testing, while Heylen and Janter (1989) applied MAC for dynamic model updating (Marwala, 2010).

The development of MAC over the last several decades has led researchers to use a number of similar assurance criteria for determining the degree of correlation between the experimental and analytically simulated modes of a structure. The application of MAC principle can be extended in several ways. Some of other extensions and similar assurance criteria of MAC are: Weighted Modal Analysis Criterion (WMAC), Partial Modal Analysis Criterion (PMAC), Modal Analysis Criterion Square Root (MACSR), Scaled Modal Analysis Criterion (SMAC), Coordinate Modal Assurance Criterion (COMAC), Modal Assurance Criterion with Frequency Scales (FMAC), Modal Assurance Criterion Using Reciprocal Vectors (MACRV), Enhanced Coordinate Modal Assurance Criterion (ECOMAC), Frequency Domain Assurance Criterion (FDAC), Frequency Response Assurance Criterion (FRAC), Complex Correlation Coefficient (CCF), Modal Correlation Coefficient (MCC), and Coordinate Orthogonality Check (CORTHOG) (Allemang, 2002).

The use of the modal assurance criterion, and the development and use of a significant number of related criteria, has been remarkable and is most likely due to the overall simplicity of the concept (Allemang, 2002). Some of the typical uses of MAC analysis are correlation with analytical modal models (mode pairing), structural fault/damage detection, quality control evaluations, and optimal sensor placement. Due to its importance in modal correlation and damage detection, MAC analysis was used in this research to find the degree of correlation between the dynamic response of the Field Bridge and the FEA Bridge.

1.7 Literature Reviews

Bridges are vital elements in a transportation network because they control the capacity of the system by controlling the volume and weight of traffic that can be carried over the system. Besides, the construction and maintenance cost per mile for bridges is the highest in a transportation network (Barker, 2007). Therefore, extensive research has been performed to study and evaluate the health and safety of highway bridges. The main objective of structural health monitoring is to estimate the loss of structural integrity due to aging, environment and increase in traffic, which can adversely affect the performance of a structure. Consequently, these causes reduce the load bearing capacity of bridges. Concrete degradation, steel corrosion, change in boundary conditions, and weakening of connections in structures over time are major concerns in highway bridges. If a damaged bridge remains unattended, the structural integrity and service capability of the bridge worsen over time. Therefore, frequent condition assessment and load rating of bridges are vital in maintaining a healthy transportation network.

The condition assessment of a bridge based from its dynamic response can be effective in the early detection of damage in a bridge. Lynch, et al. (2006) monitored performance of the Guemdang Bridge, South Korea, using a dense network of 14 high-resolution wireless sensors. Also installed in parallel was a commercial tethered monitoring system. They collected acceleration response of the bridge under forced vibrations induced by a calibrated 40-ton truck at 40, 60 and 80 kmph by using both tethered networks and WSNs. They used MAC for statistical analyses and compared the results from both systems. The performance of the less expensive wireless monitoring system was shown to be comparable to that of the tethered counterpart. Samali, et al. (2003) described field-testing of more than 20 timber bridges across New South Wales, Australia. The bridge assessment procedure involved the attachment of

accelerometers underneath bridge girders. The vibration response and the natural frequency of the bridge superstructure were measured when a “calibrated sledgehammer” was used to hit the unloaded deck, and then again with a relatively small mass applied at mid-span. The difference in dynamic response allowed them to calculate the in-service flexural stiffness of each bridge. Cawley and Adams (1979) related changes of successive mode frequencies to the existence and location of structural deterioration in beams. Salawu and Williams (1995a) reported a study on forced vibrations of a bridge before and after repair. The test results demonstrated the changes in natural frequency induced by the repair. Mazurek and DeWolf (1990) showed in laboratory tests that changes in the support condition and crack development affect natural frequencies and modal amplitudes (FHWA, 2005).

The literature reviews show the use and importance of dynamic response in the damage detection and bridge condition assessment. It can be concluded that more research is needed to relate the dynamic response of a PSBB bridge to its current condition and load bearing capacity. Vehicular loads with WSN have been used on bridges in these past studies in detecting damage and monitoring health, and were helpful for the scope of this research. The goal of this study is to develop an application tool for the condition assessment of a PSBB bridge by analyzing its dynamic response under vehicular loads collected through WSN.

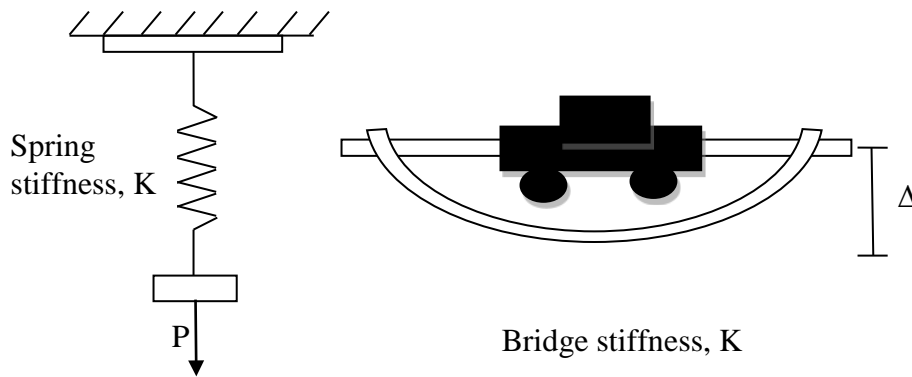


Figure 1-1: Behavior of a bridge as an elastic spring.

The load rating of bridges has been studied by many researchers. Some of them have focused on using the dynamic response of bridges to estimate their in-service stiffness and load bearing capacity. The main goal of Chen, et al. (2002) was to develop a new method to perform load rating of bridges. The researchers used the ambient vibration measurement technology, which assumes that a bridge behaves like an elastic spring, as shown in Fig. 1-1, and the load bearing capacity of a bridge is directly related to the stiffness of the spring. By knowing the vibration frequency, f , and mass, m , of the bridge, the bridge stiffness, K , can be calculated by using Eq. 1.2. Due to the deterioration of materials and loss of structural integrity over time, the stiffness of a structure decreases over time. In other words, a bridge will be more flexible and will have a lower frequency of vibration. The reduced stiffness of the current bridge, \tilde{K} , can also be calculated using Eq. 1.2 to determine the change in stiffness ($\Delta K = K - \tilde{K}$).

$$K = f^2 * m \quad (1.2)$$

In order to verify this method, Chen, et al. (2002) constructed a miniature bridge model, which consisted of four plastic girders that were bonded to a Plexiglas deck with a 20-degree skew. Both static and dynamic tests were performed on the miniature bridge model. After a cut through the mid-span, static and dynamic tests were repeated to simulate the deterioration in the miniature bridge model. A FEA model was also created to verify the results from miniature bridge model tests.

Samali, et al. (2003) found a new, simple, non-expensive, and safe procedure to determine the load bearing capacity of short-span timber bridges. They attached highly sensitive

accelerometers underneath the bridge and used a model impact hammer for bridge excitation. The dynamic response of the bridge was recorded in two cases: (1) with an extra load applied at the bridge mid-span, and (2) without any external load on the bridge. From the bridge response, the first natural frequencies, ω_1 and ω_2 for cases (1) and (2), respectively, were determined. By knowing the added weight, ΔM , the flexural stiffness, K , of the bridge can be calculated using Eq. 1.3.

$$K = \frac{\omega_1^2 * \omega_2^2}{\omega_1^2 - \omega_2^2} * \Delta M \quad (1.3)$$

The load bearing capacity was estimated from the relationship between the actual measured stiffness, EI , and the bending capacity of timber. This relationship was derived by incorporating the uncertainties in geometric and test-based strength properties of some 1,200 round timber poles.

Chowdhury (1999) proposed a nondestructive dynamic method to estimate the load capacity of beams. This method included a shaker to excite the beams and to record three forced responses, such as displacement, velocity, and acceleration, using four different types of sensors to measure the effectiveness of each sensor. Dynamic responses of beams were analyzed to estimate their static stiffness. The calculated stiffness of beams was used to estimate their load bearing capacity using the load-displacement relationship. For example, the load bearing capacity of a beam with deflection limited to $L/400$ can be calculated using Eq. 1.4.

$$\text{Load Bearing Capacity} = K * \frac{L}{400} \quad (1.4)$$

Chowdhury concluded that the proposed method can estimate the bending stiffness of a beam. Also concluded that the measured stiffness is a sensitive indicator of physical changes, which can be used for monitoring bridge performances during its service life.

In all of the above efforts, the target of the researchers was to find an acceptable method for predicting the load bearing capacity of a structure from its dynamic response. Researchers in the references listed above used the dynamic response to determine the stiffness, and the calculated stiffness to determine load bearing capacity of a structure. Both Chowdhury (1999) and Chen, et al. (2002) found the stiffness of a structure using the generalized single degree of freedom (SDOF) method. Samali, et al. (2003) found the stiffness of a structure using the first natural frequencies of the dynamic response, as shown in Eq. 1.3. The proposed load rating method in this research includes analysis of dynamic response of a single span PSBB bridge in

order to find the maximum peak amplitudes and their corresponding frequencies. Using the SDOF method and the analysis data, the bending stiffness of a bridge can be determined. By using the load-displacement relationship, the load bearing capacity of a bridge can be estimated as well.

CHAPTER 2: Field Investigations

2.1 Bridge Selection

Prestressed box beam bridges are widely used in new bridge construction and have many advantages over other bridge types due to the speed and ease of construction, aesthetics, span to depth ratio, and cost. Although early construction practices may have led to serviceability issues, improved practices have made the PSBB bridge a viable and cost-effective structural system (Prestressed Concrete Institute, 2009). Three PSBB bridges were selected for this study. Two of them were used for data collection and modeling. The third one was used to validate the application software developed based on the response from the first two bridges. Following points were taken into consideration during the final selection of the three bridges:

1. Single-span bridges were selected for ease of modeling and simulation.
2. Bridges with low average daily traffic (ADT) were preferred to minimize traffic disruption during data collection.
3. Relatively older bridges were selected for data collection to ensure the presence of sufficient deterioration, whereas a newer bridge was selected for software validation.
4. Larger bridges were selected for better and longer vibration response.
5. Bridges close to the YSU campus were preferred for convenience, and to minimize time and cost of travel.

From a list of available single-span PSBB bridges in ODOT District 4, a set of six bridges, as shown in Table 2-1, was proposed for data collection and modeling. Two out of six proposed bridges were finally selected for data collection and a separate bridge from Trumbull County was selected for software validation.

Table 2-1: List of bridges proposed to ODOT for data collection

Cty	Rte	SLM	Feature intersected	SFN	Date built	Total spans	Max span length	Overall structure length
ATB	322R	1916	Pymatuning creek	0406430	7/1/1988	1	84	85
ATB	193R	2019	Griggs creek	0405620	7/1/1991	1	60	64
ATB	006R	2469	Gravel Run	0400432	7/1/1991	1	60	61
MAH	045R	0579	W BR Meander creek	5001544	7/1/1993	1	85	88
MAH	534R	0925	Turkey Broth creek	5005809	7/1/1986	1	55	56
TRU	046R	2515	Mosquito creek	7802994	7/1/1985	1	75	76

2.2 Bridge Descriptions

The first selected PSBB bridge, as shown in Fig. 2-1, was built in July 1993 in the Mahoning County, Ohio. It is a simply supported single span composite PSBB bridge with the structural reference number MAH-45-0579 on Route 45 over Meander Creek with a 30° skew in the horizontal alignment (referred hereafter as the “Mahoning Bridge”). The length and width of the Mahoning Bridge are 84.5 ft and 44 ft, respectively. It has 11 prestressed box beams; each of them is 48 in. wide and 42 in. deep. A concrete deck of 5.5 in. thick was laid on the top of the box beams. The beams are transversely connected through 18 in. thick equally spaced concrete diaphragms and staggered tie rods. The bridge has two 12 ft wide traffic lanes with 10 ft wide shoulders on both sides. Steel railings are attached on the exterior edges of the bridge.



A: Side view

B: Top view (Google Maps)

Figure 2-1: Elevation and plan of views Mahoning Bridge.

The second bridge, constructed in July 1988, is a fixed supported single span PSBB bridge with structural reference number ATB-322-1916 on Route 322 over Pymatuning Creek in Ashtabula County, Ohio (referred hereafter as the “Ashtabula Bridge”). The Ashtabula Bridge, as shown in Fig. 2-2, is 85 ft long and 36 ft wide. It consists of nine adjacent 48 in. wide and 42 in. deep prestressed box beams with a 2.5 in. thick layer of asphalt concrete on top. Three equally spaced 18 in. thick concrete diaphragms and staggered tie rods transversely connected the box beams together. The horizontal alignment of the bridge is straight with no skew. The bridge has two 12 ft wide lanes of traffic, and two 6 ft wide shoulders. Steel railings are attached at both edges of the bridge.



A: Side view

B: Top view (Google Maps)

Figure 2-2: Elevation and plan views of Ashtabula Bridge.

2.3 SunSPOT Sensors and WSN

Sun Small Programmable Object Technology (SunSPOT) sensors are Java programmable embedded devices, which were used for the collection of real-time dynamic structural response of the two bridges selected for this study. A basic SunSPOT sensor contains accelerometer sensors, temperature and light sensors, radio transmitter, eight multicolored LEDs, 2 push-button control switches, 5 digital I/O pins, 6 analog inputs, 4 digital outputs, and a rechargeable battery (Oracle, 2012). A SunSPOT hardware kit shown in Fig. 2-3 includes two SunSPOT sensors, and a base station to communicate wirelessly with the sensors. Figure 2-4 shows the internal parts of a base station and a free-range SunSPOT sensor. Each SunSPOT sensor and base station has a unique 16-digit MAC address, of which the first 8-digit is same for all and the remaining 8-digit is different for each one. Therefore, the last 8-digit MAC address was used to identify each sensor. The SunSPOT sensors capture acceleration with time in all three axes simultaneously and transmit the data package wirelessly to base station, which is connected to a laptop via a universal serial bus (USB) cable and transfers the data package to the laptop real-time. In this research, only Z-axis (vertical axis) acceleration of the bridge was collected at 100 Hz frequency and 2g scale.



Figure 2-3: SunSPOT hardware kit.

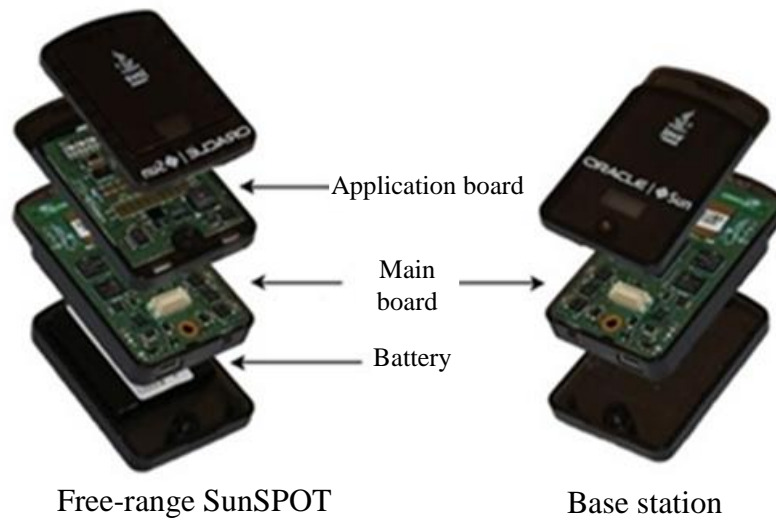


Figure 2-4: Internal parts of SunSPOT sensor and base station.

In order to prepare the SunSPOT sensors for data collection, two separate application packages were developed using Java. One application was developed to control the functions of the base station to establish communication with SunSPOT sensors to collect data and save them in Microsoft Excel format. The second application controls the functions of SunSPOT sensors, the data collection sampling rate, and the data transmission to the base station. The performance of the sensor data was very important; therefore, the accelerometers were calibrated and customized in a laboratory environment before deploying them on the field.

2.4 Moving Loads on Bridges

Three standard dump trucks provided by the ODOT Maintenance and Repair Outposts in Mahoning and Ashtabula Counties were used to produce vibrations on both bridges. A standard dump truck used in this study is shown in Fig. 2-5. The truck axle loads and dimensions were measured by the Ohio State Highway Patrol. The axle dimensions of the three trucks were the same; however, their weights were different. The distance between the front and rear axle was 14.9 ft and the axle width was 6 ft. Three different truck weights were used in this study – an empty, a half-loaded, and a fully-loaded truck. The axle loads and dimensions data for each truck are attached in Appendix A.

2.5 WSN Setup and Data Collection

Once the SunSPOT sensors were customized and prepared for field deployment, tests were run in coordination with ODOT Maintenance and Repair personnel for data collection on bridges.



A: Measuring truck axle dimensions

B: Measuring truck axle weights

Figure 2-5: Recording axle dimensions and weights of dump trucks.

2.5.1 WSN Setup

Two sets of wireless sensor networks were deployed simultaneously on the bridge during each truck run. Each set of the WSN included four SunSPOT sensors, one base station, and a laptop. SunSPOT sensors were numbered from 1 to 4 for base station 1 and 5 to 8 for base station 2. The base station and the sensors were customized in such a way that the sensors transmit data only to the assigned base station. In this way, the base station 1 in WSN 1 collects data only from sensors 1 to 4, while the base station 2 in WSN 2 collects data from sensors 5 to 8 only. Figure 2-6 shows the configuration of the two WSNs built with SunSPOT sensors, base stations and laptops. Each base station was connected to a laptop via a USB cable to get the needed power and to send the collected data to the laptop. In order to ensure adequate power supply to the sensors, each of them was connected to an external battery throughout the entire test, as shown in Fig. 2-7.

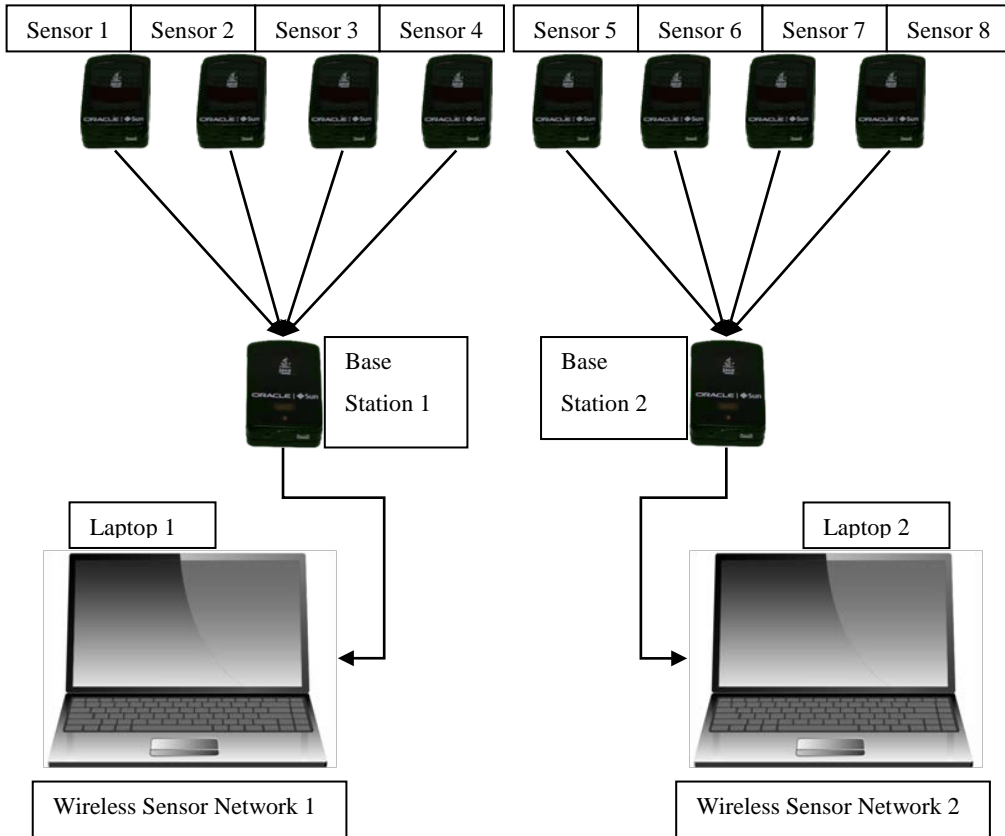


Figure 2-6: Configuration of two WSNs used on bridges.



Figure 2-7: SunSPOT sensors with external battery.

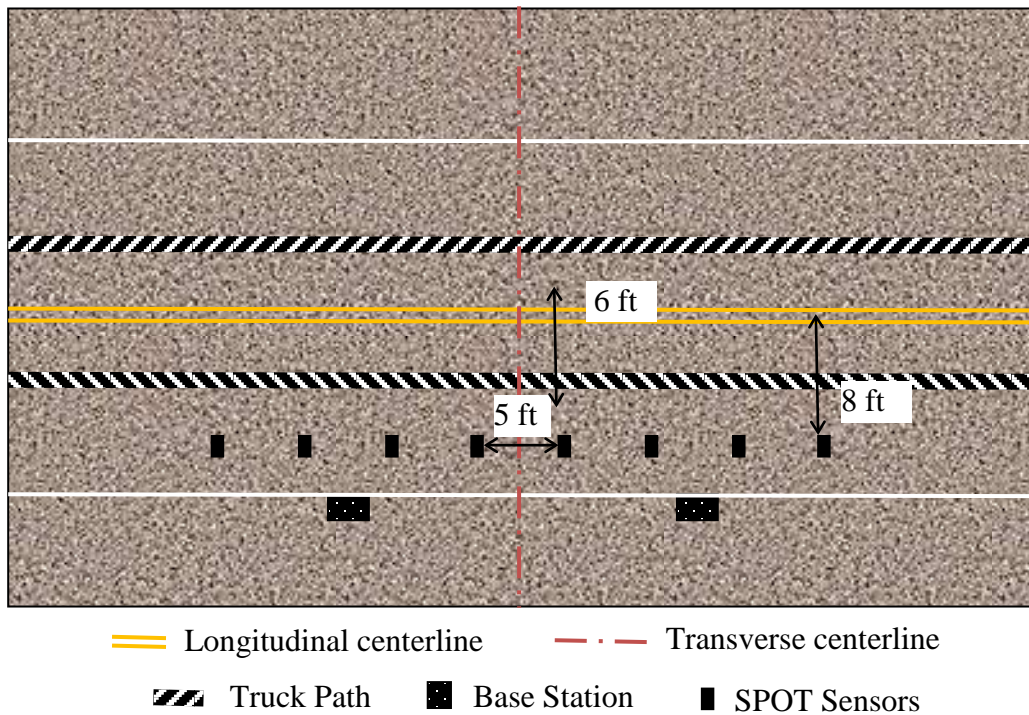


Figure 2-8: Graphical representation of truck path and sensor locations.

2.5.2 Sensors and Truck Locations

Two sets of wireless sensor networks were installed on the bridge deck using the arrangement shown in Fig. 2-6. Since the maximum bridge vibration is anticipated in the middle of the bridge, sensors were attached on the middle half of the bridge at 5 ft spacing, which also helped better communication between sensors and base stations. For even distribution of truck loads across the bridge, the truck path was delineated in such a way that its centerline coincided with the longitudinal centerline of the bridge.

During the first attempt in collecting the dynamic response of Mahoning Bridge with sensors attached on the bridge centerline, a test truck accidentally ran over and destroyed all eight sensors and the batteries. The data sets collected before the accident were incomplete and therefore, were discarded. In order to avoid such damage to sensors and batteries during future data collection, sensor locations were shifted from the centerline to the side of the bridge, as shown in Fig. 2-8 for both Mahoning and Ashtabula Bridge. Figure 2-9 shows pictures of data collection on both bridges.



A: Data collection on Mahoning Bridge B: Data collection on Ashtabula Bridge

Figure 2-9: Field data collection of Mahoning and Ashtabula Bridge.

2.6 Acceleration Data Collection

Before the test runs, ODOT Maintenance and Repair personnel closed one lane of traffic on the bridge during taking measurements and installing sensors. Sensors locations were marked and cleaned before applying quick-setting epoxy (available in local stores, such as in Home Depot by the brand name “Super Glue: 5 Minute Quick Setting Epoxy”) to hold the flexi-glass plates. The sensor clips, which grip the sensors, were screwed onto the flexi-plates. The epoxy was set to harden for 30 minutes before data collection to prevent unexpected vertical movement of the sensors. In other words, the sensors were made to be an integral part of the bridge. The same procedure was used prior to running trucks on the Mahoning and Ashtabula Bridge. Figure 2-9 shows the attachment of sensors on both bridges.

An empty, a half-loaded, and a fully-loaded truck were used for collecting bridge dynamic response. During the test runs, the truck drivers were instructed to drive over the centerline of the bridge by maintaining a uniform speed. On the Mahoning Bridge, each truck ran three times at 10, 15, and 20 mph. Every single run produced 8 subsets of sensor data – one subset for each sensor. Since a total of 9 runs were performed on the bridge, a total of 72 subsets of acceleration data were collected from the Mahoning Bridge. While on the Ashtabula Bridge, each truck ran four times at 10, 15, 20, and 25 mph. Therefore, a total of 96 subsets of acceleration data were collected from the Ashtabula Bridge. The bridge acceleration versus time

data for each truck run was recorded in real-time; sample of recorded data is shown in Appendix B. The accelerometer inside the SunSPOT sensors captured the analog bridge acceleration signals and converted them into electrical voltage. The voltage data are then converted into digital signals using the built-in analog-to-digital converter (ADC) in the sensor. All data collected from the sensors were time-stamped along with the 8-digit MAC address of respective sensor for easier identification and synchronization.

Acceleration data from the Mahoning Bridge were transformed from time domain into frequency domain using Fast Fourier Transform (FFT) technique and found inconsistent with no significant peak in the frequency domain data. Due to near-freezing temperature during data collection on the Mahoning Bridge, it was found that the glue used for holding sensor clips on the bridge deck did not set enough to provide a firm interface between sensors and the bridge. Consequently, the glue itself might have absorbed part of the bridge vibration. Therefore, acceleration data from the Mahoning Bridge were not considered useful for this research. In order to avoid such problems in future, a different type of quick-setting epoxy was used during the data collection on the Ashtabula Bridge. Some representative samples of acceleration data from Field Bridge (Ashtabula Bridge) are shown in Fig. 2-10.

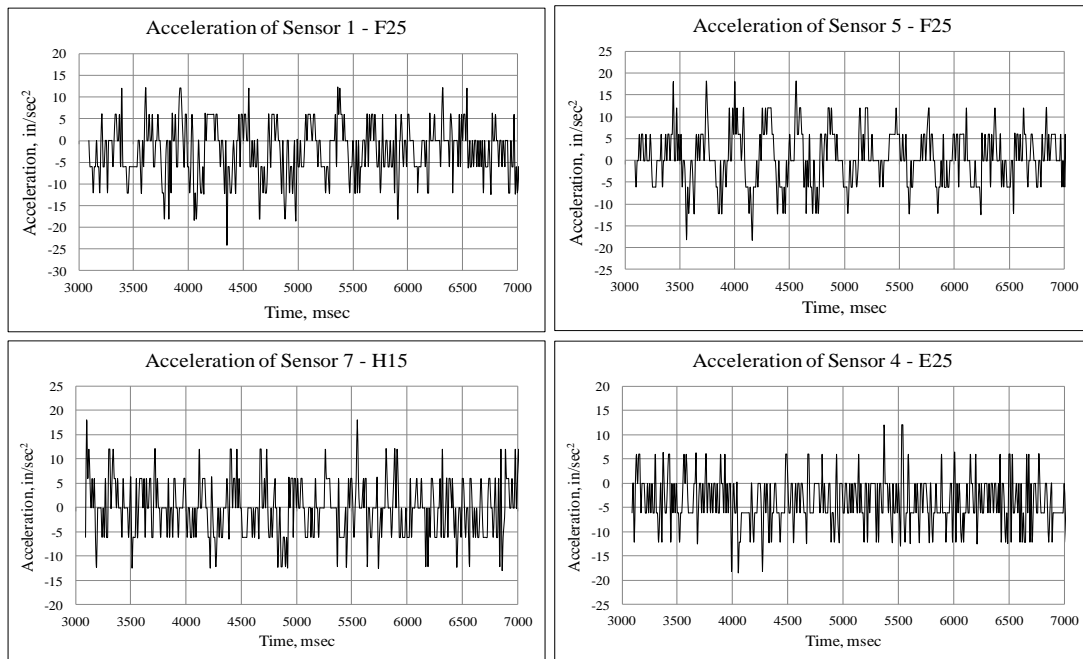


Figure 2-10: Acceleration of Field Bridge in time domain.

CHAPTER 3: Modeling and Simulation

3.1 Finite Element Analysis

Finite element analysis (FEA) is a numerical technique, which is used to model and solve complex engineering problems in a virtual environment. With the advancement in technology and dramatic increase in computer processing capacity, FEA has become a popular choice for numerically solving a variety of problems that would otherwise require expensive experimental testing.

In this study, the FEA software ABAQUS 6.12 (ABAQUS, 2013) was used to build a full-scale 3D finite element (FE) model of the Ashtabula Bridge. The model represents the FEA Bridge, which refers to the Ashtabula Bridge right after construction. ABAQUS includes three main parts for analysis and simulation, which are ABAQUS CAE, ABAQUS Standard, and ABAQUS Explicit. ABAQUS CAE provides a simple interface for creating a wide range of shapes and structures, submitting and monitoring jobs, and evaluating the results from ABAQUS Standard and ABAQUS Explicit simulations. The modeling consistency in ABAQUS CAE makes it an easy-to-use, and yet highly productive and attractive, tool for FEA users. Some of the common modules in ABAQUS CAE are: Part, Material, Section, Assembly, Steps, Field Output Requests, Interactions and Constraints, Loads, BCs, Mesh, Job Analysis, and Post-Processing. Both ABAQUS Standard and ABAQUS Explicit are supported within the ABAQUS CAE modeling environment, and they are designed to provide the user with two complementary mechanisms.

3.2 Bridge Descriptions

The FEA Bridge was modeled from the PSBB cross-section, bridge cross-section and plan of the Ashtabula Bridge, as shown in Figs. 3-1 to 3-3, provided by ODOT. The prestressing stress applied to the model was also adopted from the bridge plans.

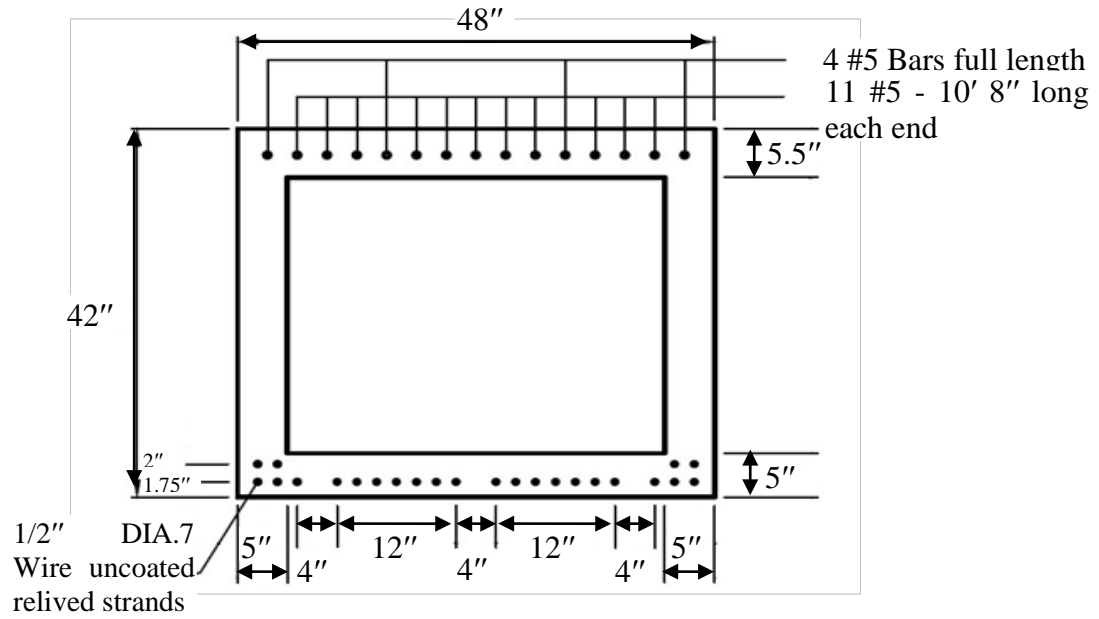


Figure 3-1: Cross-section of PSBB in FEA Bridge.

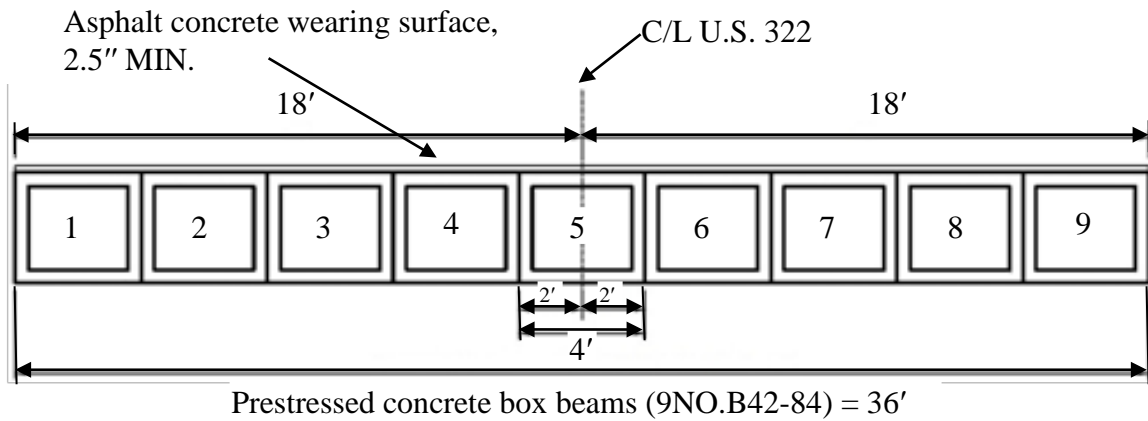


Figure 3-2: Cross-section of FEA Bridge.

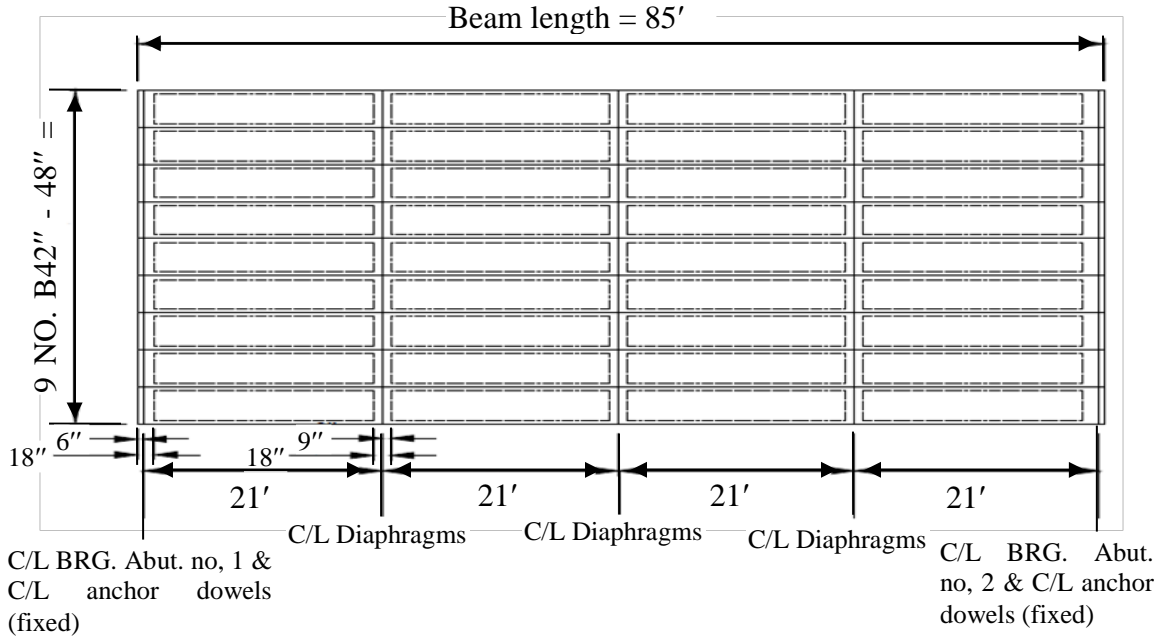


Figure 3-3: PSBB layout plan of FEA Bridge.

3.3 Modeling of FEA Bridge

The finite element modeling and simulation of the FEA Bridge (Ashtabula Bridge) was performed using commercially available software ABAQUS CAE 6.12 (ABAQUS, 2013). The brief details of modeling are described herein.

3.3.1 Creating Model Parts

The part module was used to create and edit five different parts for the model using two features. Each one of these parts is located in its local coordinate system. Prestressed concrete box beam and asphalt concrete wearing surface parts were created using solid features, while reinforcing steel and prestressing strands parts were created using wire features. After creating the solid parts of the bridge model, multiple ‘cut extrude’ and ‘cell partition’ commands were used to create beam ends, internal diaphragms, truck paths, and sensor locations. The mesh module was used to control the element shape, meshing technique, element type, part seeds, etc. The hexahedral element shape was used with structured meshing technique to generate the mesh. This technique applies pre-established mesh patterns for the model parts, which provide the most

control over the mesh. For both PSBB and wearing surface, ‘3D stress’ eight-node linear brick elements were used. The two-node linear ‘3D truss’ elements were used for the reinforcing steel and the prestressing strands. Size of elements in the mesh was defined to be 10 in. This mesh size divided the bridge model into 50,772 elements. Various finite element model parts are shown in Fig. 3-4.

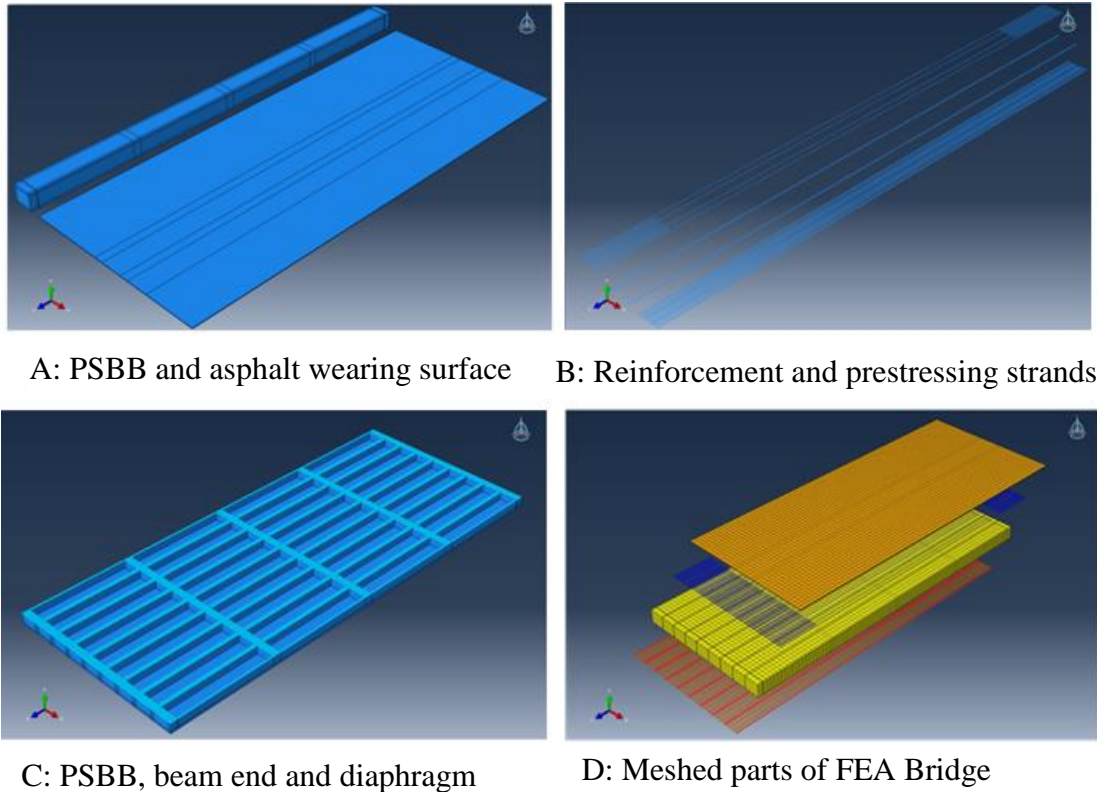


Figure 3-4: Various parts of FEA Bridge.

3.3.2 Defining Part Properties

The property module was used to define material properties and part sections. Four material properties were created to define prestressed concrete, asphalt concrete, steel reinforcement, and prestressing strands. Material properties used in the FE model are shown in Table 3-1. The ‘section editor’ command was used to define part sections. The solid category with homogenous type was used to define the PSBB and the asphalt concrete wearing surface.

The beam category with truss type was used to define the reinforcing steel and the prestressing strands.

Table 3-1: Material properties used in FEA Bridge

Part	Material	Properties		
		Density (lbf s ² /in ⁴)	Modulus of Elasticity (psi)	Poisson's Ratio
Prestressed concrete box beam	Prestressed concrete	2.246520589 E-4	4496060.776	0.15
Asphalt concrete wearing surface	Asphalt concrete	2.246520589 E-4	350000	0.35
Reinforcing steel	Steel	7.338633924 E-4	29000000	0.3
Prestressing strands	Steel	7.338633924 E-4	28500000	0.3

3.3.3 Creating Model Assembly

The assembly module was used to create part instances and to position the instances relative to each other in a global coordinate system. The part instances were positioned together by sequentially applying position constraints that align selected faces or edges, or by applying simple translations and rotations (ABAQUS, 2013). Figure 3-5(a) shows different part instances that represent the bridge model assembly, while Fig. 3-5(b) shows the entire bridge model assembly after the reinforcing steel and the strands were embedded in the PSBB. The assembly module was also used to create the contact surfaces between part instances. These contact surfaces were used to define the interaction between instances in the interaction module. In addition, the assembly module was used to define a set of sensor nodes mimicking field locations.

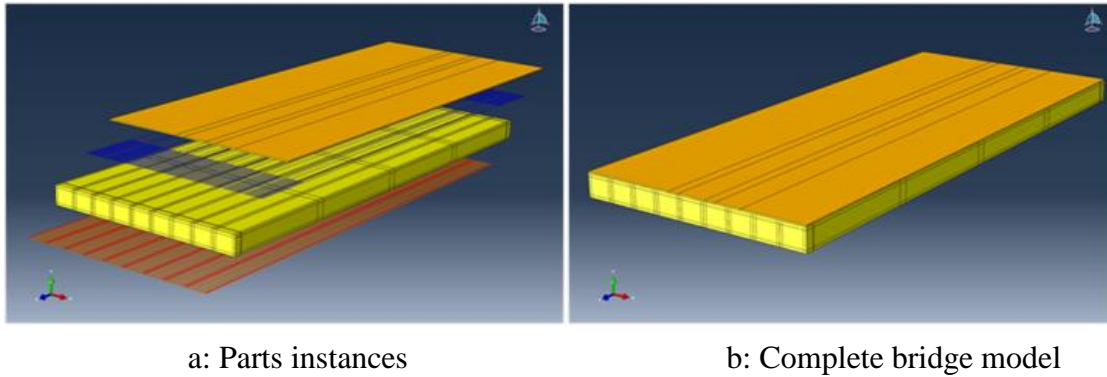


Figure 3-5: Assembled model of FEA Bridge.

The interaction module was used to define and manage the interaction and constraints between parts instances. The interaction properties section was used to define the concrete friction coefficient of 0.6 according to ACI Section 11.6.4.3 (ACI, 2008). Contact surfaces were used as pairs to define interaction surfaces between adjacent PSBBs. No part was created for the transverse tie rod during the modeling, but the effect of the tie rods was taken into consideration by creating tie constraints at diaphragm locations between PSBBs. Another tie constraint was created between the bottom of the asphalt concrete wearing surface and the top of PSBBs. An embedded element technique was used to define the contact between the reinforcement or the prestressing strands and PSBBs. This type of constraint is used to specify a group of embedded elements that lies in a group of host elements. The response of host elements is used to constrain translational degrees of freedom of embedded elements (ABAQUS, 2013).

3.4 Load Generation

Loads, predefined fields, and boundary conditions were defined using the load module. Dead loads and truck loads were defined under the mechanical category. The dead load of the structure was defined using the gravity load (g). To define the truck load, VDLOAD user-subroutine was written using Fortran10.1.034. A VDLOAD user-subroutine defines a truck as functions of position, time, and velocity. Twelve VDLOAD subroutines were created for three trucks at four different speeds. For each one of these files, the weight of each wheel was assumed to be uniformly distributed over the contact area. The contact area was taken as a single

rectangular area of 20 in. width and 10 in. length according to AASHTO Section 3.6.1.2.5 (AASHTO, 2007). Moreover, axle spacing, truck width, and truck paths were taken into consideration during the development of VDLOAD subroutines. The effect of prestress was included in the models by applying stress in prestressing strands. The stress was applied under the mechanical category in the predefined section. The value of stress was calculated by dividing the final tension force of 21,700 lb per strand (adopted from ODOT plans) after all losses (ODOT, 1972) by the area of a prestressing strand. The fixed type of anchor dowels was used at beams ends. Therefore, fixed boundary conditions were assumed during simulations and applied at the bottom of beams ends, as shown in Fig. 3-6.

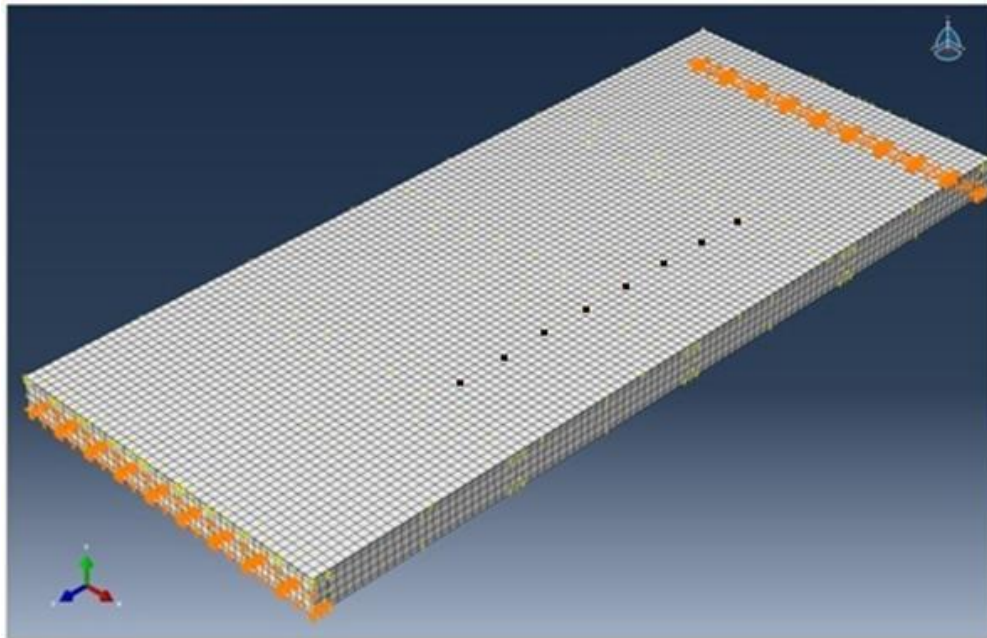


Figure 3-6: Sensor locations and boundary conditions in FEA Bridge model.

3.5 Bridge Model Analysis

Several analyses of FEA Bridge models were performed under various truck weights and speeds mimicking field conditions. These analysis details are described herein.

3.5.1 Static and Dynamic Analyses

After developing the 3D FE model of the FEA Bridge, the input file was submitted to ABAQUS Standard and ABAQUS Explicit using the job module to perform analysis and generate an output database. The analysis of the model was performed in two stages using two types of simulation procedure: static-general and dynamic-explicit. The first stage of analysis was performed using ABAQUS Standard to analyze the effect of prestress, as shown in Fig. 3-7. ABAQUS Standard is a general-purpose analysis product that can solve a wide range of linear and nonlinear problems involving static, dynamic, and thermal problems, when accurate stress solutions are of main interest (ABAQUS, 2013).

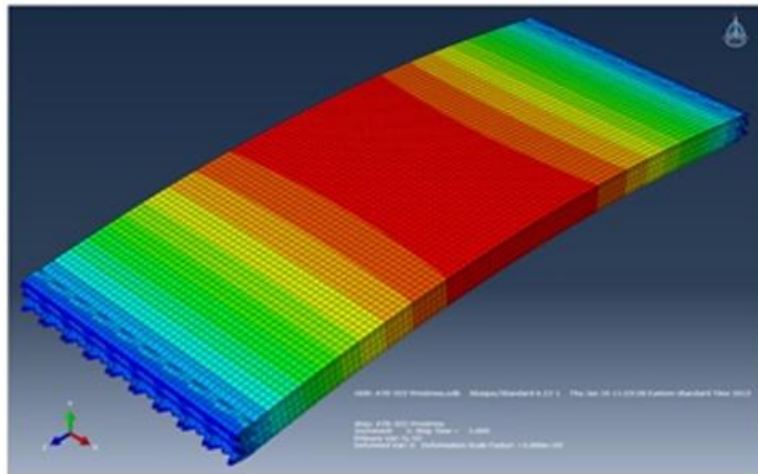


Figure 3-7: Prestressing effect on FEA Bridge model (exaggerated).

The second stage of analysis was performed using ABAQUS Explicit to find the bridge dynamic response under vehicular loads. ABAQUS Explicit is a special-purpose analysis product that uses an explicit dynamic finite element formulation. It is a suitable and very efficient tool that provides accurate solutions for high-speed, large, and non-linear dynamics simulations (ABAQUS, 2013). During the real-time data collection, trucks passed the bridge at four different

speeds, and the sensors collected acceleration data at 100 Hz. Therefore, the analysis time period, the maximum time increment in the dynamic-explicit analysis procedure, and the data output request were modified during the FE model simulation to mimic conditions during the real-time data collection. Time needed for trucks to pass the bridge at each speed was calculated and taken into consideration to determine analysis time period for the bridge modeling. In addition, time increment and data output request were changed to 0.01 second to mimic the real-time data collection rate in the field. Before the second stage of analysis, the effect of prestress from the first stage of analysis was imported to the dynamic model using the initial state type of load under the predefined field section. The analysis was performed 12 times on the FEA Bridge model with 12 different VDLOAD user-subroutines. At the end of each analysis, the acceleration data in Y (vertical) direction at each sensor node location were requested for output. Finally, the requested output was saved as Microsoft Excel files. Graphs in Fig. 3-8 show the acceleration responses from the FEA Bridge at various sensor locations. In addition to the acceleration data, the displacement of the bridge model under vehicular loads were also requested for output and saved as Microsoft Excel files. Samples of acceleration and displacement data are shown in Appendix B. Acceleration data of the FEA Bridge were compared with Field Bridge data to determine the loss of frequency of the Ashtabula Bridge over time.

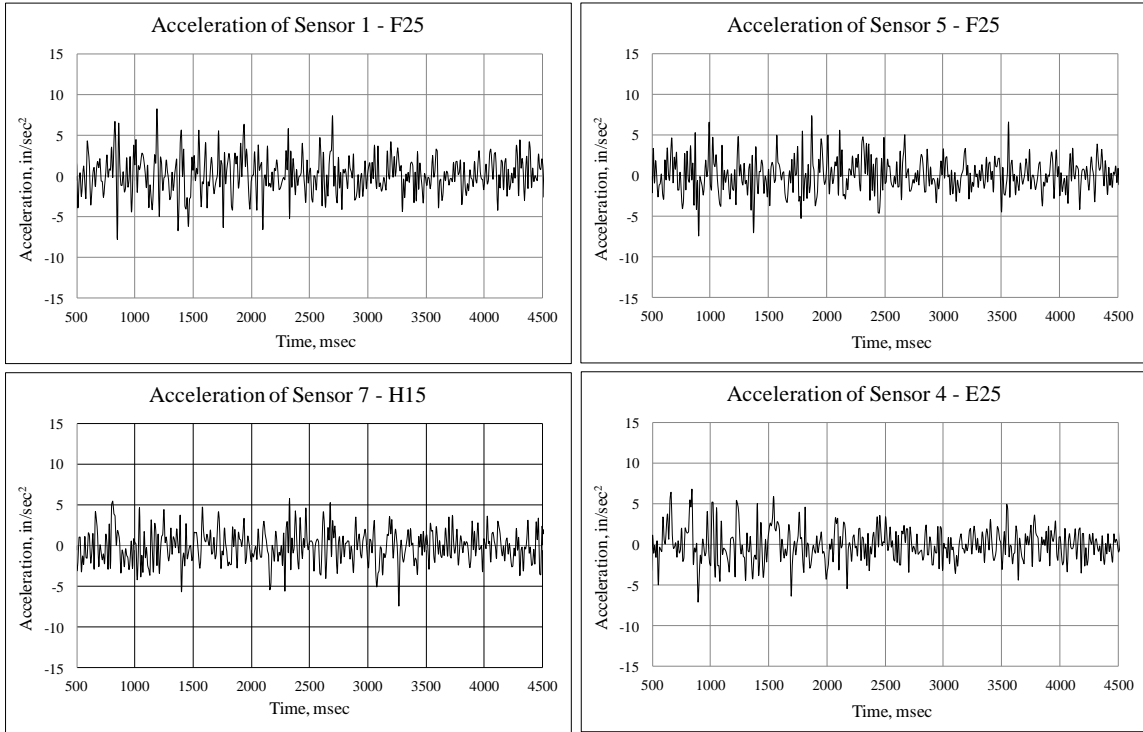


Figure 3-8: Acceleration of FEA Bridge in time domain.

3.5.2 Frequency Analysis

The frequency analysis was also performed to extract natural frequencies and corresponding mode shapes of the FEA Bridge. The frequency analysis was later used in validating the FEA model of the bridge. ABAQUS Standard provides three eigenvalue extraction methods: Lanczos, automatic multi-level substructuring (AMS), and subspace iteration. The Lanczos method was used to perform the frequency analysis to find the first four natural frequencies and their corresponding mode shapes, as shown in Fig. 3-9.

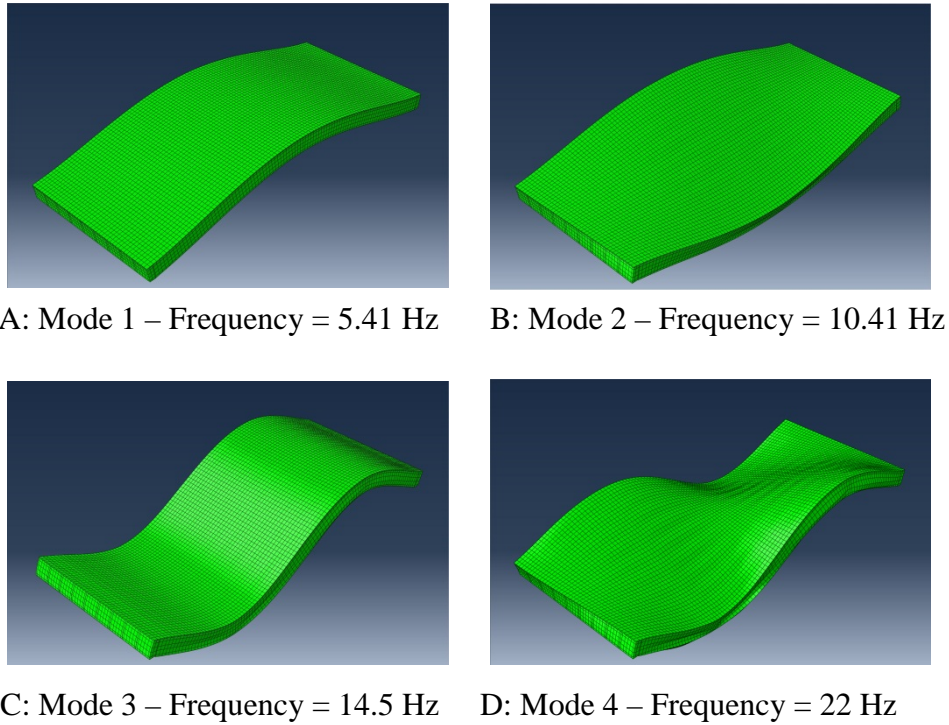


Figure 3-9: Vibration mode shapes of FEA Bridge.

3.6 FEA Model Validation

The most challenging task in finite element modeling and analysis is to validate a finite element model assumed to represent a real structure. The FEA model in this study was validated using two methods: experimental validation by using frequency analysis and theoretical validation by using static analysis.

3.6.1 Experimental Validation

The modulus of elasticity (MOE) of concrete is a variable that plays important role in the dynamic bridge response. It is the primary material property of the bridge in the FE simulation. The MOE of the Field Bridge was calculated and detail calculations are shown in Appendix C. An FE model was created based on the current MOE of the bridge, and the frequency analysis was performed to extract the fundamental frequency of the bridge.

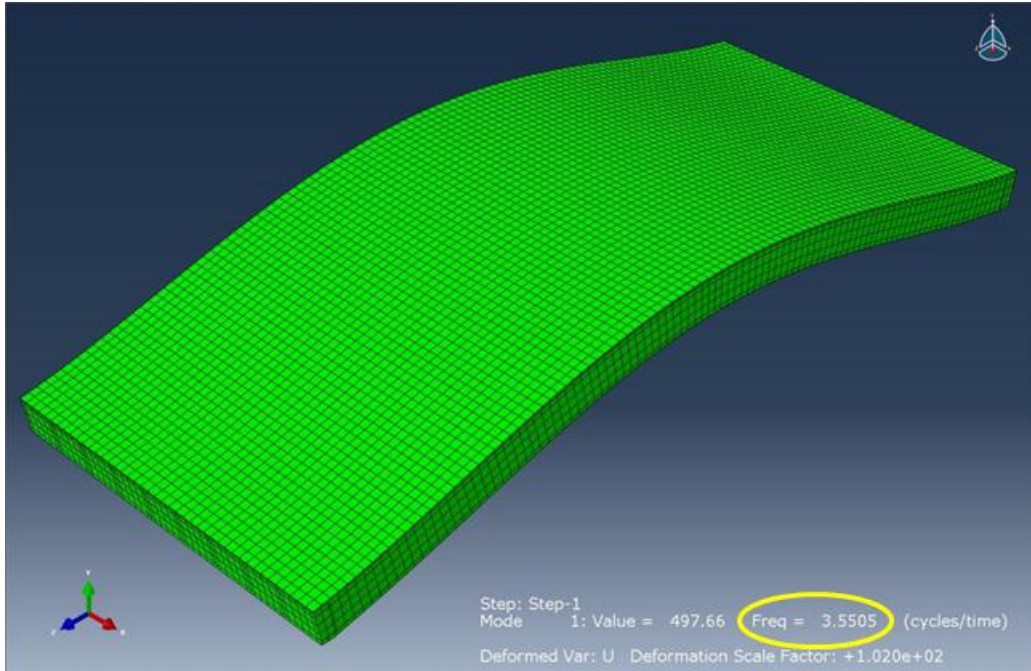
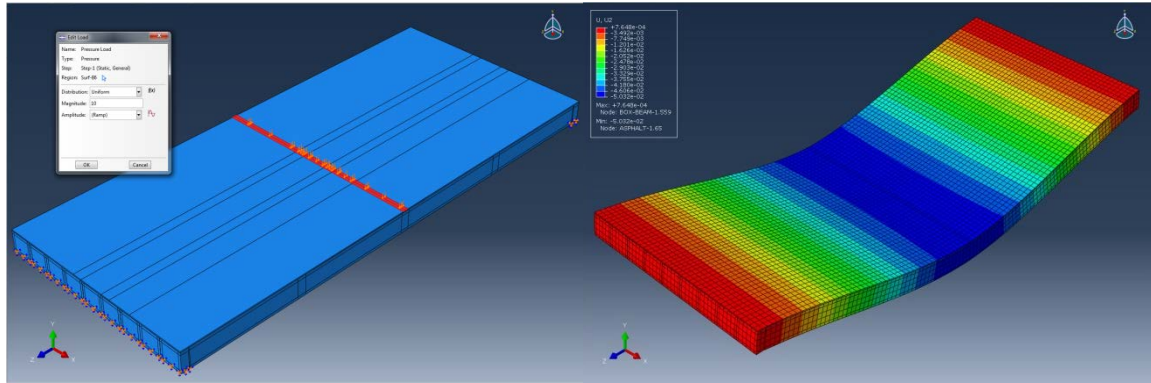


Figure 3-10: FEA Bridge model validation by frequency analysis.

From the results of the FEA, the fundamental frequency of the FE model bridge was obtained as 3.5505 Hz, as shown in Fig. 3-10. This result was very close to the fundamental frequency of 3.44 Hz of the Field Bridge.

3.6.2 Theoretical Validation

A static pressure of 10 psi was applied through a 12 in. wide and 432 in. long strip across the bridge, as shown in Fig. 3-11. The pressure was applied at the middle of the bridge so that its effect is uniformly distributed. A static analysis of the FE model bridge was performed, and the values for maximum stress, maximum deflection and the total mass of the bridge were obtained from the FEA output. On the other hand, theoretical hand calculations were carried out to find the maximum stress, maximum deflection and the total mass of the bridge under the same loading condition. Hand calculated results and those obtained from the FEA output are shown in Table 3-2. The comparison of both results shows that they are fairly close.



(a)

(b)

Figure 3-11: FE model validation: a) pressure, b) deflected shape (exaggerated view).

Table 3-2: Comparison of results from FEA and approximate calculations

Items	FEA	Hand Calculations
Maximum stress	73 psi	78.14 psi
Maximum deflection	0.05 in.	0.036 in.
Total mass	2193.1 lb.s ² /in	2154.321 lb.s ² /in
Fundamental frequency	3.5505 Hz	3.4383 Hz*

Note: * means the value is found from FFT and peak-picking method.

In view of the above analyses and comparisons, it can be concluded from the experimental and theoretical validations that the FEA Bridge modeled in ABAQUS represents the Ashtabula Bridge right after construction.

Chapter 4: Bridge Condition Assessment

4.1 Modal Analysis

Modal analysis is performed on a structure under dynamic conditions in terms of its frequency, damping, and mode shapes. The vibration amplitude in a structure diminishes if excitation forces are removed. The reduction in vibration amplitude is caused by the damping property of a structure. The simulation of damping mechanism, however, is beyond the scope of this study. On the other hand, frequencies and mode shapes of a structure are affected by its mass and stiffness. Mass of a structure does not change significantly over time when there is no big loss in the cross-section of the structure. In the Ashtabula Bridge, no significant loss in cross-section was noticed. Therefore, it was assumed that the mass of the bridge did not change over time. The variable that plays important role in the health of a structure is the stiffness or flexural rigidity, which can be determined from the geometric and material properties of the structure. The stiffness of a structure decreases over time due to structural deterioration and cracks. This phenomenon reduces the capacity of the structure. Moreover, the natural frequency of a structure is directly proportional to the square root of its stiffness. Therefore, any change in stiffness causes a change in the frequency and the capacity of a structure. By determining the change in frequency of a structure between its new and old conditions, the amount of deterioration and the health condition of the structure can be estimated. Dynamic properties of a system under vibration can be determined analytically using modal analysis.

From the theory of structural dynamics, the equation of motion of any linearly elastic system subjected to external dynamic force can be described by Eq. 4.1.

$$[M]\{\ddot{x}\} + [C]\{\dot{x}\} + [K]\{x\} = \{f(t)\} \quad (4.1)$$

Where, $[M]$ = mass matrix, $[C]$ = damping matrix, $[K]$ = stiffness matrix, $\{f(t)\}$ = nodal force vector, $\{x\}$ = nodal displacement vector, $\{\dot{x}\}$ = nodal velocity vector, $\{\ddot{x}\}$ = nodal acceleration vector.

In case of a force-free vibration, $\{f(t)\} = 0$, and Eq. 4.1 becomes Eq. 4.2.

$$[M]\{\ddot{x}\} + [C]\{\dot{x}\} + [K]\{x\} = 0 \quad (4.2)$$

After some calculations, the natural circular frequency (ω) of the system can be expressed by Eq. 4.3.

$$\omega = \sqrt{\frac{k}{m}} \quad (4.3)$$

From structural dynamics, the modal frequency, f , of a system is equal to its circular frequency divided by 2π , and is given by Eq. 4.4.

$$f = \frac{1}{2\pi} \sqrt{\frac{k}{m}} \quad (4.4)$$

4.2 Dynamic Analysis of Beam Systems

Idealizing a complex real structure into a simplified system is an essential part in the theory of structural engineering. A continuous system with distributed mass has an infinite number of degrees of freedom and an infinite variety of deformation patterns. Analyzing a system with such complexities is impractical. In this study, the bridge was idealized as a beam, as shown in Fig. 4.1, with distributed mass, flexural rigidity and fixed-fixed support conditions for dynamic analysis.

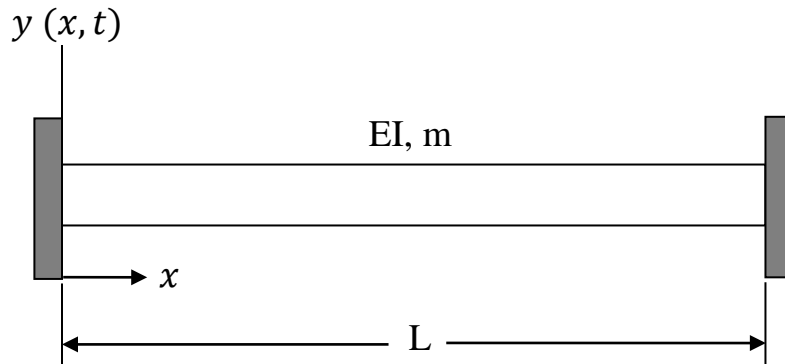


Figure 4-1: Idealization of Field Bridge.



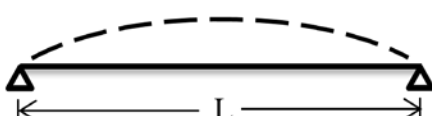
The vertical deflection of the beam is defined in term of distance and time by Eq. 4.5.

$$y(x, t) = \phi(x) f(t) \quad (4.5)$$

Where, x = distance along the length of the beam, y = vertical deflection, t = time, $\phi(x)$ = shape function.

By solving Eq. 4.5, the fundamental frequency of the beam can be found. Table 4.1 shows fundamental frequencies and mode shapes for beams with different support conditions (Paz, 1985).

Table 4-1: Fundamental frequencies of beams with different support systems

Support Condition	Fundamental frequency, Hz	Mode shape
Fixed-Fixed	$f = 3.5608 \sqrt{\frac{EI}{mL^4}}$	
Fixed-Hinged	$f = 2.4529 \sqrt{\frac{EI}{mL^4}}$	
Simply Supported	$f = 1.5708 \sqrt{\frac{EI}{mL^4}}$	

Where, f = fundamental frequency, E = Young's modulus of elasticity, I = moment of inertia, m = mass per unit length, and L = length of the beam.

The fundamental frequency of the Field Bridge can be determined by analyzing its real-time acceleration data. On the other hand, the fundamental frequency of the FEA Bridge can be found from the FEA or theoretical analysis shown in Table 4.1. The change in frequency between FEA Bridge and Field Bridge indicates deterioration of the bridge over its service life. Type and location of damage are beyond the scope of this study; rather the overall change in frequency is the main focus. From this change, the overall structural condition of the bridge is estimated and correlated to the reduction in standard condition rating of the bridge.

4.3 Fast Fourier Transform

The acceleration data collected from each sensor location on the bridge are time-dependent. The peak amplitude and its corresponding fundamental frequency, however, were needed to assess the overall structural condition of the bridge. Therefore, the acceleration data in the time domain need to be transformed into the frequency domain to determine the peak

amplitudes and corresponding frequencies. This transformation of the time domain data can be performed by Discrete Fourier Transform using the Fast Fourier Transform (FFT) algorithm developed and proposed by Cooley and Tukey in 1965 (Cooley, et al., 1965). The FFT requires the number of data points to be of a power of 2, such as 256, 512, or 1024. Figures 4.2 and 4.3 show time domain and corresponding frequency domain data from the Field Bridge and the FEA Bridge, respectively.

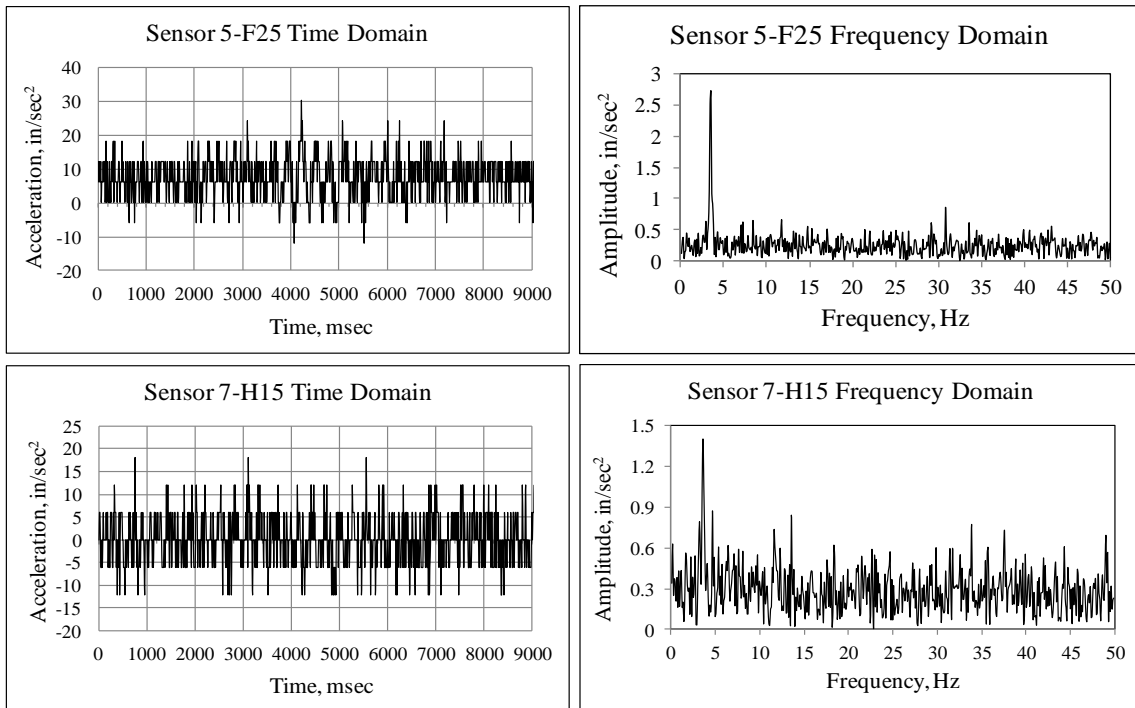


Figure 4-2: Representative acceleration of Field Bridge in time and frequency domain.

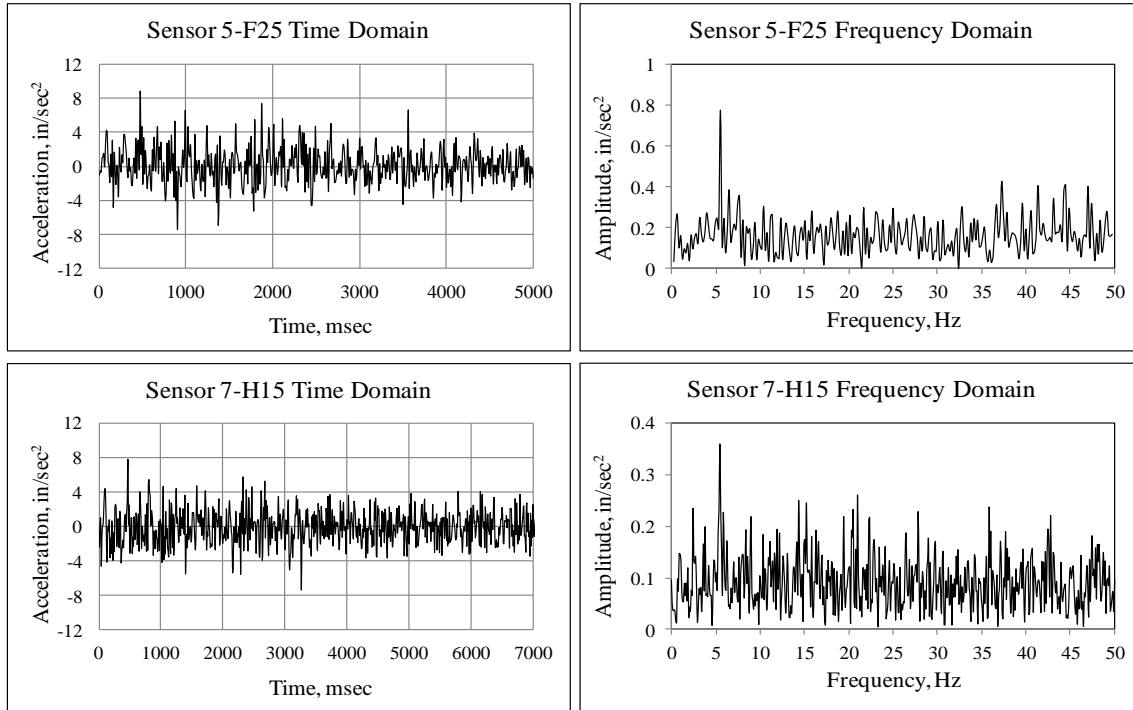


Figure 4-3: Representative acceleration of FEA Bridge in time and frequency domain.

4.4 Peak-Picking Method

For acceleration data in the frequency domain, the peak-picking method was used to select peak amplitudes and their corresponding fundamental frequencies. Peak-picking is a fast method for the identification of modal characteristics of a bridge. It is a nonparametric method, which is mostly used for acceleration data in the frequency domain. The concept of this method is based on the fact that the frequency response of a structure goes through peak values around natural frequencies (Ren, et al., 2003). Frequencies at these peak values are good estimates of frequencies of the system. The fundamental frequency of the bridge was determined as the frequency corresponding to the first dominant peak amplitude. Figures 4.4 and 4.5 show the peak-picking method in selecting peak amplitudes and their corresponding fundamental frequencies at various sensor locations on the Field Bridge and the FEA Bridge, respectively.

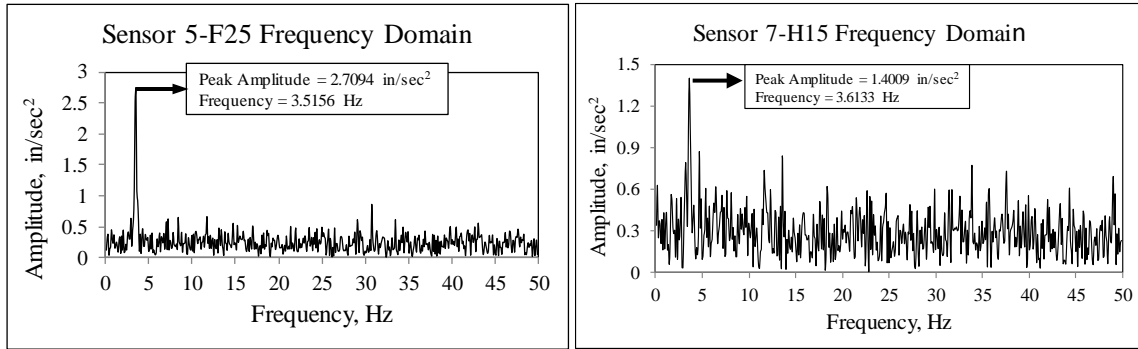


Figure 4-4: Peak amplitude and corresponding fundamental frequency of Field Bridge.

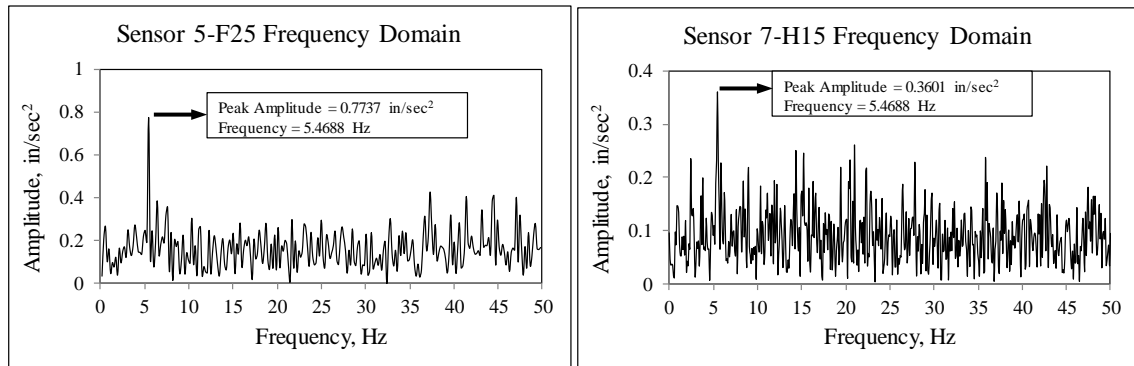


Figure 4-5: Peak amplitude and corresponding fundamental frequency of FEA Bridge.

Peak amplitudes for all truck runs from the Field Bridge and the FEA Bridge are shown in Tables 4.2 and 4.3, respectively. Fundamental frequencies corresponding to peak amplitudes from the Field Bridge and FEA Bridge are shown in Tables 4.4 and 4.5, respectively.

Table 4-2: Peak amplitude of Field Bridge

Truck	Speed (mph)	Bridge Peak Acceleration Amplitude-Field (in/sec ²)							
		1	2	3	4	5	6	7	8
Empty	10	0.7499	0.5698	0.8015	0.7739	0.8177	0.6032	0.76	0.4036
	15	0.7403	0.8494	0.8672	0.964	0.9174	0.8463	0.7496	1.06
	20	0.604	0.67	0.6731	0.7939	0.718	0.6533	0.4172	1.0856
	25	0.5717	0.6828	0.6269	0.7475	0.5611	0.4449	0.4683	0.536
Half-loaded	10	0.7968	0.5372	1.1876	1.0212	1.1997	0.764	0.7868	0.7979
	15	1.1896	1.3009	1.3067	1.4836	1.5935	1.2862	1.4009	1.0629
	20	1.0671	1.1051	2.2269	1.619	1.6344	1.5373	1.3762	1.4366
	25	0.7756	0.9033	0.7905	0.6671	0.944	0.7674	1.013	0.8163
Fully-loaded	10	0.856	0.5005	0.6876	0.9099	0.5487	0.7202	0.6857	0.4597
	15	1.1336	1.3086	1.2047	1.3405	1.1901	1.3547	1.3529	1.1107
	20	0.8125	0.9708	1.1406	1.0386	1.055	1.1537	1.1223	0.8568
	25	2.1988	2.3635	2.6689	2.2605	2.7094	2.9505	2.5981	1.8354

Table 4-3: Peak amplitude of FEA Bridge

Truck	Speed (mph)	Bridge Peak Acceleration Amplitude-Abaqus (in/sec ²)							
		1	2	3	4	5	6	7	8
Empty	10	0.3938	0.2763	0.4914	0.4645	0.4385	0.487	0.2731	0.4472
	15	0.3132	0.3064	0.2361	0.3591	0.4023	0.3767	0.3377	0.2871
	20	0.496	0.6078	0.701	0.6699	0.7919	0.7049	0.5976	0.7733
	25	0.5818	0.4896	0.5979	0.7699	0.9861	0.6733	0.5728	0.4653
Half-loaded	10	0.2798	0.3254	0.342	0.3833	0.4774	0.3154	0.2956	0.3594
	15	0.4349	0.3951	0.404	0.373	0.3919	0.3537	0.3601	0.265
	20	0.6783	0.5045	0.4883	0.7517	0.5461	0.7238	0.5604	0.6152
	25	0.4818	0.5701	0.6864	0.8603	0.7394	0.5213	0.5829	0.6485
Fully-loaded	10	0.373	0.3348	0.3412	0.3697	0.4146	0.4257	0.3822	0.2905
	15	0.492	0.3419	0.4074	0.3349	0.3647	0.2758	0.304	0.3739
	20	0.6706	0.826	0.7616	0.5884	0.7719	0.599	0.713	0.5601
	25	0.6876	0.6921	0.7019	0.925	0.7737	0.8321	0.7175	0.6336

Table 4-4: Fundamental frequency of Field Bridge

Truck	Speed (mph)	Bridge Frequency-Field (Hz)							
		1	2	3	4	5	6	7	8
Empty	10	2.9297	3.3203	3.418	4	3.5156	3.5156	3.5156	3.3203
	15	3.6133	3.7109	3.5156	3.5156	3.6133	3.6133	3.6133	3.5156
	20	3.6133	3.418	3.6133	3.418	3.0273	3.2227	3.027	3.2227
	25	3.3203	3.3203	3.3203	3.6133	3.8086	3.3203	3.125	3.0273
Half-loaded	10	3.3203	3.418	3.5156	3.5156	3.418	3.418	3.418	3.5156
	15	3.5156	3.5156	3.5156	3.6133	3.6133	3.5156	3.6133	3.6133
	20	3.418	3.418	3.418	3.418	3.5156	3.418	3.418	3.5156
	25	3.418	3.2227	3.809	3.7109	3.418	3.3203	3.418	3.3203
Fully-loaded	10	3.418	3.418	3.7109	3.418	3.2227	3.125	3.125	3.6133
	15	3.5156	3.418	3.418	3.5156	3.418	3.5156	3.418	3.5156
	20	3.5156	3.5156	3.2227	3.3203	3.3203	3.418	3.125	3.2227
	25	3.418	3.418	3.418	3.5156	3.5156	3.418	3.5156	3.5156

Table 4-5: Fundamental frequency of FEA Bridge

Truck	Speed (mph)	Bridge Frequency-Abaqus (Hz)							
		1	2	3	4	5	6	7	8
Empty	10	5.5664	5.4688	5.4688	5.3711	5.3711	5.4688	5.3711	5.3711
	15	5.4688	5.3711	5.3711	5.3711	5.4688	5.3711	5.4688	5.3711
	20	5.4688	5.4688	5.4688	5.4688	5.4688	5.4688	5.4688	5.4688
	25	5.4688	5.4688	5.4688	5.4688	5.4688	5.4688	5.4688	5.4688
Half-loaded	10	5.4688	5.3711	5.3711	5.3711	5.4688	5.3711	5.4688	5.3711
	15	5.4688	5.3711	5.4688	5.3711	5.4688	5.4688	5.4688	5.4688
	20	5.4688	5.4688	5.4688	5.4688	5.4688	5.4688	5.4688	5.4688
	25	5.4688	5.4688	5.4688	5.4688	5.4688	5.4688	5.4688	5.4688
Fully-loaded	10	5.3711	5.3711	5.566	5.3711	5.4688	5.3711	5.4688	5.3711
	15	5.4688	5.4688	5.4688	5.3711	5.3711	5.4688	5.3711	5.4688
	20	5.4688	5.4688	5.4688	5.4688	5.4688	5.4688	5.4688	5.4688
	25	5.4688	5.4688	5.4688	5.4688	5.4688	5.4688	5.4688	5.4688

4.5 MAC Analysis

The modal analysis between each sensor location at both FEA Bridge and Field Bridge under different loads and speeds was carried out by using MAC technique. The MAC analysis of peak amplitudes indicates the degree of correlation or linearity between each set of data from the Field Bridge and the FEA Bridge. The MAC value for each pair of similar sensors is calculated by Eq. 4.6.

$$MACn = \frac{(N_n^T \cdot O_n^T)^2}{(N_n^T \cdot N_n) * (O_n^T \cdot O_n)} \quad (4.6)$$

Where,

$MACn$ = MAC value for the n^{th} sensor nodes

N_n = Amplitude response matrix of n^{th} sensor of FEA Bridge model

O_n = Amplitude response matrix of n^{th} sensor of Field Bridge.

N_n^T = Transpose of amplitude response matrix of N_n .

O_n^T = Transpose of amplitude response matrix of O_n .

Details of MAC calculations for Sensors 1 and 4 are shown in Appendix D. Values of MAC analysis of all sensor data are shown in Table 4.6.

Table 4-6: Sensors with corresponding MAC values

Sensors	MAC Value
1	0.866
2	0.819
3	0.752
4	0.817
5	0.718
6	0.778
7	0.789
8	0.851

4.6 Results

The overall dynamic response of the bridge was tested under different load scenarios. Acceleration data were collected on the bridge at eight sensor nodes, which represented the response of the entire bridge. It became evident from the analyses that there are distinct differences between the responses of the Field Bridge and the FEA Bridge indicating some deterioration of the bridge condition. As a bridge ages, damage and deterioration in terms of loss in cross-section, material degradation, corrosion in steel, etc., cause reduction in stiffness or flexural rigidity of the bridge. From the theory of structural dynamics, the natural frequency of a structure is directly proportional to the square root of its stiffness or flexural rigidity.

From Tables 4.4 and 4.5, it was found that the change in the fundamental frequency of the bridge between sensor locations is fairly small. However, the goal of this study is to estimate the overall structural condition of the bridge rather than the condition at a specific location. Therefore, the average fundamental frequencies at all sensor locations under various load cases were used in calculating the change in frequency.

From Table 4.4, the average fundamental frequency of the Field Bridge is 3.44 Hz. From Table 4.5, the average fundamental frequency of the FEA Bridge is 5.45 Hz. The reduction in the fundamental frequency of the Ashtabula Bridge was calculated as 36.9 percent. The detail calculations are shown in Appendix D.

The Ashtabula Bridge has a current condition rating of “6”, as reported by ODOT. It was found from the analysis results that the fundamental frequency of the Field Bridge was less than that of the FEA Bridge, while the amplitude was higher in the Field Bridge than in the FEA Bridge. Therefore, the change in fundamental frequency between these two bridge conditions indicates some amount of deterioration of the bridge over time. The fundamental frequency of the bridge has been reduced by 36.9 percent over a service life of 25 years. Assuming the FEA Bridge had a condition rating of “9”, this 36.9 percent reduction in frequency has been assigned to the structural condition deterioration of the bridge by 3 points (from “9” to “6”). The explanations of condition rating numbers are shown in Table 4.7 (FHWA, 2011).

Table 4-7: National Bridge Inventory general condition rating guidance

Code	Description	Commonly Employed Feasible Actions
9	EXCELLENT CONDITION.	Preventive Maintenance
8	VERY GOOD CONDITION No problems noted.	
7	GOOD CONDITION Some minor problems.	
6	SATISFACTORY CONDITION Structural elements show some minor deterioration.	Preventive Maintenance; and/or Repairs
5	FAIR CONDITION Primary structural elements are sound but may have some minor section loss, cracking, spalling or scour.	
4	POOR CONDITION Advanced section loss, deterioration, spalling or scour.	Rehabilitation or Replacement
3	SERIOUS CONDITION Loss of section, deterioration spalling or scour have seriously affected primary structural components. Local failures are possible. Fatigue cracks in steel or shear cracks in concrete may be present.	
2	CRITICAL CONDITION Advanced deterioration of primary structural elements. Fatigue cracks in steel or shear cracks in concrete may be present or scour may have removed substructure support. Unless closely monitored, the bridge may have to be dosed until corrective action is taken.	
1	IMMINENT FAILURE CONDITION Major deterioration or section loss present in critical structural components or obvious vertical or horizontal movement affecting structure stability. Bridge is closed to traffic but corrective action may put back in light service.	
0	FAILED CONDITION Out of service - beyond corrective action.	

4.7 Application Software Algorithms

In order to estimate the condition of a bridge, two fundamental frequencies are required to calculate the percent of reduction in fundamental frequency: one from the current condition of the bridge, and the other one from the newest condition of the bridge. The current fundamental frequency can be obtained from the field acceleration data captured through WSN. The fundamental frequency at the newest condition can be determined using two methods: FE simulation and theory of structural dynamics. Since the application software developed in this

study mainly focuses on instantly estimating the current condition rating of a PSBB bridge, the use of FE simulation in the field is not practical. Therefore, the theory of structural dynamics is used to determine the fundamental frequency of a bridge at its newest condition. However, finite element analysis was used in this study to find the fundamental frequency of the FEA Bridge (new Ashtabula Bridge). Therefore, the fundamental frequency found by the theory of structural dynamics needs to be correlated to that of the FEA Bridge. A relationship between these two frequencies was determined in order to develop algorithms for the application software.

The fundamental frequency of a bridge at its newest condition can be determined from the theory of structural dynamics by using equations in Table 4.1. For a beam with fixed-fixed support conditions, the fundamental frequency is given by Eq. 4.7.

$$f = 3.5608 * \sqrt{\frac{EI}{mL^4}} \quad (4.7)$$

Assume, $mL = m_t$ (4.8)

Where, m_t = total mass of beam.

By substituting values from Eq. 8, Eq. 4.7 can be re-written as Eq. 4.9.

$$f = 3.5608 * \sqrt{\frac{EI}{m_t L^3}} \quad (4.9)$$

In the above equation, the fundamental frequency is a function of total mass, flexural rigidity, and length of the bridge. The total mass of the bridge does not change significantly over time. Therefore, it was assumed constant and found from the FE model output. The total mass of the bridge: $m_t = 2193.1 \frac{lb.s^2}{in}$, and the length of the PSBB: $L = 1020 in$.

The flexural rigidity, EI , of the bridge can be determined from its geometry and material properties. According to ACI 8.5.1 (ACI, 2008), the modulus of elasticity, E_c , for concrete is given by Eq. 4.10.

$$E_c = 33 w_c^{1.5} \sqrt{f'_c} \quad (4.10)$$

Where, E_c = modulus of elasticity of concrete in (psi), w_c = unit weight of concrete in (lb/ft³), f'_c = 28-day compressive strength of concrete in (psi).

From the design data of the Ashtabula Bridge, the unit weight of concrete of the box beam was 150 lb/ft³, and the 28-day compressive strength of concrete was 5,500 psi. Substituting these values in Eq. 4.10 produces the value of E_c to be 4,496,061 psi.

The moment of inertia, *I*, of the box beams was found by Eq. 4.11.

$$I = \left(\frac{W_o H_o^3}{12} - \frac{W_i H_i^3}{12} \right) * n_b \quad (4.11)$$

Where,

W_o : box beam outside width (in.)

H_o : box beam outside height (in.)

W_i : box beam inside width (in.)

H_i : box beam inside height (in.)

n_b : number of box beams.

The moment of inertia (*I*) of the Ashtabula Bridge was calculated as 1,776,376 in⁴. By using Eq. 4.9, the theoretical fundamental frequency of the bridge was calculated as 6.6 Hz.

The percentage difference between fundamental frequencies of the bridge found by FEA and theory is calculated as 17.4 percent. The detail calculations are shown in Appendix D. The 17.4 percent difference in frequency was expected, which confirms that the theoretical method produces higher frequency values than the FEA method. Therefore, multiplying the theoretical frequency by (1-.174) or 0.826 produces the frequency in the FEA method.

The 36.9 percent decrease in frequency is equivalent to the reduction of condition rating three units (from “9” to “6”) according to the NBI numerical scale. This produces a 12.3 percent decrease in frequency for each unit of rating. The reduction in the condition of a bridge, *G*, is expressed by Eq. 4.12.

$$G = \Delta f * \frac{1000}{123} \quad (4.12)$$

Where Δf stands for the percentage difference in frequencies between the FEA Bridge and the Field Bridge. The current condition rating of the Field Bridge is calculated by Eq. 4.13.

$$\text{Bridge Condition Rating} = \text{integer } (9 - G) \quad (4.13)$$

The flow chart in Figs. 4.6 to 4.8 shows algorithms for the application software and the procedures for bridge condition assessment developed in this study. Figure 4.9 shows schematic diagrams of bridge geometric parameters used in the flow chart.

Input:	
1. L: box beam length	<input type="text"/> (in)
2. W_o : box beam outside width	<input type="text"/> (in)
3. W_i : box beam inside width	<input type="text"/> (in)
4. H_o : box beam outside height	<input type="text"/> (in)
5. H_i : box beam inside height	<input type="text"/> (in)
6. n_b : number of box beams	<input type="text"/>
7. n_d : number of diaphragms per box beam	<input type="text"/>
8. t_d : thickness of diaphragm	<input type="text"/> (in)
9. t_e : thickness of box beam end	<input type="text"/> (in)
10. t_w : thickness of wearing surface	<input type="text"/> (in)
11. f'_c : 28-day compressive strength of concrete	<input type="text"/> (psi)
12. w_c : unit weight of concrete	<input type="text"/> (lb/ft ³)
13. bridge end supports (drop down menu)	
a) fixed-fixed	
b) fixed-hinged	
c) simply supported	

Figure 4-6: Bridge condition assessment input page.

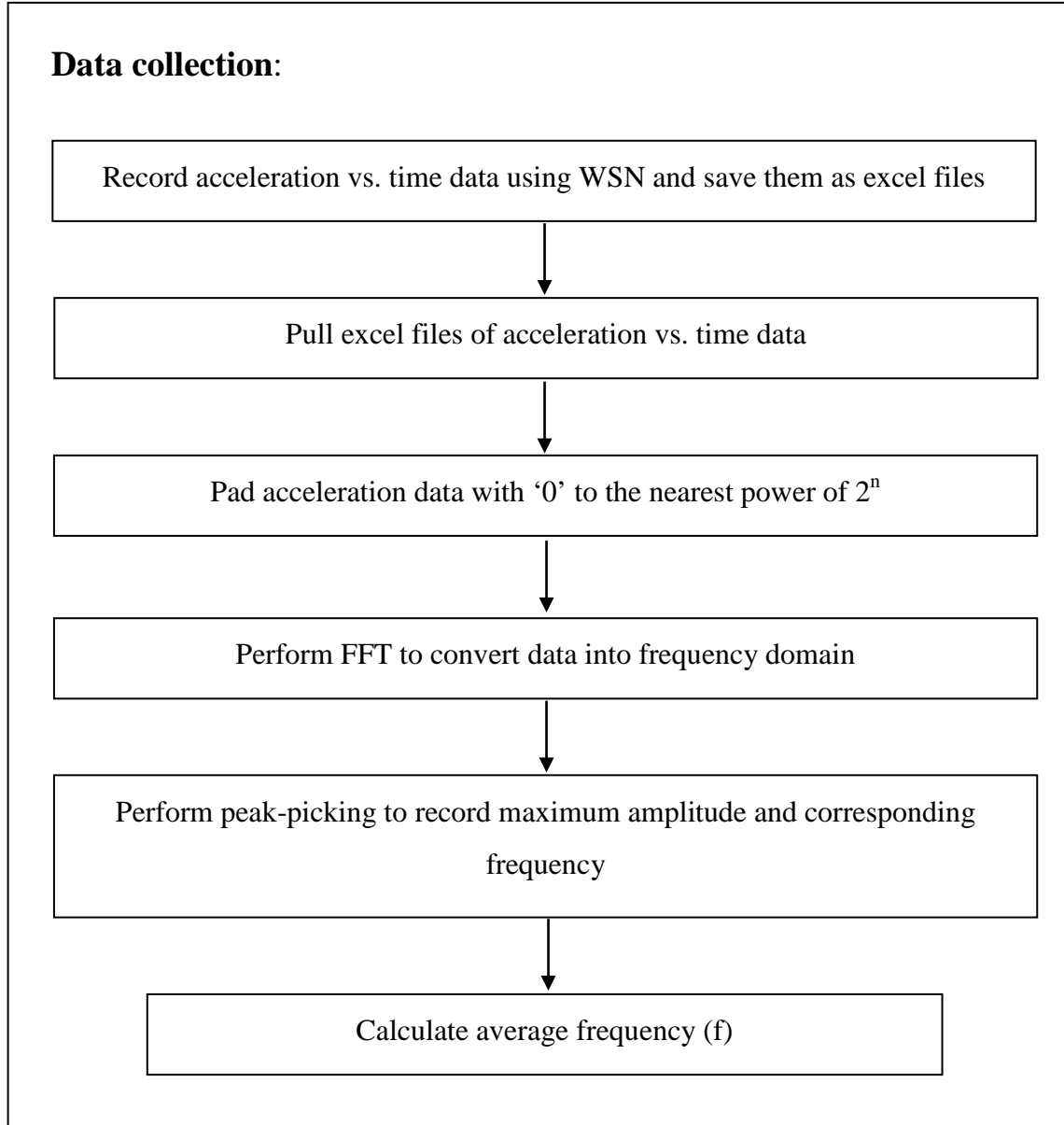


Figure 4-7: Bridge condition assessment flow chart.

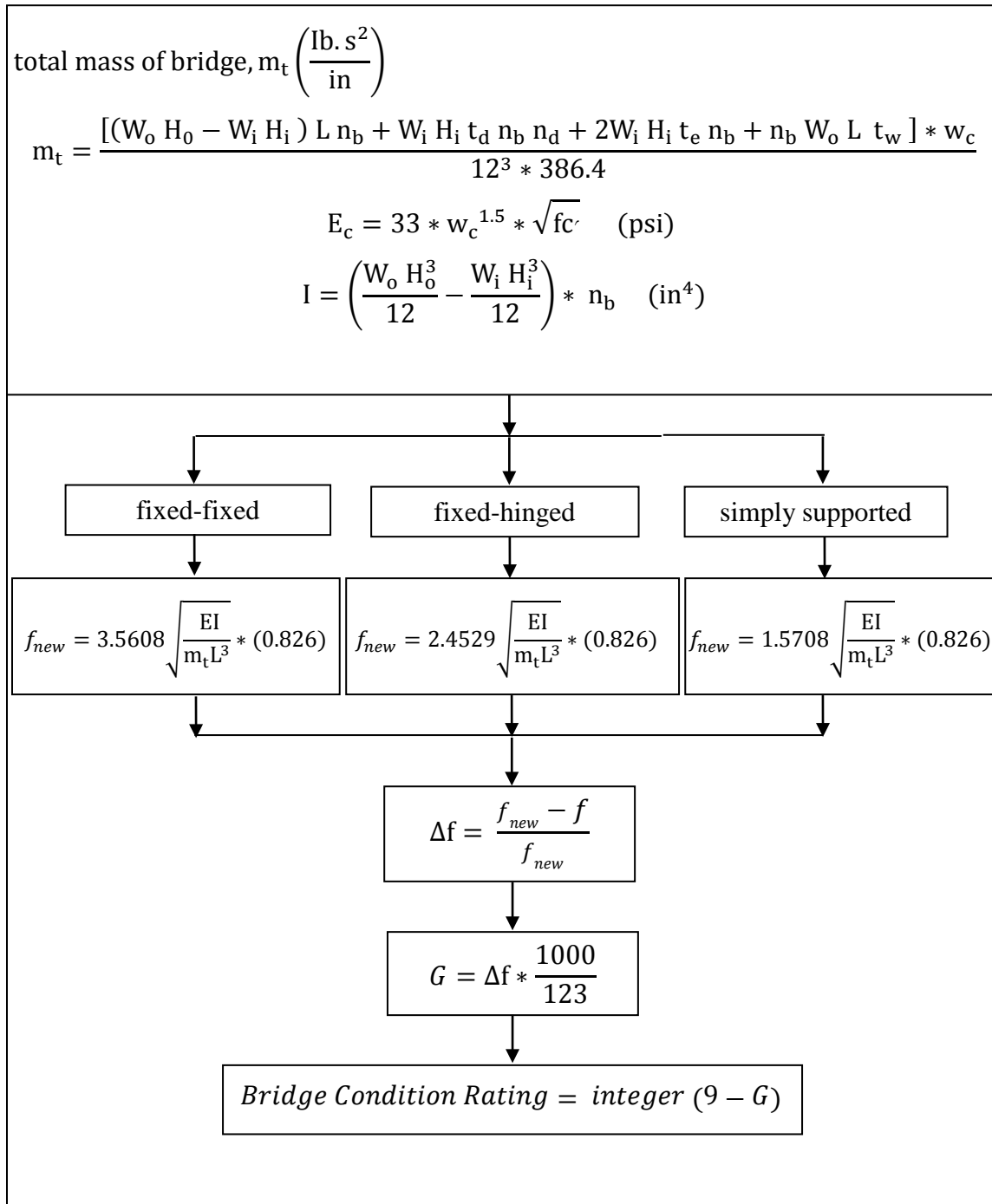


Figure 4-8: Bridge condition assessment flow chart (continued).

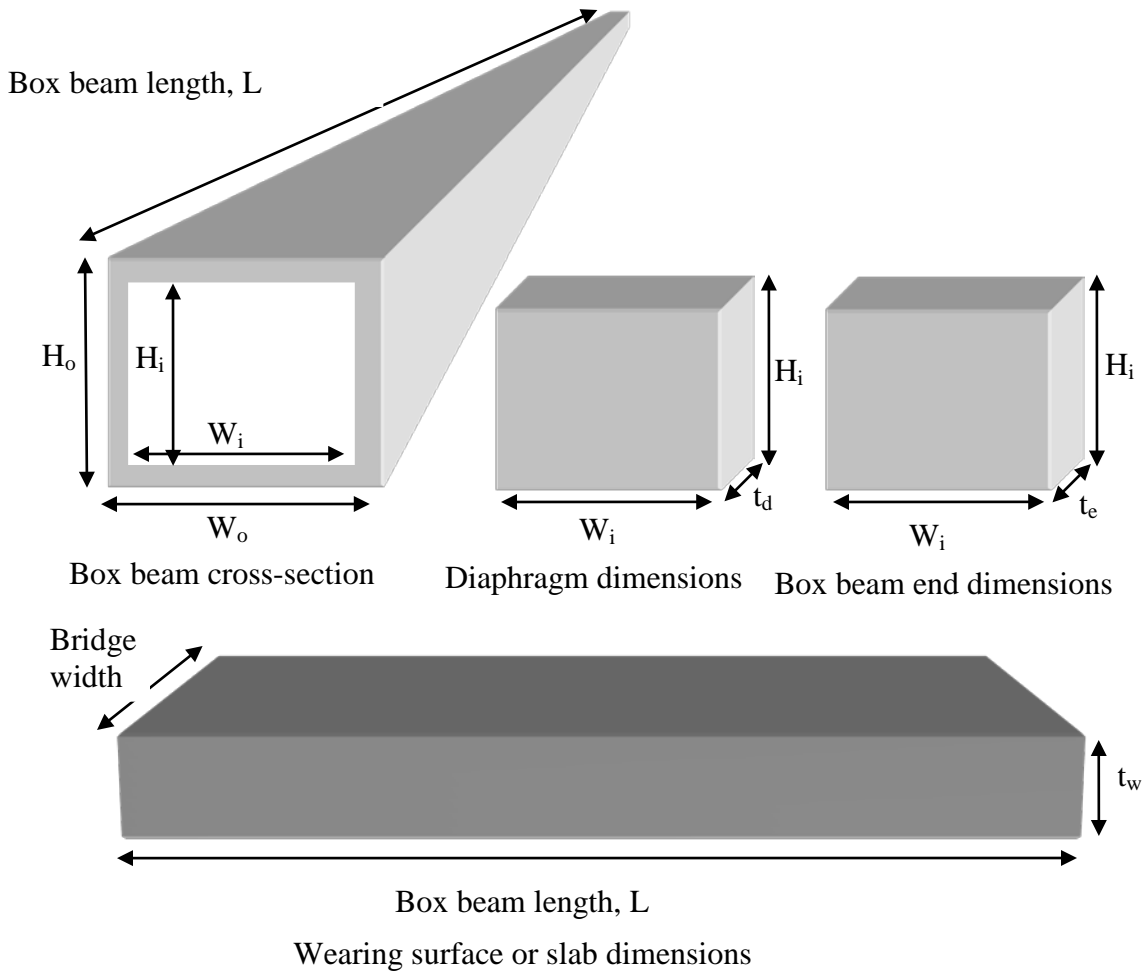


Figure 4-9: PSBB bridge geometric property.

4.8 Discussions

The objective of this research was to develop a tool for condition assessment and load rating of a PSBB bridge under vehicular loads by analyzing its dynamic response collected through WSN. The stated objective was achieved by determining the relationship between the response data of the FEA Bridge and the Field Bridge. The hypothesis is based on the assumption that the dynamic response is a sensitive and important indicator of the physical integrity of a structure. The following findings are summarized from the outcome of the condition assessment:

- After 25 years in service, the frequency of the bridge has decreased by 36.9 percent. This reduction in frequency was correlated to the reduction in condition rating of the bridge, as reported by ODOT. The bridge was given a rating of “6” on the numerical scale of 0-9 according to NBI. The explanation of this rating by NBI is "Satisfactory Condition, Structural elements show some minor deterioration". Those bridges are usually designed and built to last around 50 years. However, the bridge still has sufficient capacity for supporting current traffic. Therefore, the 36.9 percent decrease in frequency after 25 years of service is expected, practical and reasonable.
- The values of MAC analysis vary along the length of the bridge. Sensors closer to bridge ends produce higher MAC values than those close to the middle of the bridge. The average of MAC values was 0.8, which estimates the degree of correlation between the Field Bridge and the FEA Bridge. In practice, MAC values greater than 0.9 are considered as well correlated sets of data (Ewins, 2000).
- From Tables 4.4 and 4.5, it can be noticed that the fundamental frequency was not much affected by the changes in the weight and speed of trucks. This is because the weight of a truck is very negligible compared to the weight of the bridge itself. Therefore, in the modal analysis of the bridge using the theory of beam system, the mass of a truck does not affect the calculation of fundamental frequency. On the other hand, the amplitudes of the bridge, as shown in Tables 4.2 and 4.3, were greatly affected by the changes in the weight and speed of trucks.
- From Tables 4.2 to 4.5, it can be found that the frequency of the Field Bridge is less than that of the FEA Bridge, while the amplitude of the Field Bridge is higher than that of the FEA Bridge. These results agree with the fact that a bridge ages and deteriorates over time, and its frequency decreases while amplitude increases under the same loading condition.

CHAPTER 5: Bridge Load Rating

5.1 Equation of Motion and Natural Frequency

Degrees of freedom (DOF) can be defined as the number of independent coordinates, which are needed to describe the configuration of a structure at any instant of time. In reality, structures have an infinite number of DOF. Therefore, an infinite number of independent coordinates are needed to determine the configuration of a structure (Tedesco, 1999). However, if a structure is idealized as a single degree of freedom (SDOF) spring-mass system, as shown in Fig. 5-1, then the equation of motion can be expressed by Eq. 5.1.

$$m\ddot{X} + c\dot{X} + kX = F(t) \quad (5.1)$$

Where, \ddot{X} is the acceleration of the system, \dot{X} is the velocity of the system, X is the displacement of the system, m is the system mass, c is the system damping coefficient, k is the system stiffness, and $F(t)$ is the time-dependent force that acts on the system to create forced vibrations.

After some calculations, the natural circular frequency, ω , of the system can be expressed by Eq. 5.2. At the same time, it can be expressed in term of the natural frequency, f , of the system by Eq. 5.3. Therefore, the natural frequency of the system can be expressed by Eq. 5.4.

$$\omega = \sqrt{\frac{k}{m}} \quad (5.2)$$

$$\omega = 2 \pi f \quad (5.3)$$

$$f = \frac{1}{2 \pi} \sqrt{\frac{k}{m}} \quad (5.4)$$

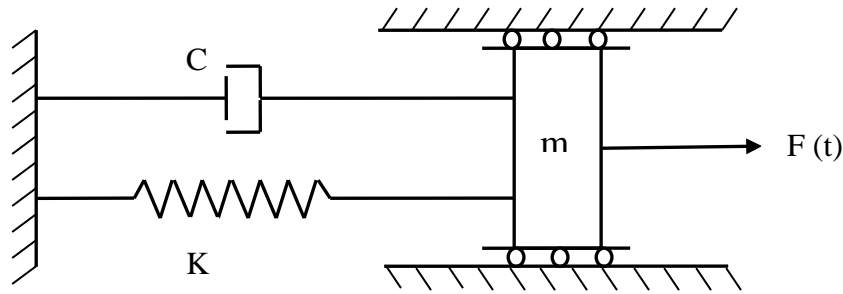


Figure 5-1: SDOF spring-mass system.

Assuming that a bridge behaves like a SDOF spring-mass system, the stiffness of the spring (herein the FEA Bridge) can be calculated by Eq. 5.5. The calculated system stiffness can be used to estimate the load bearing capacity of a bridge.

$$k = 4 \pi^2 f^2 m \quad (5.5)$$

5.2 Bridge Response Analysis

The peak amplitude and fundamental frequency of a bridge under forced vibration are two important parameters for estimating the load bearing capacity of a bridge. The bridge dynamic response under forced vibrations was captured as acceleration in the time domain. Acceleration data of the Field Bridge and the FEA Bridge was transformed into frequency domain by performing FFT. The peak-picking algorithm was used to pick peak amplitudes and their corresponding frequencies from the FFT data the Field Bridge and the FEA Bridge.

Acceleration data in the frequency domain may have multiple peaks, which represent various modes of movement, but the most dominant peak will represent the most critical mode. The FFT data shows the dynamic response of the Field Bridge has clear dominant peaks for all 8 sensors. Figure 5-2 shows the dynamic response of the Field Bridge in the frequency domain due to vibration caused by the fully-loaded truck at 25 mph. By using the peak-picking algorithm, peak amplitudes and their corresponding frequencies for the Field Bridge were recorded and shown in Tables 4-2 and 4-3. The FFT data from the dynamic response of the FEA Bridge under truck loads also show clear dominant peaks. Peak amplitudes and their corresponding frequencies of the FEA Bridge are shown in Tables 4-4 and 4-5. Figure 5-3 shows the dynamic response of the FEA Bridge due to the fully-loaded truck at 25 mph.

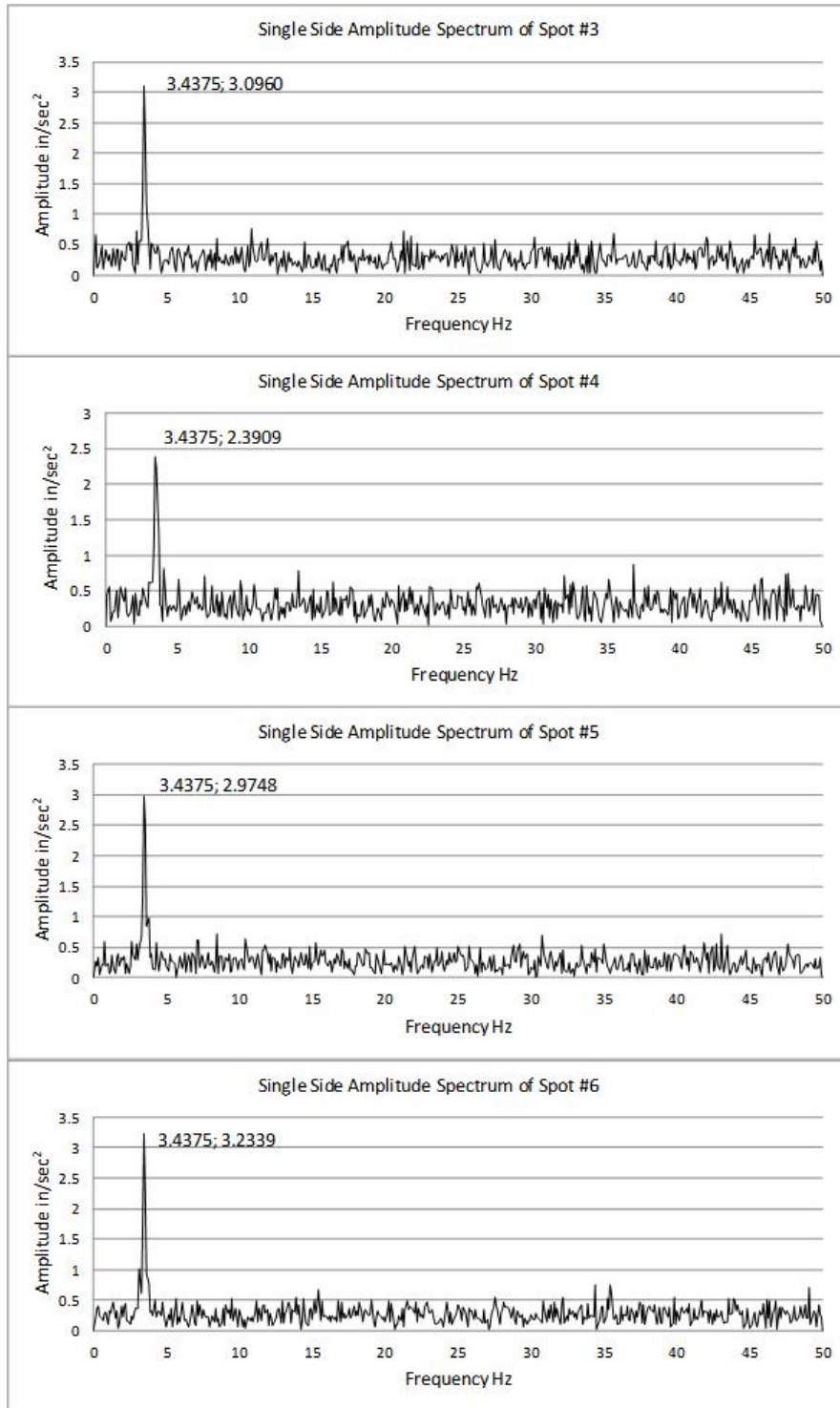


Figure 5-2: Frequency-amplitude graphs of Field Bridge.

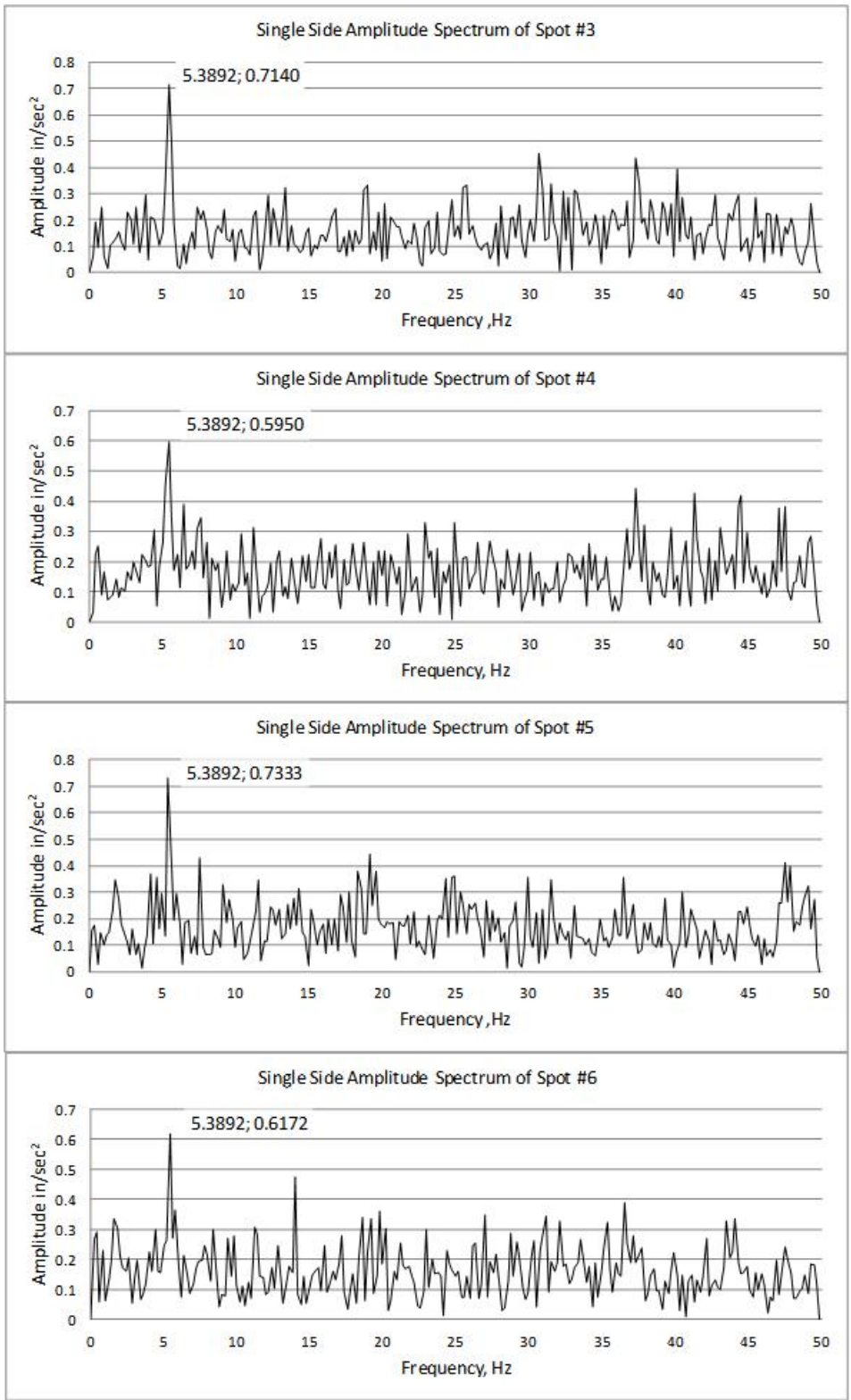


Figure 5-3: Frequency-amplitude graphs of FEA Bridge.

5.3 Load Rating Method

In order to estimate the load rating of a bridge, the stiffness of a bridge in the current field condition should be calculated. For calculating the stiffness of the FEA Bridge, it was assumed to be a single beam with distributed mass and stiffness, and fixed end support conditions. A structure with these assumptions will exhibit an infinite number of degrees of freedom due to its flexural deformation. However, if a structure is idealized as a SDOF system by assuming that the structure vibrates only in one predetermined vibration pattern (Tedesco, 1999), then the equation of motion can be expressed by Eq. 5.1, and the stiffness of the bridge can be calculated by Eq. 5.4. The system stiffness can be used accordingly to estimate the load bearing capacity of a bridge. Systems idealized with these assumptions are known as generalized single degree of freedom system.

5.4 FEA Bridge Fundamental Frequency

The fundamental (or the first bending) frequency of a bridge is needed prior to calculating its bending stiffness. It was assumed that the frequency at the most dominant peak amplitude for each sensor is the fundamental frequency. This is a reasonable assumption for a single span bridge (Chen, 2002). To verify this assumption, the displacement data of the FEA Bridge under various truck runs were collected and saved as Microsoft Excel files. The displacement data in time domain were transformed into frequency domain by using FFT. The most dominant amplitude peaks in frequency domain were recorded, as shown in Table 5-1, to verify the vibration mode shape through plotting the amplitude with sensor locations, as shown in Fig. 5-4. As expected, the vibration mode of the FEA Bridge model under the vehicular loads was the first bending mode shape with frequency equal to 5.47 Hz.

Table 5-1: FEA Bridge data for fully-loaded truck at 25 mph

Sensors	Bridge frequency (Hz)	Displacement amplitude (in)	Sensor location on bridge (ft)
1	5.47	0.168	25
2	5.47	0.198	30
3	5.47	0.219	35
4	5.47	0.230	40
5	5.47	0.230	45
6	5.47	0.219	50
7	5.47	0.198	55
8	5.47	0.168	60

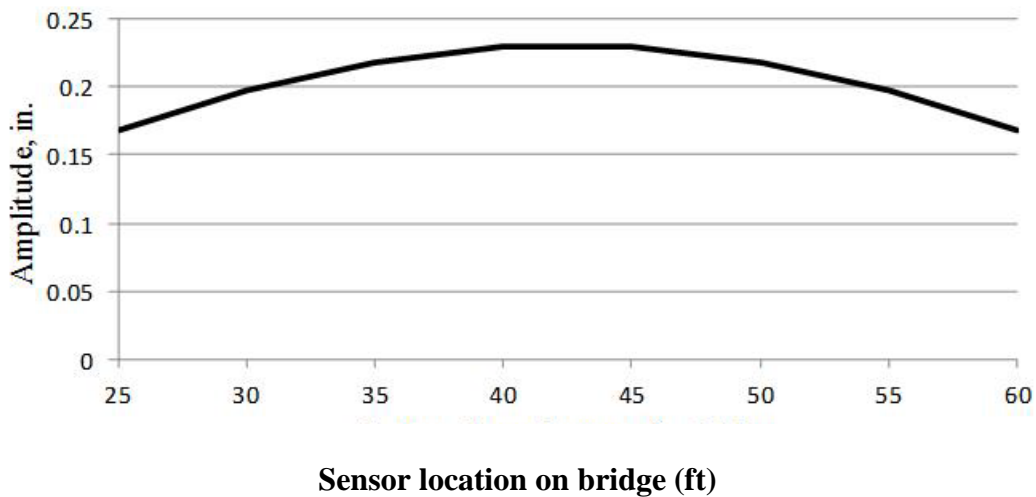


Figure 5-4: FEA Bridge mode shape under vehicular loads.

In addition, frequency analysis results show that the first vibration mode is, in fact, a bending mode at the frequency of 3.55 and 5.42 Hz for the Field Bridge and the FEA Bridge, respectively. Comparing these results with frequencies of the Field Bridge (Table 4-4) and the FEA Bridge (Table 4-5) verify the assumption that the frequency of the Ashtabula Bridge under vehicular loads is its first bending frequency.

5.5 Idealized Bridge and Load Rating Equations

In order to idealize the Ashtabula Bridge as a single beam with fixed supports in a generalized SDOF system, as shown in Fig. 5-5, it is necessary to assume a displacement configuration or shape function, $\varphi(x)$, for the beam that satisfies its kinematic and natural boundary conditions. Once the fundamental frequency of the beam is known, the effective stiffness, K_e , and the effective mass, M_e , can be calculated after deriving the shape function of the vibration pattern. The shape function of a fixed-fixed beam can be expressed by Eq. 5.6.



Figure 5-5: Beam with fixed end supports.

$$\varphi(x) = y_0 \left(\frac{x}{L}\right)^2 \left(1 - \frac{x}{L}\right)^2 \quad (5.6)$$

Where, y_0 is the vibration coefficient, and L is the PSBB beam length. By using the shape function, the effective mass and the effective stiffness were calculated using Eqs. 5.7 to 5.9, respectively.

$$M_e = \int_0^L m \{\varphi(x)\}^2 dx \quad (5.7)$$

$$M_e = \frac{y_0^2 m_t}{630} \quad (5.8)$$

$$K_e = \int_0^L EI \{\varphi''(x)\}^2 dx \quad (5.9)$$

$$K_e = \frac{4 EI y_0^2}{5 L^3} \quad (5.10)$$

Where, m_t is the total mass of the bridge ($\text{lb}\cdot\text{S}^2/\text{in.}$), and EI is the effective flexural rigidity of the bridge ($\text{lb}\cdot\text{in.}^2$). Using Eqs. 5.11 to 5.13, the effective flexural rigidity, $EI_{\text{Effective}}$, of the system can be calculated.

$$f = \frac{1}{2\pi} \sqrt{\frac{K_e}{M_e}} \quad (5.11)$$

$$f = \frac{1}{2\pi} \sqrt{\frac{\frac{4 EI y_0^2}{5 L^3}}{\frac{y_0^2 m_t}{630}}} \quad (5.12)$$

$$EI_{\text{Effective}} = \frac{f^2 * \pi^2 * L^3 * m_t}{126} \quad (5.13)$$

The maximum deflection, Δ , at the middle of the beam can be expressed by Eq. 5.14. Using the load displacement relationship in Eq. 5.15, the bridge stiffness can be calculated using Eq. 5.16.

$$\Delta = \frac{PL^3}{192 EI} \quad (5.14)$$

$$K = \frac{P}{\Delta} \quad (5.15)$$

$$K = \frac{192 * EI_{\text{Effective}}}{L^3} \quad (5.16)$$

Where, P is the load bearing capacity of the bridge. According to AASHTO Section 2.5.2.6.2 (AASHTO, 2007), the maximum allowable deflection for bridges with and without sidewalks are $L/1000$ and $L/800$, respectively. Using the maximum allowable deflection of the bridge and its calculated stiffness, the bridge maximum allowable load capacity can be determined by Eq. 5.17.

$$P = K * \Delta \quad (5.17)$$

In order to eliminate the dynamic effect of a moving truck to achieve the static load capacity of a bridge, the dynamic load allowance or the dynamic load factor of acceleration (DLFA) should be used. The dynamic load allowance suggested in AASHTO Table 3.6.2.1-1 (AASHTO, 2007) is 1.33. On the other hand, the DLFA, which is the dynamic interaction between a moving vehicle and a bridge, can be obtained by using the acceleration data. The DLFA is the ratio of the acceleration amplitude of a bridge under a vehicle at high speed to the acceleration amplitude of the bridge under a vehicle at low speed, as shown in Eq. 5.18. Therefore, the static bridge capacity after incorporating the dynamic effect can be expressed by Eq. 5.19.

$$DLFA = \frac{\text{acceleration amplitude for a vehicle at high speed}}{\text{acceleration amplitude for a vehicle at low speed}} \geq 1.33 \quad (5.18)$$

$$\text{Bridge Capacity} = \frac{P}{DLFA} \quad (5.19)$$

The derivations of load rating equations for other ends support conditions are shown in Appendix E.

5.6 Load Rating of Ashtabula Bridge

Using equations in Section 5.3, the load rating of the Ashtabula Bridge was calculated for the three trucks (empty, half-loaded, and fully-loaded), as shown in Table 5-2. By knowing frequencies at peak amplitudes, the effective flexural rigidity of the bridge was calculated using Eq. 5.13. The bending stiffness of the Field Bridge was calculated by using Eq. 5.16. This bending stiffness was later used in Eq. 5.19 to estimate the load bearing capacity at each sensor location during each truck run. Finally, in order to estimate the load rating of the bridge for each truck, the truck speed weighted average capacity was calculated as shown in Table 5-2. Appendix F includes calculations of $EI_{\text{Effective}}$, bending stiffness, and DLFA.

Table 5-2: Ashtabula Bridge load rating for different trucks

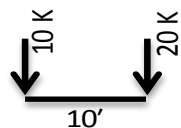
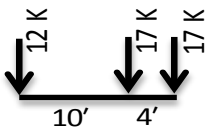
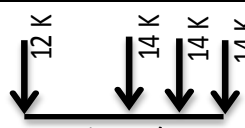
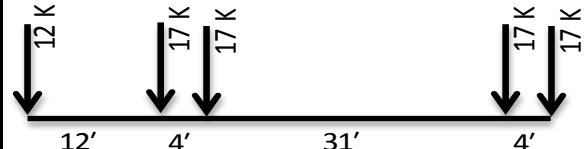
Truck weight (Ton)	Truck speed (mph)	Bridge capacity (Ton)		
		Average capacity for 8 sensors	Truck speed weighted average capacity	Rating factor
9.75	10	185.986	157.797	16.184
	15	207.878		
	20	144.358		
	25	127.224		
13.55	10	132.412	139.119	10.267
	15	154.072		
	20	141.923		
	25	130.587		
16.15	10	64.481	66.977	4.147
	15	70.680		
	20	63.142		
	25	68.822		

The load rating summary of Ashtabula Bridge provided by ODOT is shown in Table 5-3. BARS software was used to perform the load rating of the bridge. VIRTIS is new software developed and recommended by AASHTO (AASHTO, 2013) for load rating of highway bridges. Load rating factors from BARS and VIRTIS seem very close. The load rating of a bridge using BARS and VIRTIS is expressed as a rating factor for a particular vehicle. Vehicle weights and load configurations are shown in Table 5-4, which was taken from the ODOT Bridge Design Manual (ODOT BDM, 2004). The heaviest vehicle used for data collection on the Ashtabula Bridge was around 16.15 tons (Table 5-3), which is similar to the Ohio legal vehicle OH-2F1 (Table 5-4). By comparing Tables 5-2 and 5-3, it is interesting to note that the load rating factor for Ashtabula Bridge from the research using a 16-ton vehicle is 4.147 and the same by ODOT using a 15-ton OH-2F1 is 4.708 (VIRTIS) and 4.867 (BARS). The load rating factor from the research is very similar to that found by ODOT using BARS and VIRTIS. This comparison strengthens the proposed algorithms and validates the application software developed in this research.

Table 5-3: Ashtabula Bridge load rating using VIRTIS and BARS

VIRTIS Software			BARS Software		
Live load	Load rating (ton)	Rating factor	Live load	Load rating (ton)	Rating factor
OH-2F1	70.63	4.708	OH-2F1	73	4.867
OH-3F1	72.03	3.132	OH-3F1	74.4	3.234
OH-4F1	74.18	2.747	OH-4F1	76.7	2.84
OH-5C1	110.45	2.761	OH-5C1	110.5	2.762

Table 5-4: Ohio legal vehicle weights and load configurations.

OHIO LEGAL LOADS		
Load designation	Load configuration	Gross vehicle weight
2F1		15 Tons
3F1		23 Tons
4F1		27 Tons
5C1		40 Tons

5.7 Load Rating Flow Chart

This research mainly focused at developing a method and application software for load rating of PSBB bridges based on their dynamic response. The geometric inputs for the application software are based on bridge element dimensions shown in Fig. 4-9. Figures 5-6 and 5-7 show the flow chart of the load rating method, which was used to develop the load rating application software. This tool can be quickly deployed in the field to estimate the load bearing capacity of a PSBB bridge by collecting its dynamic response under trucks with known weights and speeds. The load rating output of the application software will be in terms of a rating factor (RF) for a particular vehicle. In order to find the load rating of a bridge, a particular vehicle needs to be run at least at two different speeds.

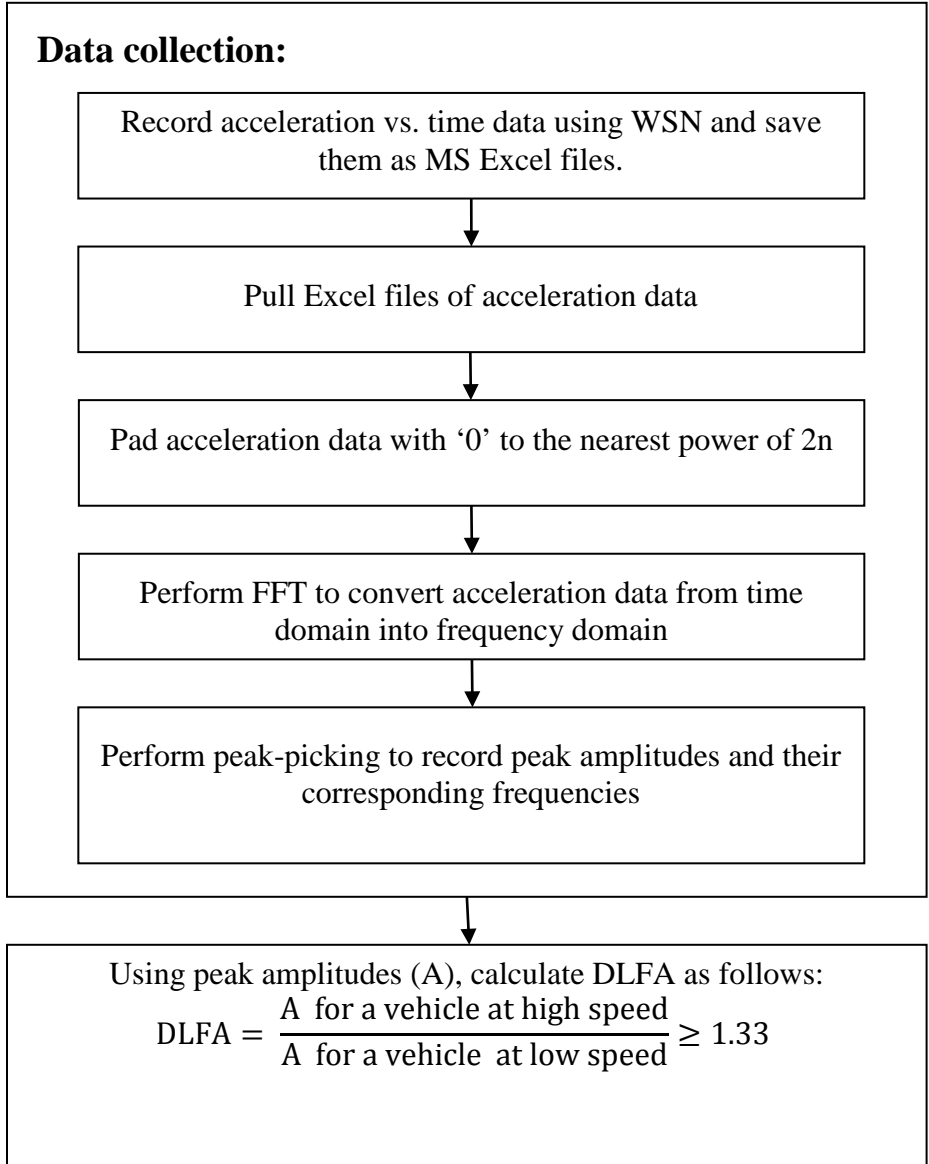


Figure 5-6: Load rating flow chart.

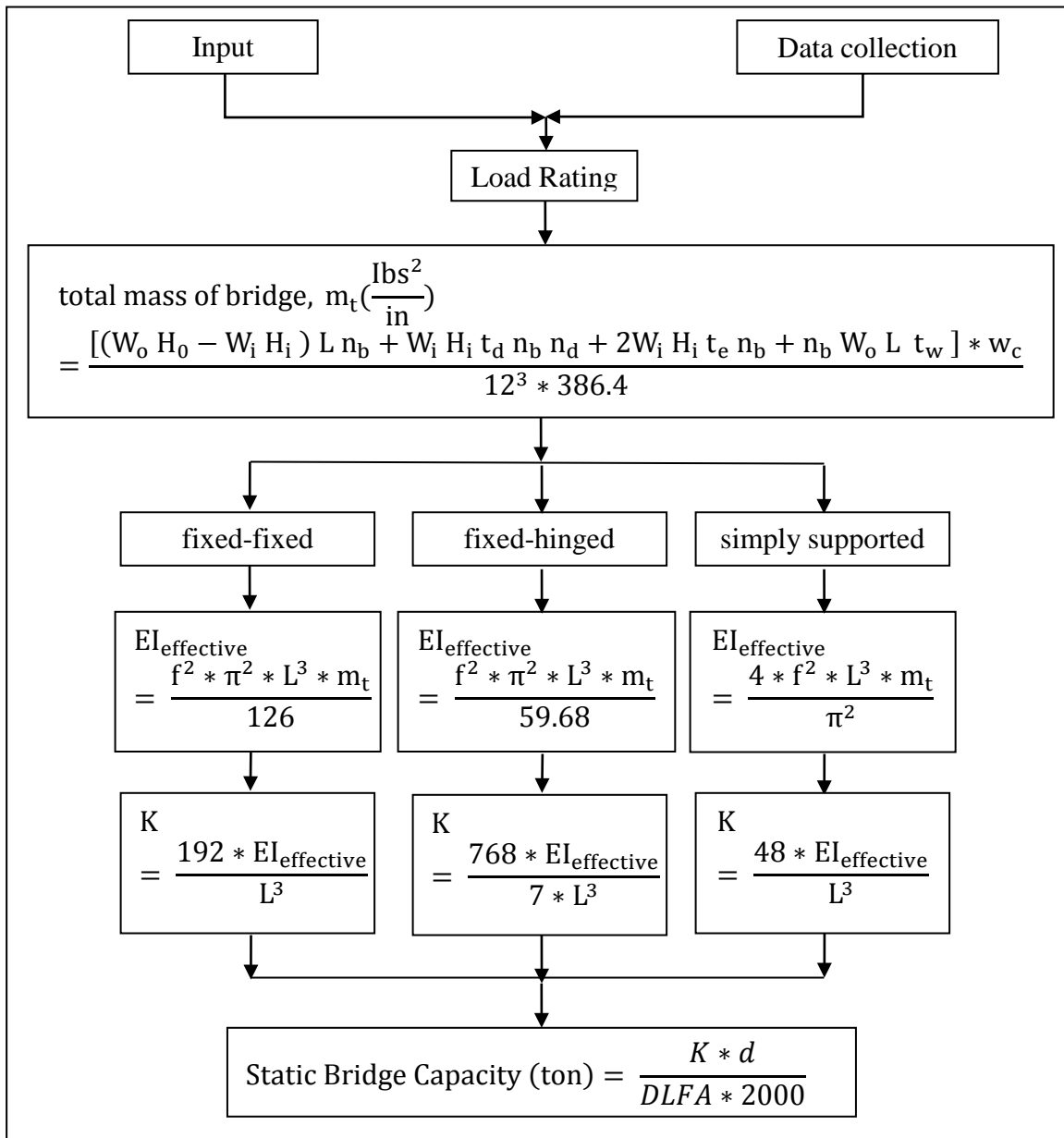


Figure 5-7: Load rating flow chart (continued).

CHAPTER 6: Field Testing and Software Validation

6.1 Application Software Validation

The application software was developed on the Microsoft's .NET4.5 framework based on flow charts for both condition assessment and load rating. Both flow charts were combined to develop a single standalone software that will be able to determine condition and load rating of a PSBB bridge from the same acceleration data. The application software requires inputs for bridge geometric, materials and support conditions, truck parameters and dynamic response of a bridge under a heavily loaded truck at two different speeds, such as 10 and 25 mph. It was developed based on the research outcomes of the Ashtabula Bridge. Figures 6.1 and 6.2 show the 'Input Parameters' and 'Bridge Assessment' tabs, respectively, from the application software called "ODOTApp". The User's Manual for the application software and instructions on preparing WSNs and laptops is attached in Appendix G.

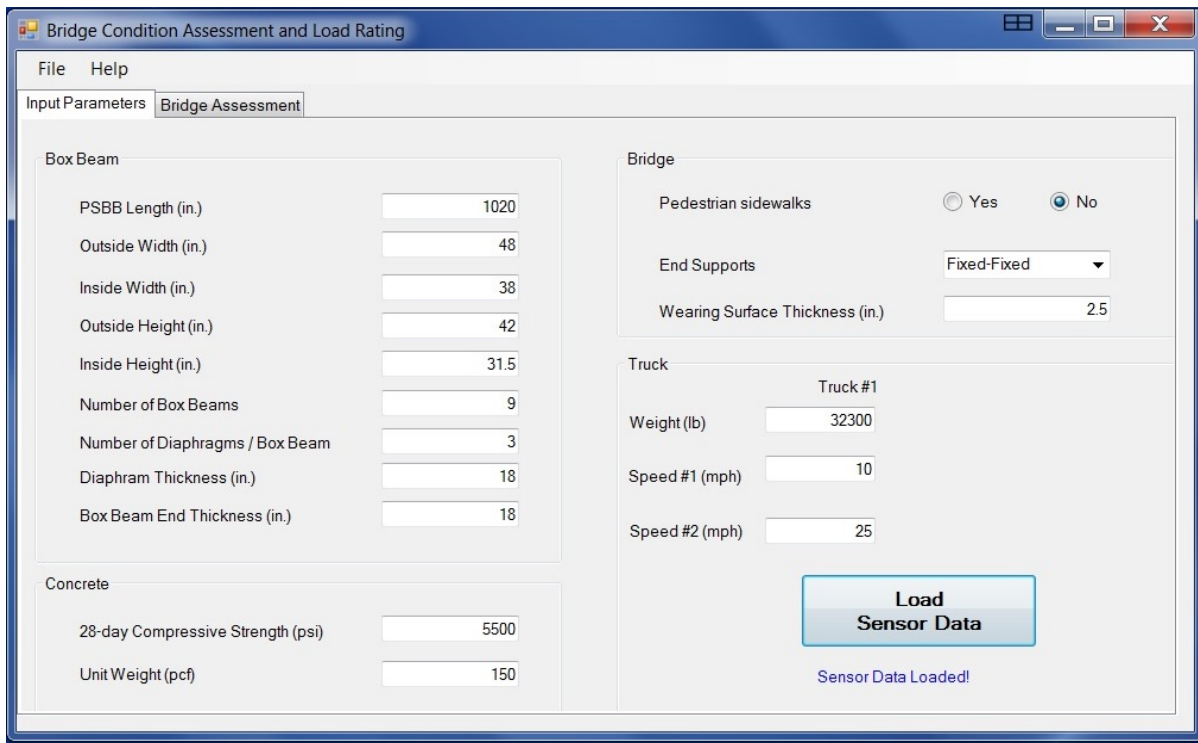


Figure 6-1: Input Parameters tab of ODOTApp with Ashtabula Bridge data.

The input parameters are self-explanatory. Usually, these data are available from the bridge design and construction plans. The 'Load Sensor Data' button requires selection of files of bridge dynamic response. The sensor data, which are acceleration data of a bridge, must be loaded before going to the 'Bridge Assessment' tab to run the analysis.

The 'Bridge Assessment' tab has two buttons, 'Start Analysis' and 'View Report', as shown in Fig. 6.2. The analysis can be started by clicking the 'Start Analysis' button. Once the analysis is complete, the analysis report can be viewed by clicking the 'View Report' button. The report will contain the tables and results of the analysis. The left box shows the bridge load rating based on the truck weight, and the right box provides the bridge condition rating based on a scale of 0-9.

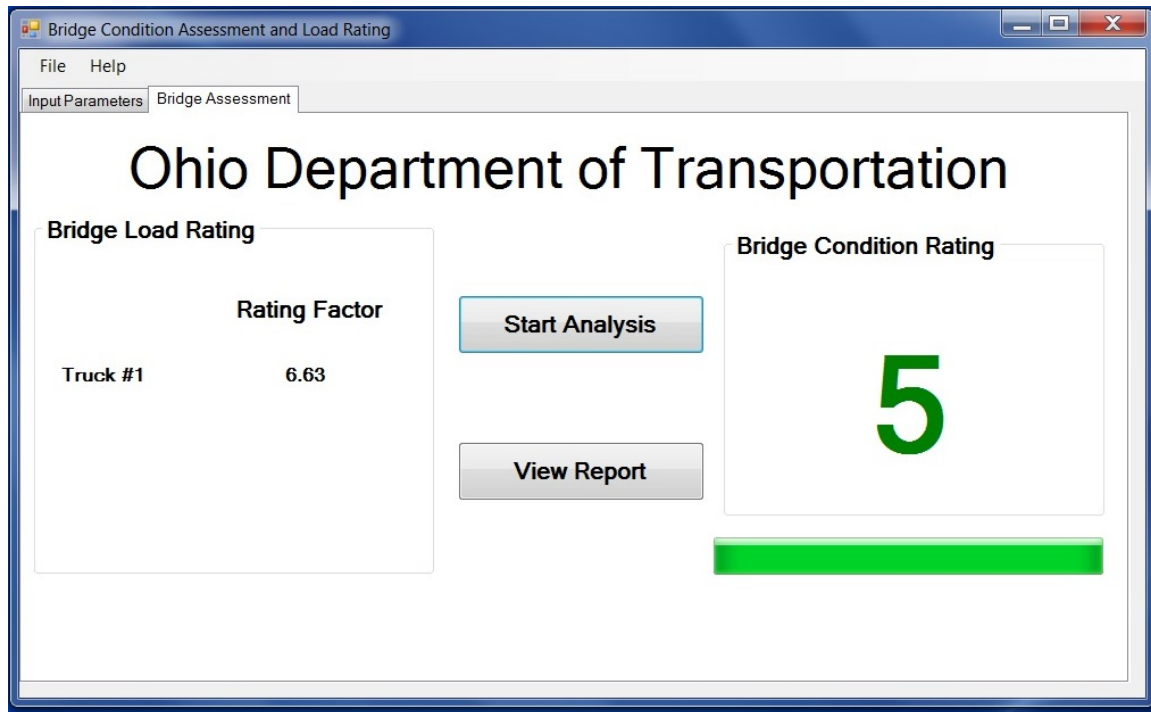


Figure 6-2: Bridge Assessment output tab of ODOTApp after analysis.

The validation of the ODOTApp application software was extremely important in order to check if the methods and algorithms proposed are reasonable in estimating the condition and load rating of a PSBB bridge. It was also important to make sure the codes and formulas used in developing the software were accurate. Therefore, the dynamic response data from the Trumbull

Bridge (TRU-45.1699 on Route 45 over Center Creek in Trumbull County, Ohio, built in 2005) under a 43,100 lb truck at 10 and 25 mph were collected. Truck dimension and weight data sheet is attached in Appendix A. After changing names of acceleration data files, the ODOTApp was run on site to estimate the load and condition rating of the bridge. Figures 6.3 and 6.4 show the input and output tabs, respectively, using dynamic response of Trumbull Bridge.

The input data were adopted from bridge design and construction plans provided by ODOT, and truck parameters were recorded on site. Once the analysis was performed, the output tab shows a load rating factor of 13.69 for a 22-ton truck (similar to a 23-ton OH-3F1 truck) and a condition rating of “8”. No load rating factor is available for this bridge from ODOT since this is a relatively new bridge and has not been load rated yet. But the condition rating of “8” from this research is comparable to ODOT’s calculated general appraisal of “7”. After on-site validation, the researchers believe that the application software is expected to produce acceptable load and condition ratings of a PSBB bridge on site, which can be performed quickly and cost-effectively.

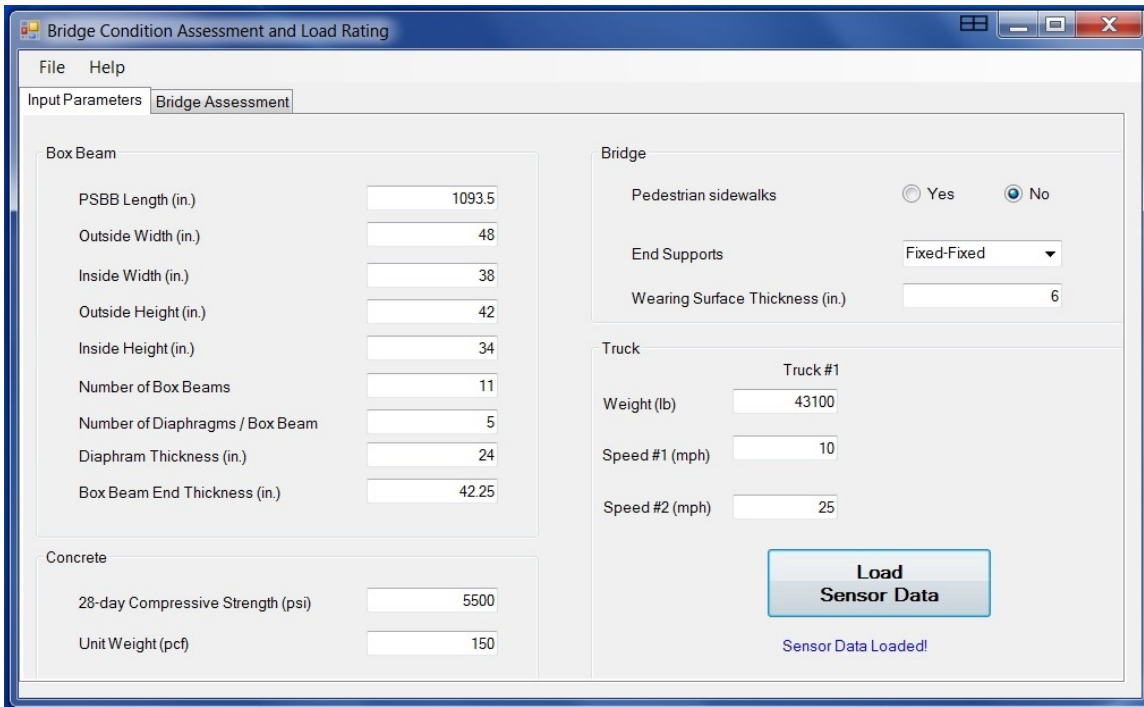


Figure 6-3: Input tab of ODOTApp with Trumbull Bridge dynamic response.

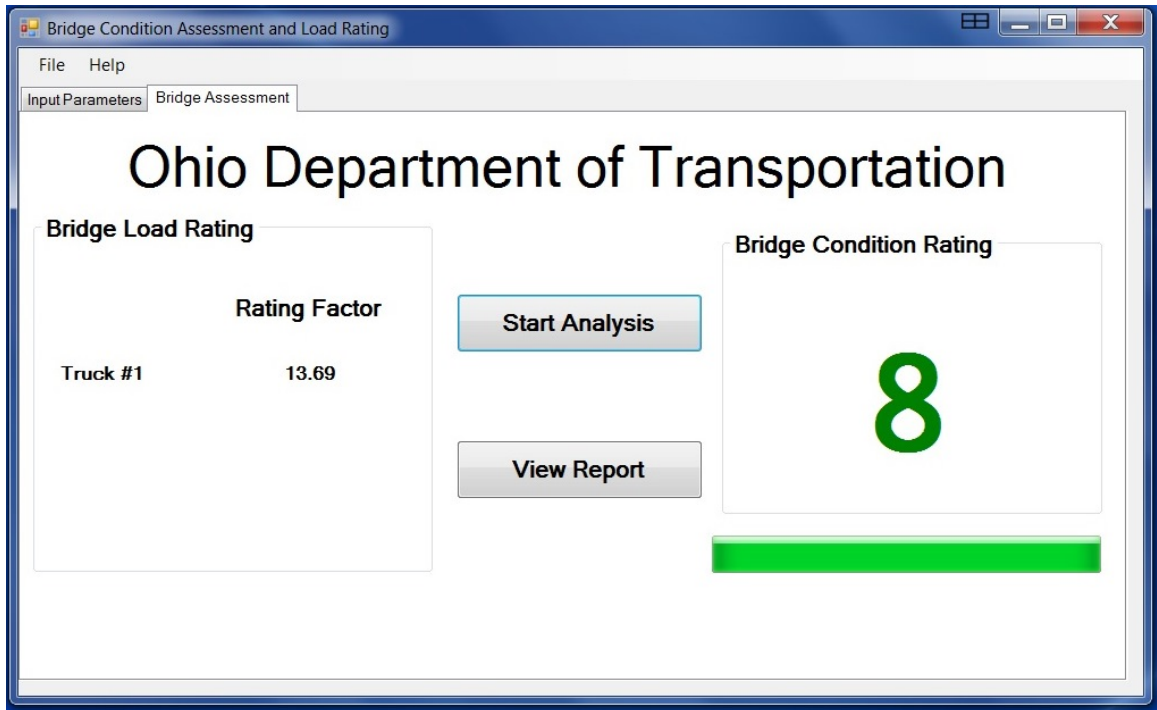


Figure 6-4: Output tab of ODOTApp with Trumbull Bridge dynamic response.

6.2 Recommendations for Implementation of Research Findings

The application software and the wireless sensor networks developed in this research can be used on any single span PSBB bridge to determine its current condition and load rating within a reasonable accuracy at a minimal cost. The entire process takes approximately half a day to get the assessment results. This application software will in no way replace the existing methods of bridge condition assessment and load rating, but may be used simultaneously to develop a database of dynamic response of single span PSBB bridges. The researchers suggest that a database of condition assessment and load rating of single span PSBB bridges be developed and incorporated into the software to help refine the algorithms as well as the application software to make them more robust and more reliable.

CHAPTER 7: Conclusions and Recommendations

7.1 Conclusions

The role of health monitoring is vital to ensure public safety by detecting structural damage and deterioration of a bridge from its dynamic response under vehicular loads. In bridge engineering, the concept of health monitoring is widely applied to assess structural integrity of bridges, and to maintain their safe and continuous operation. The method described in this study and the application software developed from the data analysis provide cost-effective solution for assessing the overall condition and load rating of single span PSBB bridges.

The concept used in this study of bridge condition assessment is based on the hypothesis that the dynamic structural response of a new bridge under vehicular loads will be quite different than that of the same bridge after 20 years due to deterioration of the bridge over time. Therefore, this difference, which estimates the amount and average rate of bridge deterioration, can be assessed by analyzing the dynamic structural response of a bridge at its newest and existing conditions.

Although the percentage of either functionally obsolete or structurally deficient bridges has been declining slowly over the last decade, a significant number of bridges are still closed to traffic or posted for load restrictions. For posting load limits, the load bearing capacity of bridges needs to be evaluated. Considering the fact that the current theoretical load rating of bridges is a very conservative approach and sometimes proposes capacity well below the actual structural capacity, this research focused at developing a state-of-the-art method and application software for condition and load rating of single-span PSBB bridges based on their dynamic response under vehicular loads collected through wireless sensor networks.

The outline of the methods used in this study can be summarized as follows:

- Collecting acceleration response of an existing PSBB bridge under vehicular loads through a system of wireless sensor networks. These data represent the condition of the Field Bridge.

- Developing a full-scale 3D bridge model using ABAQUS to represent the bridge at its newest condition (FEA Bridge), and simulating the FEA Bridge to obtain its acceleration data.
- Performing FFT to transform collected acceleration data from time domain into frequency domain for further analysis.
- Performing peak-picking method to record peak amplitudes and corresponding fundamental frequencies.
- Analyzing frequency data from the Field Bridge and FEA Bridge to assess the overall structural condition of the bridge.
- Calculating bridge bending stiffness in current condition using analysis data along with the bridge geometric parameters.
- Estimating bridge load bearing capacity using the load-displacement relationship and the calculated bending stiffness.

From the data analysis results, it was observed that the MAC values change along the length of the bridge. The values are higher values at points closer to the end support and decreases as it gets closer to the middle of the bridge. Also, it is shown that the fundamental frequency of the bridge has decreased while its amplitude has increased over its 25-year service life. The reduction in the fundamental frequency over 25 years of service is 36.9 percent, and this reduction in frequency has been assigned to the structural condition deterioration of the bridge by 3 points (from “9” to “6”).

The fundamental frequency of the FEA Bridge is also calculated using the theoretical method, and compared with the fundamental frequency found from the FEA Bridge simulation. A relationship between two these frequencies was established and incorporated in calculating the fundamental frequency in the application software.

Using the results from the FEA Bridge simulations, it has been found that the vibration frequency at the peak amplitude under vehicular loads is the first bending frequency of the bridge. Therefore, this first bending frequency of the Field Bridge was used to determine its bending stiffness and estimate the load bearing capacity. The load rating factors of Ashtabula Bridge estimated from this research were compared to those reported by ODOT using VIRTIS and BARS. The gross weight of the two-axle fully-loaded truck used for data collection is 16.15 tons (similar to 15-ton OH-2F1 truck). The load rating factor of Ashtabula Bridge for this truck

was 4.147 from the research. On the other hand, BARS and VIRTIS load rating factors of Ashtabula Bridge for OH-2F1 truck were 4.708 and 4.867, respectively, as reported by ODOT. The 16.15-ton truck used in the research and 15-ton OH-2F1 truck used by ODOT for load rating are similar in geometry and weight, and produced very close load rating factors. Therefore, the load rating method developed herein appears reliable for use in a single span PSBB bridge. The research outcome and the software will help in performing quick and cost-effective condition assessment and load rating of PSBB bridges, and may provide a better ability to plan replacements and develop load ratings.

7.2 Recommendations

This research combines bridge response and wireless sensor technology in health monitoring, and reinforces the possibility of bridge condition assessment and load rating using its dynamic response. In light of the outcome of this research, some possible areas of future work have been identified in the following areas:

- The primary focus of this research was on prestressed concrete box beam bridges. Therefore, it is suggested that future work be performed on various bridge types such as truss, steel, and long span bridges.
- The effect of structural damage on the higher frequency modes should be further investigated.
- Dynamic response of bridges can also be further investigated under the effect of multiple moving trucks.
- Condition assessment and load rating with sensors relocated on the bridge centerline should be investigated as well to find out any difference from the proposed sensor location.
- In addition, the dynamic response of bridges could be used to investigate substructure conditions of a bridge after an extreme event, such as an earthquake.
- A database of condition assessment and load rating of single span PSBB bridges needs to be developed and incorporated into the software to help refine the algorithms as well as the application software to make them more robust and more reliable.

REFERENCES

- AASHTO (2007). AASHTO LRFD Bridge Design Specifications, SI Units (4th Edition). Washington, DC.
- AASHTO (2008). "Bridging the Gap." American Association of State Highway and Transportation Officials, 444 North Capitol Street, NW Suite 249 Washington, DC 20001.
- AASHTO (2013). "AASHTOWare: Bridge Analytical Rating Software (BARS)." <<http://www.aashtoware.org/Bridge/Pages/Rating.aspx?PID=3>> (Oct. 16, 2013)
- ABAQUS. (2012). ABAQUS CAE User's Manual, Dassault Systemes Simulia Corp, Providence, Rhode Island.
- ACI (2008). "Building Code Requirements for Structural Concrete and Commentary." American Concrete Institute, 38800 Country Club Drive, Farmington Hills, MI 48331.
- ASCE (2013). "Report Card on America's Infrastructure." 1801 Alexander Bell Drive, Reston, Virginia.
- Chen, S. E., Siswobusono, P., Delatte, N., and Stephens B. J. (2002). "Feasibility Study on Dynamic Bridge Load Rating." University Transportation Center for Alabama, (UTCA).
- Chowdhury, M. R. (1999). "Rapid Beam Load Capacity Assessment Using Dynamic Measurements." Research Structural Engineering, Structures Laboratory, U.S. Army Engineering Waterways Experimental Station, Vicksburg, MS 39180-6199.
- Cooley, J. W., and Tukey, J. W. (1965). "An algorithm for the machine calculation of complex Fourier series." IBM Watson Research Center, Yorktown Heights, NY; Bell Telephone Laboratories, Murray Hill; and Princeton University, NJ.
- Doebling, S. W., Farrar C. R., Prime, M. B., and Shevitz, D. W. (1996). "Damage Identification and Health Monitoring of Structural and Mechanical Systems from Changes in their Vibration Characteristics: a Literature Review." Report No. LA-13070-MS, Los Alamos National Laboratory. Los Alamos, NM.
- Ewins, D. J. (1997). "Model Validation: Correlation for Updating." Sadhana-Academy Proceedings in Engineering Sciences, Vol. 25, Part 3, ISSN: 0256-2499, pp. 221-234.
- FHWA (2004). "NBIS Regulations", Federal Highway Administration, Rules and Regulations, Vol. 69, No. 239.

- FHWA (2004). "Status of the Nation's Highways, Bridges, and Transit: 2004 Conditions and Performance." Federal Highway Administration, <<http://www.fhwa.dot.gov/policy/2004cpr/chap3c.htm#body>> (October 26, 2013).
- FHWA (2011). "National Bridge Inventory General Condition Rating Guidance." Federal Highway Administration (FHWA), Bridge Preservation Guide, FHWA-HIF-11042.
- FHWA (2012). National Bridge Inventory. Inspection and Evaluation. Bridges by Structure Type.
- Gangone, M. V, Whelan, M. J., Janoyan, K. D., and Jha, R. (2008). "Field deployment of a dense wireless sensor network for condition assessment of a bridge superstructure." SPIE Smart Structures Symposium, San Diego, California.
- Kim, S., Pakzad, S., Culler, D., Demmel, J., Fenves, G., Glaser, S., and Turon, M. (2007). "Health Monitoring of Civil Infrastructures Using Wireless Sensor Networks." Proceedings of the 6th International Conference on Information Processing in Sensor Networks (IPSN 2007), ACM Press, Cambridge, MA, pp. 254-263.
- Lichtenstein, A. (1993). "Bridge Rating Through Non-Destructive Load Testing", Final Draft, NCHRP Report 12-28(13)A, Transportation Research Board, Washington, D.C.
- Logan, D. L. (2001). "A first Course in the Finite Element Method." 2nd Edition, PWS Publishing Company, Boston, Massachusetts.
- Lynch, J. P. (2005). "Design of a wireless active sensing unit for localized structural health monitoring", Structural Control and Health Monitoring, Wiley InterScience, 12:405-423
- Lynch, J. P., Wang, Y., Loh, K. J., Yi, J., and Yun, C. (2006). "Performance monitoring of the Geumdang Bridge using a dense network of high-resolution wireless sensors." Smart Materials and Structures, Vol. 15, pp. 1561-1575.
- Microsoft (2012). "Microsoft Visual Studio 2012." One Microsoft Way, Redmond, WA 98052-6399.
- NCHRP (2009). "NCHRP Synthesis 393." National Cooperative Highway Research Program (NCHRP), Adjacent Precast Concrete Box Beam Bridges: Connection Details.
- NSTP (2007). Transportation for Tomorrow Report of the National Surface Transportation Policy (NSTP) and Revenue Study Commission. Final report. Volume II, Chapter 4, p. 6.

- ODOT (1972). "Prestressed Concrete Bridge (48") CBP2." Ohio Department of Transportation, <www.dot.state.oh.us/Divisions/Engineering/Structures/standard/ArchivedStandardDrawings/Pages/ConcreteBeam%28prestressed%29.aspx> (October 16, 2013).
- ODOT (2010). "Manual of Bridge Inspection (MBI)." Ohio Department of Transportation, Columbus, Ohio.
- ODOT (2011). "Bridge Design Manual (BDM)." Ohio Department of Transportation, Columbus, Ohio.
- ODOT (2013). "Bridge Design Manual." Ohio Department Of Transportation, Columbus, Ohio.
- Oracle, Inc. (2013). Sun Small Programmable Object Technology (Sun SPOT) Sensors, Redwood City, California.
- Paz, M. (1985). "Structural Dynamics." Theory & Computation (Second Edition). ISBN: 0442275358 (ISBN13: 9780442275358). Published November 13th 1985 by Van Nostrand Reinhold Company, New York.
- Ren, W. and Zong, Z. (2003). "Output-only modal parameter identification of civil engineering structures." Fuzhou University, China.
- Russell, H. G. (2008). "Adjacent Precast Box Beam Bridges: Connection Details." National Cooperative Highway Research Program (NCHRP) Synthesis, 20-05/ Topic 39-10.
- Samali, B., Crews, K., Li, J., Bakoss, S., and Champion, C. (2003). "Assessing the Load Carrying Capacity of Timber Bridges using Dynamic Methods." Institute of Public Works Engineering, Sydney, NSW, Australia.
- Straser, E. G. and Kiremidjian, A. S. (1998). "A modular, wireless damage monitoring system for structures." John A. Blume Center Technical Report No. 128, Stanford University, Stanford, CA.
- Tedesco, J. W., McDougal, W. G., and Ross, C. A. (1999). "Structural Dynamics: Theory and Applications." Addison-Wesley Longman Inc., Menlo Park, CA.
- USDOT (2012). "Transportation Statistics Annual Report", Bureau of Transportation Statistics, Table 1-28: Condition of U.S. Highway Bridges.
- USDOT (2012). "Deficient Bridges by State and Highway System." <www.fhwa.dot.gov/bridge/deficient.cfm> (October 16, 2013).

APPENDICES

Appendix A

Information of trucks used on Mahoning Bridge



OHIO DEPARTMENT OF PUBLIC SAFETY
OHIO STATE HIGHWAY PATROL

Portable Scale Arrest and Weight Record

Date/Time of Violation _____ @ _____ Date/Time Vehicle Weighed 11-5-12 @ 0810
 Violation Occurred at _____ Distance Traveled _____
 Vehicle Weighed at ODOT BAILEY RD County of Arrest _____
 Citation Number _____ Court Date _____ Total Fine Including Court Costs _____
 Driver Name _____ Operator License # _____ State _____
 Carrier Name ODOT Description of Load EMPTY
 Power Unit: Make INTL Model Year 99 Color WH Style of Vehicle DUMP
 Registration: Power Unit T4827 State _____ Trailer _____ State _____

Reasonable Suspicion for Traffic Stop (check all that apply)

- Bulging Tires Visible Load Pulling Hard Slow Speed Insecure Load Vehicle Defect
 Oversize Load (5577.05) Registration Violation Other Violation _____

Axles	Axle Spacing	Scale #	Axle #	Left	Right	Axle #	Scale #	Total Weight
		<u>131</u>	Steer	<u>4,000</u>	<u>3,900</u>	Steer	<u>129</u>	<u>7,900</u>
1-2	<u>11-9</u>	<u>139</u>	2	<u>5,500</u>	<u>5,200</u>	2	<u>115</u>	<u>10,700</u>
1-3			3			3		
1-4			4			4		
1-5			5			5		
1-6			6			6		
1-7			7			7		
1-8			8			8		
1-9			9			9		
1-10			10			10		
1-11			11			11		

5577.04 (B) Maximum Gross Weight Allowed _____ lbs 5577.04 (D) Maximum Gross Weight Allowed _____ lbs

	Actual Weight In Pounds	Allowed Weight In Pounds	Number of Pounds Overweight	Issued Citation
Gross Weight	<u>18,600</u>	<u>40,000</u>		<input type="checkbox"/>
Axles 1	<u>7,900</u>	<u>20,000</u>		<input type="checkbox"/>
Axles 2	<u>10,700</u>	<u>20,000</u>		<input type="checkbox"/>
Inner-Bridge				<input type="checkbox"/>

Vehicle Length 11 Ft 9 In Vehicle Width 6 Ft 0 In Vehicle Height _____ Ft _____ In
 Arresting Officer _____ Unit _____ LLI Unit # 432 LLI Unit # _____
 Level Checked By 3022 Unit _____ All Scales Department of Agriculture Sealed Yes No
 Disposition of Vehicle: Axles shifted Vehicle off loaded Driven to closest safe haven to get legal
 Other (Explain) _____
 Check box for citations issued (check all that apply): Oversize IFTA Unsafe Permit Violation
 Other Arrest (List all) _____

OHP 0468 3/08 Page 1 of 2
(OSP-201.06)



OHIO DEPARTMENT OF PUBLIC SAFETY
OHIO STATE HIGHWAY PATROL

Portable Scale Arrest and Weight Record

Date/Time of Violation _____ @ _____ Date/Time Vehicle Weighed 11-5-12 @ OTM6
 Violation Occurred at _____ Distance Traveled _____
 Vehicle Weighed at ODOT Bailey Rd County of Arrest _____
 Citation Number _____ Court Date _____ Total Fine Including Court Costs _____
 Driver Name _____ Operator License # _____ State _____
 Carrier Name ODOT Description of Load 1/2 LOAD
 Power Unit: Make INTL Model Year 07 Color WHI Style of Vehicle Dump
 Registration: Power Unit T4577 State _____ Trailer _____ State _____

Reasonable Suspicion for Traffic Stop (check all that apply)

- Bulging Tires Visible Load Pulling Hard Slow Speed Insecure Load Vehicle Defect
 Oversize Load (5577.05) Registration Violation Other Violation _____

Axes	Axle Spacing	Scale #	Axle #	Left	Right	Axle #	Scale #	Total Weight
		<u>131</u>	Steer	<u>5,600</u>	<u>5,800</u>	Steer	<u>129</u>	<u>11,400</u>
1-2	<u>14-8</u>	<u>139</u>	2	<u>9,600</u>	<u>10,100</u>	2	<u>115</u>	<u>19,700</u>
1-3			3			3		
1-4			4			4		
1-5			5			5		
1-6			6			6		
1-7			7			7		
1-8			8			8		
1-9			9			9		
1-10			10			10		
1-11			11			11		

5577.04 (B) Maximum Gross Weight Allowed _____ lbs 5577.04 (D) Maximum Gross Weight Allowed _____ lbs

	Actual Weight in Pounds	Allowed Weight in Pounds	Number of Pounds Overweight	Issued Citation
Gross Weight	<u>31,100</u>	<u>40,000</u>		<input type="checkbox"/>
Axes 1	<u>11,400</u>	<u>20,000</u>		<input type="checkbox"/>
Axes 2	<u>19,700</u>	<u>20,000</u>		<input type="checkbox"/>
Inner-Bridge				<input type="checkbox"/>

Vehicle Length 14 Ft 8 In Vehicle Width 6 Ft 0 In Vehicle Height _____ Ft _____ In
 Arresting Officer _____ Unit _____ LLI Unit # 432 LLI Unit # _____
 Level Checked By 3022 Unit _____ All Scales Department of Agriculture Sealed Yes No
 Disposition of Vehicle: Axles shifted Vehicle off loaded Driven to closest safe haven to get legal
 Other (Explain) _____
 Check box for citations issued (check all that apply): Oversize IFTA Unsafe Permit Violation
 Other Arrest (List all) _____



OHIO DEPARTMENT OF PUBLIC SAFETY
OHIO STATE HIGHWAY PATROL

Portable Scale Arrest and Weight Record

Date/Time of Violation _____ @ _____ Date/Time Vehicle Weighed 11-5-12 @ 0834
 Violation Occurred at _____ Distance Traveled _____
 Vehicle Weighed at ODOT BAILEY RD County of Arrest _____
 Citation Number _____ Court Date _____ Total Fine Including Court Costs _____
 Driver Name _____ Operator License # _____ State _____
 Carrier Name ODOT Description of Load FULL LOAD
 Power Unit: Make INTL Model Year 03 Color WHITE Style of Vehicle Dump
 Registration: Power Unit T 4 946 State _____ Trailer _____ State _____

Reasonable Suspicion for Traffic Stop (check all that apply)

- Bulging Tires Visible Load Pulling Hard Slow Speed Insecure Load Vehicle Defect
 Oversize Load (5577.05) Registration Violation Other Violation _____

Axes	Axle Spacing	Scale #	Axle #	Left	Right	Axle #	Scale #	Total Weight
		<u>131</u>	Steer	<u>6,000</u>	<u>5,900</u>		<u>129</u>	<u>11,900</u>
1-2	<u>14-9</u>	<u>139</u>	2	<u>13,900</u>	<u>13,700</u>	2	<u>115</u>	<u>27,600</u>
1-3			3			3		
1-4			4			4		
1-5			5			5		
1-6			6			6		
1-7			7			7		
1-8			8			8		
1-9			9			9		
1-10			10			10		
1-11			11			11		

5577.04 (B) Maximum Gross Weight Allowed _____ lbs 5577.04 (D) Maximum Gross Weight Allowed _____ lbs

	Actual Weight in Pounds	Allowed Weight in Pounds	Number of Pounds Overweight	Issued Citation
Gross Weight	<u>39,500</u>	<u>40,000</u>		<input type="checkbox"/>
Axes 1	<u>11,900</u>	<u>20,000</u>		<input type="checkbox"/>
Axes 2	<u>27,600</u>	<u>20,000</u>		<input type="checkbox"/>
Inner-Bridge				<input type="checkbox"/>

Vehicle Length 14 Ft 9 In Vehicle Width 6 Ft 0 In Vehicle Height _____ Ft _____ In
 Arresting Officer _____ Unit _____ LLI Unit # 432 LLI Unit # _____

Level Checked By 3022 Unit _____ All Scales Department of Agriculture Sealed Yes No

Disposition of Vehicle: Axles shifted Vehicle off loaded Driven to closest safe haven to get legal

Other (Explain) _____

Check box for citations issued (check all that apply): Oversize IFTA Unsafe Permit Violation

Other Arrest (List all) _____

Information of trucks used on Ashtabula Bridge:



OHIO DEPARTMENT OF PUBLIC SAFETY
OHIO STATE HIGHWAY PATROL

Portable Scale Arrest and Weight Record

Date/Time of Violation _____ @ _____ Date/Time Vehicle Weighed 11-13-12 @ 0828
 Violation Occurred at _____ Distance Traveled _____
 Vehicle Weighed at ODOT 512322 County of Arrest _____
 Citation Number _____ Court Date _____ Total Fine Including Court Costs _____
 Driver Name _____ Operator License # _____ State _____
 Carrier Name ODOT Description of Load EMPTY
 Power Unit: Make INTL Model Year 06 Color WHITE Style of Vehicle DUMP
 Registration: Power Unit T4614 State OH Trailer _____ State _____

Reasonable Suspicion for Traffic Stop (check all that apply)

- Bulging Tires Visible Load Pulling Hard Slow Speed Insecure Load Vehicle Defect
 Oversize Load (5577.05) Registration Violation Other Violation _____

Axles	Axle Spacing	Scale #	Axle #	Left	Right	Axle #	Scale #	Total Weight
		<u>162</u>	Steer	<u>5,100</u>	<u>4,900</u>	Steer	<u>129</u>	<u>10,000</u>
1-2	<u>14-10</u>	<u>144</u>	2	<u>5,100</u>	<u>4,480</u>	2	<u>115</u>	<u>9,500</u>
1-3			3			3		
1-4			4			4		
1-5			5			5		
1-6			6			6		
1-7			7			7		
1-8			8			8		
1-9			9			9		
1-10			10			10		
1-11			11			11		

5577.04 (B) Maximum Gross Weight Allowed _____ lbs 5577.04 (D) Maximum Gross Weight Allowed _____ lbs

	Actual Weight in Pounds	Allowed Weight in Pounds	Number of Pounds Overweight	Issued Citation
Gross Weight	<u>19,500</u>	<u>40,000</u>		<input type="checkbox"/>
Axles 1	<u>10,000</u>	<u>20,000</u>		<input type="checkbox"/>
Axles 2	<u>9,500</u>	<u>20,000</u>		<input type="checkbox"/>
Inner-Bridge				<input type="checkbox"/>

Vehicle Length 14 Ft 10 In Vehicle Width 6 Ft 0 In Vehicle Height _____ Ft _____ In
 Arresting Officer _____ Unit _____ LLI Unit # 432 LLI Unit # _____
 Level Checked By 3022 Unit _____ All Scales Department of Agriculture Sealed Yes No
 Disposition of Vehicle: Axles shifted Vehicle off loaded Driven to closest safe haven to get legal
 Other (Explain) _____
 Check box for citations issued (check all that apply): Oversize IFTA Unsafe Permit Violation
 Other Arrest (List all) _____



OHIO DEPARTMENT OF PUBLIC SAFETY
OHIO STATE HIGHWAY PATROL

Portable Scale Arrest and Weight Record

Date/Time of Violation _____ @ _____ Date/Time Vehicle Weighed 11-13-12 @ 0824
 Violation Occurred at _____ Distance Traveled _____
 Vehicle Weighed at 0001-52322 County of Arrest _____
 Citation Number _____ Court Date _____ Total Fine Including Court Costs _____
 Driver Name _____ Operator License # _____ State _____
 Carrier Name 0001 Description of Load SALT - HALF LOAD
 Power Unit: Make INTL Model Year 05 Color WHI Style of Vehicle DAMP
 Registration: Power Unit T4947 State OH Trailer _____ State _____

Reasonable Suspicion for Traffic Stop (check all that apply)

- Bulging Tires Visible Load Pulling Hard Slow Speed Insecure Load Vehicle Defect
 Oversize Load (5577.05) Registration Violation Other Violation _____

Axles	Axle Spacing	Scale #	Axle #	Left	Right	Axle #	Scale #	Total Weight
		<u>162</u>	Steer	<u>5,500</u>	<u>5,500</u>	Steer	<u>139</u>	<u>11,000</u>
1-2	<u>14-10</u>	<u>144</u>	2	<u>7,800</u>	<u>8,300</u>	2	<u>115</u>	<u>16,100</u>
1-3			3			3		
1-4			4			4		
1-5			5			5		
1-6			6			6		
1-7			7			7		
1-8			8			8		
1-9			9			9		
1-10			10			10		
1-11			11			11		

5577.04 (B) Maximum Gross Weight Allowed _____ lbs 5577.04 (D) Maximum Gross Weight Allowed _____ lbs

	Actual Weight in Pounds	Allowed Weight in Pounds	Number of Pounds Overweight	Issued Citation
Gross Weight	<u>27,100</u>	<u>40,000</u>		<input type="checkbox"/>
Axles 1	<u>11,000</u>	<u>20,000</u>		<input type="checkbox"/>
Axles 2	<u>16,100</u>	<u>20,000</u>		<input type="checkbox"/>
Inner-Bridge				<input type="checkbox"/>

Vehicle Length 12 Ft 10 In Vehicle Width 6 Ft 0 In Vehicle Height _____ Ft _____ In
 Arresting Officer 432 Unit _____ LLI Unit # _____ LLI Unit # _____
 Level Checked By 3022 Unit _____ All Scales Department of Agriculture Sealed Yes No
 Disposition of Vehicle: Axles shifted Vehicle off loaded Driven to closest safe haven to get legal
 Other (Explain) _____
 Check box for citations issued (check all that apply): Oversize IFTA Unsafe Permit Violation
 Other Arrest (List all) _____



OHIO DEPARTMENT OF PUBLIC SAFETY
OHIO STATE HIGHWAY PATROL

Portable Scale Arrest and Weight Record

Date/Time of Violation _____ @ _____ Date/Time Vehicle Weighed 11-13-12 @ 0817
 Violation Occurred at _____ Distance Traveled _____
 Vehicle Weighed at ODOT- 51322 County of Arrest _____
 Citation Number _____ Court Date _____ Total Fine Including Court Costs _____
 Driver Name _____ Operator License # _____ State _____
 Carrier Name 912 ODOT Description of Load Full Load
 Power Unit: Make FNTL Model Year 04 Color WHITE Style of Vehicle DUMP
 Registration: Power Unit T4942 State OH Trailer _____ State _____

Reasonable Suspicion for Traffic Stop (check all that apply)

- Bulging Tires Visible Load Pulling Hard Slow Speed Insecure Load Vehicle Defect
 Oversize Load (5577.05) Registration Violation Other Violation _____

Axles	Axle Spacing	Scale #	Axle #	Left	Right	Axle #	Scale #	Total Weight
		<u>102</u>	Steer	<u>6000</u>	<u>5300</u>	Steer	<u>139</u>	<u>11,300</u>
1-2	<u>14-9</u>	<u>144</u>	2	<u>10,200</u>	<u>10,800</u>	2	<u>115</u>	<u>21,000</u>
1-3			3			3		
1-4			4			4		
1-5			5			5		
1-6			6			6		
1-7			7			7		
1-8			8			8		
1-9			9			9		
1-10			10			10		
1-11			11			11		

5577.04 (B) Maximum Gross Weight Allowed _____ lbs 5577.04 (D) Maximum Gross Weight Allowed _____ lbs

	Actual Weight in Pounds	Allowed Weight in Pounds	Number of Pounds Overweight	Issued Citation
Gross Weight	<u>32,300</u>	<u>40,000</u>		<input type="checkbox"/>
Axles 1	<u>11,300</u>	<u>20,000</u>		<input type="checkbox"/>
Axles 2	<u>21,000</u>	<u>20,000</u>		<input type="checkbox"/>
Inner-Bridge				<input type="checkbox"/>

Vehicle Length 14 Ft 9 In Vehicle Width 6 Ft 0 In Vehicle Height _____ Ft _____ In
 Arresting Officer _____ Unit _____ LLI Unit # 432 LLI Unit # _____
 Level Checked By 3022 Unit _____ All Scales Department of Agriculture Sealed Yes No
 Disposition of Vehicle: Axles shifted Vehicle off loaded Driven to closest safe haven to get legal
 Other (Explain) _____
 Check box for citations issued (check all that apply): Oversize IFTA Unsafe Permit Violation
 Other Arrest (List all) _____

Information of trucks used on Trumbull Bridge:



OHIO DEPARTMENT OF PUBLIC SAFETY
OHIO STATE HIGHWAY PATROL

Portable Scale Arrest and Weight Record

Date/Time of Violation 09-27-13 @ NA Date/Time Vehicle Weighed 09-27-13 @ 1045
 Violation Occurred at SR 45 AT SR 88 Distance Traveled - 0 -
 Vehicle Weighed at SR 45/NORTH OF SR 88 County of Arrest TRUMBULL
 Citation Number NA Court Date NA Total Fine Including Court Costs NA
 Driver Name NA Operator License # NA State NA
 Carrier Name O.D.O.T. Description of Load GRINDINGS
 Power Unit: Make INTER Model Year 2012 Color WHITE Style of Vehicle DUMP
 Registration: Power Unit T 4823 State OHIO Trailer NA State NA

Reasonable Suspicion for Traffic Stop (check all that apply)

- Bulging Tires Visible Load Pulling Hard Slow Speed Insecure Load Vehicle Defect
 Oversize Load (5577.05) Registration Violation Other Violation Y.S.U. TEST

Axles	Axle Spacing	Scale #	Axle #	Left	Right	Axle #	Scale #	Total Weight
1-2	<u>146</u>	<u>115</u>	Steer	<u>5,850</u>	<u>6,850</u>	Steer	<u>160</u>	<u>12,700</u>
1-3		<u>153</u>	2	<u>15,450</u>	<u>14,950</u>	2	<u>128</u>	<u>30,400</u>
1-4			3			3		
1-5			4			4		
1-6			5			5		
1-7			6			6		
1-8			7			7		
1-9			8			8		
1-10			9			9		
1-11			10			10		
			11			11		

5577.04 (B) Maximum Gross Weight Allowed 40,000 lbs 5577.04 (D) Maximum Gross Weight Allowed 40,000 lbs

★

	Actual Weight in Pounds	Allowed Weight in Pounds	Number of Pounds Overweight	Issued Citation
Gross Weight	<u>43,100</u>	<u>40,000</u>	<u>3,100</u>	<input type="checkbox"/>
Axles				<input type="checkbox"/>
Axles REAR	<u>30,400</u>	<u>20,000</u>	<u>10,400</u>	<input type="checkbox"/>
Inner-Bridge				<input type="checkbox"/>

Vehicle Length ___ Ft ___ In Vehicle Width ___ Ft ___ In Vehicle Height ___ Ft ___ In

Arresting Officer TR L.S. WOODWARD Unit 1673 LLI Unit # 3022 LLI Unit # _____

Level Checked By 3022 Unit _____ All Scales Department of Agriculture Sealed Yes No

Disposition of Vehicle: Axles shifted Vehicle off loaded Driven to closest safe haven to get legal

Other (Explain) _____

Check box for citations issued (check all that apply): Oversize IFTA Unsafe Permit Violation

Other Arrest (List all) _____

Appendix B

Sample acceleration data collected from Ashtabula Bridge

Ashtabula Bridge acceleration data under fully-loaded truck at 25 mph

Sensor #1		Sensor #2		Sensor #3		Sensor #4	
Time (msec)	Acceleration (g)	Time (msec)	Acceleration (g)	Time (msec)	Acceleration (g)	Time (msec)	Acceleration (g)
0	0	0	0	1	0	0	0.01563
10	-0.0156	10	-0.015625	10	0	10	0.03125
20	0	20	0	20	0.015625	20	0.01563
30	0	30	0.015625	30	0.015625	30	0.03125
40	0	40	0	40	0.015625	40	0.01563
50	0	50	0.015625	50	0	50	0.03125
60	-0.0156	60	-0.015625	60	0	60	0
70	-0.0313	70	0.015625	70	0	70	0.01563
80	0.01563	80	0.03125	80	0.015625	80	0.01563
90	0.01563	90	0.015625	90	0.015625	90	0.01563
100	-0.0156	100	0	100	0.015625	100	0.03125
110	0	110	0	110	0.03125	110	0.01563
120	0	120	0.03125	120	0.015625	120	0.03125
130	0	130	0	130	0.015625	130	0.03125
140	0	140	0	140	-0.015625	140	0
150	-0.0156	150	0	150	0.03125	150	0.01563
160	0.01563	160	0	160	0	160	0.04688
170	0	174	0.03125	174	0	170	0
180	-0.0313	180	0.015625	181	0.015625	184	0.01563
190	0	190	0	190	0.03125	190	0.03125
200	0	200	0.03125	200	0.015625	200	0
.....
.....

FEA Bridge acceleration data under fully-loaded truck at 25 mph

Sensor #1		Sensor #2		Sensor #3		Sensor #4	
Time (msec)	Acceleration (g)	Time (msec)	Acceleration (g)	Time (msec)	Acceleration (g)	Time (msec)	Acceleration (g)
0	-1	0	-0.9999986	0	-1.0000013	0	-1
0.01	-1.33941	0.01	-2.4210129	0.01	-0.6754006	0.01	-1.0626
0.02	2.863717	0.02	-4.2600088	0.02	-0.1303344	0.02	-1.53078
0.03	-1.59082	0.03	-1.734302	0.03	-0.5599596	0.03	-0.49705
0.04	-2.1777	0.04	0.11662557	0.04	-0.8557031	0.04	-1.40808
0.05	-0.18549	0.05	0.31286295	0.05	1.7007868	0.05	0.231656
0.06	-3.79851	0.06	0.68159297	0.06	-1.7314424	0.06	2.692012
0.07	-0.16237	0.07	4.49513185	0.07	0.63683184	0.07	3.990912
0.08	0.515303	0.08	3.31101443	0.08	0.44790485	0.08	0.520151
0.09	3.200698	0.09	-1.5487406	0.09	4.02153726	0.09	2.686225
0.1	-0.08493	0.1	3.44664106	0.1	-2.3583765	0.1	-0.17328
0.11	2.81004	0.11	3.70786931	0.11	1.84954973	0.11	-0.57674
0.12	-1.38704	0.12	-0.9725098	0.12	-3.6362939	0.12	0.891428
0.13	-6.83073	0.13	1.59731326	0.13	-5.3822292	0.13	-2.30483
0.14	2.013323	0.14	-4.1706794	0.14	-1.205504	0.14	2.042213
0.15	0.790555	0.15	-4.8211799	0.15	-2.5130865	0.15	-3.06275
0.16	-4.50665	0.16	1.59905775	0.16	-3.359907	0.16	-1.54987
0.17	0.29366	0.17	-3.8708992	0.17	0.5515159	0.17	-2.98925
0.18	-0.69055	0.18	-0.406506	0.18	-0.3205951	0.18	-2.59804
0.19	-1.20416	0.19	-0.9300374	0.19	-2.3111066	0.19	-2.23722
0.2	-0.80467	0.2	1.75441466	0.2	-1.432016	0.2	-1.52192
0.21	-1.68634	0.21	-2.1842887	0.21	2.04453889	0.21	-0.64741
0.22	2.181287	0.22	-0.2280089	0.22	-1.2437619	0.22	-1.43687
0.23	2.654741	0.23	1.81416245	0.23	4.66441058	0.23	2.200728
0.24	0.490813	0.24	0.29528833	0.24	1.96751328	0.24	4.455553
0.25	1.369262	0.25	-2.8512008	0.25	4.49907923	0.25	-1.25128
....
....

FEA Bridge displacement data under fully-loaded truck at 25mph

Sensor #1		Sensor #2		Sensor #3		Sensor #4	
Time (msec)	Displacement (in)	Time (msec)	Displacement (in)	Time (msec)	Displacement (in)	Time (msec)	Displacement (in)
0	0.006636	0	0.00735788	0	0.00783256	0	0.00806
0.01	-0.01416	0.01	-0.0129933	0.01	-0.0116793	0.01	-0.01103
0.02	-0.06712	0.02	-0.0737669	0.02	-0.0777293	0.02	-0.07946
0.03	-0.1432	0.03	-0.1684619	0.03	-0.1861757	0.03	-0.19506
0.04	-0.24199	0.04	-0.2833486	0.04	-0.3126599	0.04	-0.32754
0.05	-0.34997	0.05	-0.4064143	0.05	-0.4457539	0.05	-0.46548
0.06	-0.4474	0.06	-0.5249617	0.06	-0.5795764	0.06	-0.60699
0.07	-0.52924	0.07	-0.623015	0.07	-0.6897362	0.07	-0.72354
0.08	-0.58944	0.08	-0.6890547	0.08	-0.759419	0.08	-0.79489
0.09	-0.61331	0.09	-0.7178884	0.09	-0.7917923	0.09	-0.82902
0.1	-0.59945	0.1	-0.7057331	0.1	-0.7813618	0.1	-0.81955
0.11	-0.5568	0.11	-0.6520655	0.11	-0.7195573	0.11	-0.75355
0.12	-0.48532	0.12	-0.5655398	0.12	-0.6218505	0.12	-0.65009
0.13	-0.38902	0.13	-0.4566343	0.13	-0.504548	0.13	-0.52869
0.14	-0.28731	0.14	-0.3364302	0.14	-0.3712385	0.14	-0.3886
0.15	-0.19153	0.15	-0.2193872	0.15	-0.238374	0.15	-0.24757
0.16	-0.10522	0.16	-0.1207163	0.16	-0.131132	0.16	-0.13614
0.17	-0.04309	0.17	-0.0499867	0.17	-0.0548781	0.17	-0.05724
0.18	-0.01692	0.18	-0.0149067	0.18	-0.0128399	0.18	-0.01152
0.19	-0.02222	0.19	-0.0214231	0.19	-0.0198976	0.19	-0.01873
0.2	-0.05768	0.2	-0.0673195	0.2	-0.0740841	0.2	-0.07746
0.21	-0.1269	0.21	-0.1462795	0.21	-0.1598024	0.21	-0.16654
0.22	-0.21745	0.22	-0.2504207	0.22	-0.2729395	0.22	-0.28398
0.23	-0.31375	0.23	-0.3679881	0.23	-0.4061485	0.23	-0.42521
0.24	-0.41154	0.24	-0.483185	0.24	-0.5341401	0.24	-0.55995
0.25	-0.50061	0.25	-0.5839254	0.25	-0.6424348	0.25	-0.6717
....
....

Appendix C

FE Model Validation

1. Experimental Validation

The flexural rigidity of the bridge can be found from the following equation:

$$EI = \frac{f^2 * m_t * L^3}{3.5608^2}$$

For the FEA Bridge:

$$\begin{aligned} EI &= \frac{5.4464^2 * 2193.1 * 1020^3}{3.5608^2} \\ &= 5.444812 * 10^{12} \text{ lb.in}^2 \end{aligned}$$

For the Field Bridge:

$$\begin{aligned} EI^* &= \frac{3.4383^2 * 2193.1 * 1020^3}{3.5608^2} \\ &= 2.169958 * 10^{12} \text{ lb.in}^2 \end{aligned}$$

The MOE of the FEA Bridge was calculated and equal to

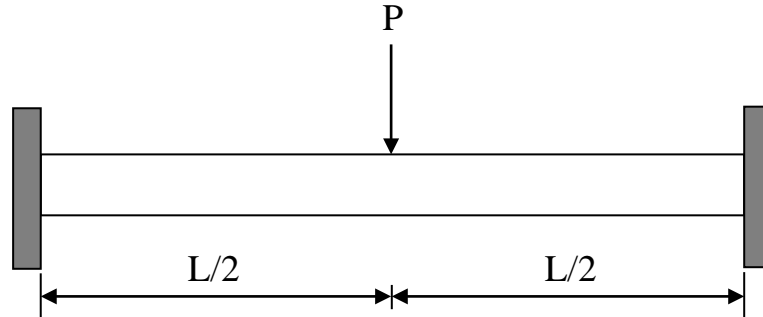
$$E_c = 4496061 \text{ psi}$$

The MOE of the Field Bridge, E_c^* , is calculated as follow:

$$\begin{aligned} E_c^* &= 4496061 * \frac{2.169958 * 10^{12}}{5.444812 * 10^{12}} \\ &= 1791846 \text{ psi} \end{aligned}$$

2. Theoretical Validation

The bridge was idealized as a beam with distributed mass and elasticity with fixed support, as shown in the following figure:



Approximate hand calculations are performed for maximum stress, maximum deflection, and total mass of the bridge as follow:

2.1 Stress Calculation

The point load, P , at the middle of the bridge is calculated by multiplying the pressure by the area as follows:

$$P = 10 * (12 * 432) = 51840 \text{ lb}$$

For a fixed beam, the maximum stress, σ , at the middle of the span is given as follow:

$$\sigma_{max} = \frac{Mc}{I}$$

Where:

σ_{max} = stress at the middle of the beam, psi.

M = bending moment at the middle of the beam, lb*in.

C = distance from the neutral axis of the box beams to the exterior fiber, in.

I = moment of inertia of the box beam, in⁴.

The maximum moment at the middle of the span is calculated as:

$$M_{max} = \frac{PL}{8}$$

$$M_{max} = \frac{51840 * 1020}{8} = 6609600 \text{ lb.in}$$

Moment of inertia of the box beams is 1776376 in^4 .

The value of C is 21 in. for a box beam of 42 in. deep.

By substituting these values into the equation of maximum stress, it produces

$$\sigma_{max} = \frac{6609600 * 21}{1776376} = 78.14 \text{ psi}$$

Maximum stress at the middle of the span from FEA was: $\sigma_{max} = 73 \text{ psi}$.

2.2 Deflection

Maximum deflection at the middle of the span is given as:

$$\Delta_{max} = \frac{PL^3}{192 EI}$$

$$\Delta_{max} = \frac{51840 * 1020^3}{192 * 4496060.776 * 1776375.563}$$

$$\Delta_{max} = 0.036 \text{ in.}$$

Maximum deflection at the middle of the span from FEA was: $\Delta_{max} = 0.05 \text{ in.}$

2.3 Total mass of the bridge

The total mass, m_t , of the bridge is calculated from its geometry and material property as follows:

$$\begin{aligned} m_t &= \frac{[(W_o H_o - W_i H_i) L n_b + W_i H_i t_d n_b n_d + 2W_i H_i t_e n_b + n_b W_o L t_w] * w_c}{12^3 * 386.4} \\ &= \frac{[(48 * 42 - 38 * 31.5) * 1020 * 9 + 9 * 48 * 1020 * 2.5] * 150}{12^3 * 386.4} \\ &\quad + \frac{[38 * 31.5 * 18 * 9 * 3 + 2 * 38 * 31.5 * 18 * 9] * 150}{12^3 * 386.4} \\ m_t &= 2154.321 \frac{\text{lb.s}^2}{\text{in}} \end{aligned}$$

The total mass of the bridge from FEA was: $m_t = 2193.1 \frac{\text{lb.s}^2}{\text{in}}$.

Appendix D

MAC Analysis

The amplitude values for Sensor 1 on both Field Bridge and FEA Bridge are:

$$N_1 = \begin{Bmatrix} 0.3938 \\ 0.3132 \\ 0.496 \\ 0.5818 \\ 0.2798 \\ 0.4349 \\ 0.6783 \\ 0.4818 \\ 0.373 \\ 0.492 \\ 0.6706 \\ 0.6876 \end{Bmatrix} \quad O_1 = \begin{Bmatrix} 0.7499 \\ 0.7403 \\ 0.6040 \\ 0.5717 \\ 0.7968 \\ 1.1896 \\ 1.0671 \\ 0.7756 \\ 0.856 \\ 1.1336 \\ 0.8125 \\ 2.1988 \end{Bmatrix}$$

$$N_1^T = \{0.3938 \quad 0.3132 \quad 0.4960 \quad 0.5818 \quad 0.2798 \quad 0.4349 \quad \dots \dots \dots 0.6876 \}$$

$$O_1^T = \{0.7499 \quad 0.7403 \quad 0.6040 \quad 0.5717 \quad 0.7968 \quad 1.1896 \quad \dots \dots \dots 2.1988 \}$$

The MAC value for Sensor 1 is calculated as follow:

$$MAC_1 = \frac{(N_1^T \cdot O_1^T)^2}{(N_1^T \cdot N_1) * (O_1^T \cdot O_1)}$$

$$MAC_1 = 0.866$$

The amplitude values for Sensor 4 on both Field Bridge and FEA Bridge are:

$$N_4 = \begin{Bmatrix} 0.4645 \\ 0.3591 \\ 0.6699 \\ 0.7699 \\ 0.3833 \\ 0.3730 \\ 0.7517 \\ 0.8603 \\ 0.3697 \\ 0.3349 \\ 0.5884 \\ 0.9250 \end{Bmatrix} \quad O_4 = \begin{Bmatrix} 0.7739 \\ 0.9640 \\ 0.7939 \\ 0.7475 \\ 1.0212 \\ 1.4836 \\ 1.6190 \\ 0.6671 \\ 0.9099 \\ 1.3405 \\ 1.0386 \\ 2.2605 \end{Bmatrix}$$

$$N_4^T = \{0.4645 \ 0.3591 \ 0.6699 \ 0.7699 \ 0.3833 \ 0.3730 \ \dots \dots \dots \ 0.9250 \}$$

$$O_4^T = \{0.7739 \ 0.9640 \ 0.7939 \ 0.7475 \ 1.0212 \ 1.4836 \ \dots \dots \dots \ 2.2605 \}$$

The MAC value for Sensor 4 is calculated as follow:

$$MAC_4 = \frac{(N_4^T \cdot O_4^T)^2}{(N_4^T \cdot N_4) * (O_4^T \cdot O_4)}$$

$$MAC_4 = 0.817$$

Reduction in fundamental frequency of Ashtabula Bridge between its newest and current conditions

The average fundamental frequency of the FEA Bridge = 5.4464 Hz.

The average fundamental frequency of the Field Bridge = 3.4383 Hz.

$$\begin{aligned} \text{Reduction in fundamental frequency of the bridge, } \Delta f &= \frac{5.4464 - 3.4383}{5.4464} * 100 \\ &= 36.9\% \end{aligned}$$

Theoretical fundamental frequency of FEA Bridge

The fundamental frequency of the bridge at its newest condition can be found from the following equation:

$$f = 3.5608 * \sqrt{\frac{EI}{m_t L^3}}$$

Total mass of the bridge, $m_t = 2193.1 \frac{lb.s^2}{in}$

The length of the PSBB, $L = 1020 in$.

The modulus of elasticity, E_c , for concrete is given by the following equation:

$$E_c = 33 w_c^{1.5} \sqrt{f'_c}$$
$$E_c = 33 * 150^{1.5} * \sqrt{5500} = 4496061 psi$$

The moment of Inertia, I , of the box beams was found as below:

$$I = \left(\frac{W_o H_o^3}{12} - \frac{W_i H_i^3}{12} \right) * n_b$$
$$I = \left(\frac{48 * 42^3}{12} - \frac{38 * 31.5^3}{12} \right) * 9$$
$$= 1776376 in^4$$

Now, the fundamental frequency of the bridge can be calculated as follow:

$$f = 3.5608 * \sqrt{\frac{4496061 * 1776376}{2193.1 * 1020^3}} = 6.5963 Hz$$

Difference in fundamental frequency of the bridge at its newest condition between FEA and theory

The fundamental frequency of the bridge at its newest condition from FEA is 5.4464 Hz.

The fundamental frequency of the bridge at its newest condition from theory is 6.5963 Hz.

The difference between the fundamental frequencies of the bridge found by FEA and Theory, is calculated as follow:

$$\frac{6.5963 - 5.4464}{6.5963} * 100 = 17.4\%$$

Appendix E

Generalized Single Degree of Freedom Systems

To idealize a single span bridge as generalized SDOF system, it is necessary to assume a displacement configuration or shape function $\varphi(x)$ that satisfies the beam kinematic and natural boundary conditions. The shape function derivation and equations for estimating the load rating of a single span bridge with different boundary conditions is shown herein.

1- Single span bridges with fixed supports.



$$\text{Vertical Displacement } Y(x, t) = \varphi(x) * \sin wt$$

Kinematic boundary conditions:

$$Y(0, t) = 0, \text{ and } Y(L, t) = 0$$

Natural boundary conditions:

$$Y'(0, t) = 0, \text{ and } Y'(L, t) = 0$$

$$Y(0, t) = 0, \text{ then } \varphi(0) * \sin wt = 0$$

$$\varphi(0) = 0$$

$$Y(L, t) = 0, \text{ then } \varphi(L) * \sin wt = 0$$

$$\varphi(L) = 0$$

$$Y'(0, t) = 0, \text{ then } \varphi'(0) * \sin wt = 0$$

$$\varphi'(0) = 0$$

$$Y'(L, t) = 0, \text{ then } \varphi'(L) * \sin wt = 0$$

$$\varphi'(L) = 0$$

$$\varphi(x) = a + bx + cx^2 + dx^3 + ex^4$$

$$\varphi'(x) = b + 2cx + 3dx^2 + 4ex^3$$

$$\varphi(0) = 0, \text{ then } a = 0$$

$$\varphi'(0) = 0, \text{ then } b = 0$$

$$\varphi'(0) = 0, \text{ then } cL^2 + dL^3 + eL^4 = 0$$

$$\varphi'(L) = 0, \text{ then } 2cL + 3dL^2 + 4eL^3 = 0$$

$$2c + 3dL = 4eL^2 = 0$$

$$- * (2c + 2dL + 2eL^2 = 0)$$

$$dL + 2eL^2 = 0$$

$$\text{then } d = -2eL, \quad \text{and } c = eL^2$$

$$\varphi(x) = eL^2x^2 - 2eLx^3 + ex^4$$

$$\varphi(x) = eL^4 \left\{ \left(\frac{x}{L}\right)^2 - 2 \left(\frac{x}{L}\right)^3 + \left(\frac{x}{L}\right)^4 \right\}$$

$$\varphi(x) = y_0 \left(\frac{x}{L}\right)^2 \left(1 - \frac{x}{L}\right)^2 \text{ shape function for fixed - fixed beam}$$

$$M_e = \int_0^L m \{\varphi(x)\}^2 dx$$

$$K_e = \int_0^L EI \{\varphi''(x)\}^2 dx$$

$$\{\varphi(x)\}^2 = y_0^2 \left\{ \left(\frac{x}{L}\right)^4 - 4 \left(\frac{x}{L}\right)^5 + 6 \left(\frac{x}{L}\right)^6 - 4 \left(\frac{x}{L}\right)^7 + \left(\frac{x}{L}\right)^8 \right\}$$

$$\varphi''(x) = y_0 \left\{ 2 \left(\frac{1}{L^2}\right) - 12 \left(\frac{x}{L^3}\right) + 12 \left(\frac{x^2}{L^4}\right) \right\}$$

$$\{\varphi''(x)\}^2 = y_0^2 \left\{ 192 \left(\frac{x^2}{L^6}\right) - 288 \left(\frac{x^3}{L^7}\right) - 48 \left(\frac{x}{L^5}\right) + 4 \left(\frac{1}{L^4}\right) + 144 \left(\frac{x^4}{L^8}\right) \right\}$$

$$M_e = \int_0^L m y_0^2 \left\{ \left(\frac{x}{L}\right)^4 - 4 \left(\frac{x}{L}\right)^5 + 6 \left(\frac{x}{L}\right)^6 - 4 \left(\frac{x}{L}\right)^7 + \left(\frac{x}{L}\right)^8 \right\} dx$$

$$M_e = m y_0^2 \left\{ \frac{L^5}{5 L^4} - \frac{4 L^6}{6 L^5} + \frac{6 L^7}{7 L^6} - \frac{4 L^8}{8 L^7} + \frac{L^9}{9 L^8} \right\}$$

$$M_e = \frac{y_0^2 * m * L}{630} = \frac{y_0^2 * m_t}{630} =$$

$$K_e = \int_0^L EI y_0^2 \left\{ 192 \left(\frac{x^2}{L^6}\right) - 288 \left(\frac{x^3}{L^7}\right) - 48 \left(\frac{x}{L^5}\right) + 4 \left(\frac{1}{L^4}\right) + 144 \left(\frac{x^4}{L^8}\right) \right\} dx$$

$$K_e = EI y_0^2 \left\{ \frac{192 L^3}{3 L^6} - \frac{288 L^4}{4 L^7} - \frac{48 L^2}{2 L^5} + \frac{4 L}{L^4} + \frac{144 L^5}{5 L^8} \right\}$$

$$K_e = \frac{4 * EI * y_0^2}{5 * L^3}$$

$$F = \frac{1}{2\pi} \sqrt{\frac{K_e}{M_e}}$$

$$F = \frac{1}{2\pi} \sqrt{\frac{\frac{4 EI y_0^2}{5 L^3}}{\frac{y_0^2 m_t}{630}}}$$

$$\text{Effective flexural rigidity, } EI_{\text{Effective}} = \frac{F^2 * \pi^2 * L^3 * m_t}{126}$$

$$\text{Beam stiffness, } K = \frac{192 * EI_{\text{Effective}}}{L^3}$$

$$P = K * \text{Deflection limit}$$

$$DLFA = \frac{\text{acceleration amplitude for a vehicle at high speed}}{\text{acceleration amplitude for a vehicle at low speed}} \geq 1.33$$

$$\text{Bridge Capacity} = \frac{P}{DLFA}$$

2- Single span bridges with fixed-hinged supports.



$$\text{Vertical displacement } Y(x, t) = \varphi(x) * \sin wt$$

Kinematic boundary conditions:

$$Y(0, t) = 0, \text{ and } Y(L, t) = 0$$

Natural boundary conditions:

$$Y''(0, t) = 0, \text{ and } Y'(L, t) = 0$$

$$Y(0, t) = 0, \text{ then } \varphi(0) * \sin wt = 0$$

$$\varphi(0) = 0$$

$$Y(L, t) = 0, \text{ then } \varphi(L) * \sin wt = 0$$

$$\varphi(L) = 0$$

$$Y''(0, t) = 0, \text{ then } \varphi''(0) * \sin wt = 0$$

$$\varphi''(0) = 0$$

$$Y'(L, t) = 0, \text{ then } \varphi'(L) * \sin wt = 0$$

$$\varphi'(L) = 0$$

$$\varphi(x) = a + bx + cx^2 + dx^3 + ex^4$$

$$\varphi'(x) = b + 2cx + 3dx^2 + 4ex^3$$

$$\varphi''(x) = 2c + 6dx + 12ex^2$$

$$\varphi(0) = 0, \text{ then } a = 0$$

$$\varphi''(0) = 0, \text{ then } c = 0$$

$$\varphi(L) = 0, \text{ then } bL + dL^3 + eL^4 = 0$$

$$\varphi'(L) = 0, \text{ then } b + 3dL^2 + 4eL^3 = 0$$

$$b + 3dL^2 + 4eL^3 = 0$$

$$\frac{-b - dL^2 - eL^3}{2dL^2 + 3eL^3} = 0$$

$$2dL^2 + 3eL^3 = 0$$

$$\text{then } d = -\frac{3eL}{2}, \text{ and } b = \frac{eL^3}{2}$$

$$\varphi(x) = \frac{eL^3}{2}x - \frac{3eL}{2}x^3 + ex^4$$

$$\varphi(x) = \frac{eL^4}{2} \left\{ \left(\frac{x}{L}\right) - 3\left(\frac{x}{L}\right)^3 + 2\left(\frac{x}{L}\right)^4 \right\}$$

$$\varphi(x) = y_0 \left\{ \left(\frac{x}{L}\right) - 3\left(\frac{x}{L}\right)^3 + 2\left(\frac{x}{L}\right)^4 \right\} \text{ shape function for fixed - hinged beam}$$

$$\{\varphi(x)\}^2 = y_0^2 \left\{ \left(\frac{x}{L}\right)^2 - 6\left(\frac{x}{L}\right)^4 + 4\left(\frac{x}{L}\right)^5 + 9\left(\frac{x}{L}\right)^6 - 12\left(\frac{x}{L}\right)^7 + 4\left(\frac{x}{L}\right)^8 \right\}$$

$$\varphi''(x) = y_0 \left\{ -18\left(\frac{x}{L^3}\right) + 24\left(\frac{x^2}{L^4}\right) \right\}$$

$$\{\varphi''(x)\}^2 = y_0^2 \left\{ 324\left(\frac{x^2}{L^6}\right) - 468\left(\frac{x^3}{L^7}\right) + 576\left(\frac{x^4}{L^8}\right) \right\}$$

$$M_e = \int_0^L m \{\varphi(x)\}^2 dx$$

$$K_e = \int_0^L EI \{\varphi''(x)\}^2 dx$$

$$M_e = \int_0^L m y_0^2 \left\{ \left(\frac{x}{L}\right)^2 - 6\left(\frac{x}{L}\right)^4 + 4\left(\frac{x}{L}\right)^5 + 9\left(\frac{x}{L}\right)^6 - 12\left(\frac{x}{L}\right)^7 + 4\left(\frac{x}{L}\right)^8 \right\} dx$$

$$M_e = m y_0^2 \left\{ \frac{L^3}{3 L^2} - \frac{6 L^5}{5 L^4} + \frac{4 L^6}{6 L^5} + \frac{9 L^7}{7 L^6} - \frac{12 L^8}{8 L^7} + \frac{4 L^9}{9 L^8} \right\}$$

$$M_e = \frac{y_0^2 * m * L}{33.15789474} = \frac{y_0^2 * m_t}{33.15789474} =$$

$$K_e = \int_0^L EI y_0^2 \left\{ 324 \left(\frac{x^2}{L^6} \right) - 468 \left(\frac{x^3}{L^7} \right) + 576 \left(\frac{x^4}{L^8} \right) \right\} dx$$

$$K_e = EI y_0^2 \left\{ \frac{324 L^3}{3 L^6} - \frac{468 L^4}{4 L^7} + \frac{576 L^5}{5 L^8} \right\}$$

$$K_e = \frac{7.2 * EI * y_0^2}{L^3}$$

$$F = \frac{1}{2\pi} \sqrt{\frac{K_e}{M_e}}$$

$$F = \frac{1}{2\pi} \sqrt{\frac{\frac{7.2 EI y_0^2}{L^3}}{\frac{y_0^2 m_t}{33.15789474}}}$$

$$\text{Effective flexural rigidity, } EI_{\text{Effective}} = \frac{F^2 * \pi^2 * L^3 * m_t}{59.6842}$$

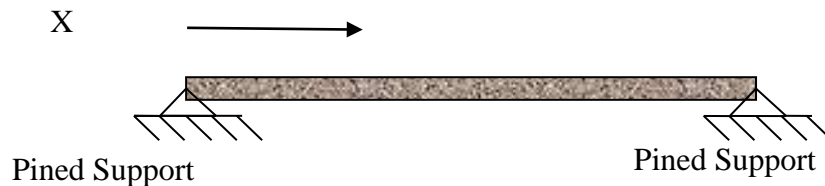
$$\text{Beam stiffness, } K = \frac{768 * EI_{\text{Effective}}}{7 * L^3}$$

$$P = K * \text{Deflection limit}$$

$$DLFA = \frac{\text{acceleration amplitude for a vehicle at high speed}}{\text{acceleration amplitude for a vehicle at low speed}} \geq 1.33$$

$$\text{Bridge Capacity} = \frac{P}{DLFA}$$

3- Single span bridges with simply supported boundary conditions.



$$\text{Vertical Displacement } Y(x, t) = \varphi(x) * \sin wt$$

Kinematic Boundary Conditions:

$$Y(0, t) = 0, \text{ and } Y(L, t) = 0$$

Natural Boundary Conditions:

$$Y''(0, t) = 0, \text{ and } Y''(L, t) = 0$$

$$Y(0, t) = 0, \text{ then } \varphi(0) * \sin wt = 0$$

$$\varphi(0) = 0$$

$$Y(L, t) = 0, \text{ then } \varphi(L) * \sin wt = 0$$

$$\varphi(L) = 0$$

$$Y''(0, t) = 0, \text{ then } \varphi''(0) * \sin wt = 0$$

$$\varphi''(0) = 0$$

$$Y''(L, t) = 0, \text{ then } \varphi''(L) * \sin wt = 0$$

$$\varphi''(L) = 0$$

$$\text{Shape Function } \varphi(x) = y_0 \sin \frac{n\pi x}{L}$$

$$\varphi'(x) = \frac{\pi}{L} y_0 \cos \frac{n\pi x}{L}$$

$$\varphi''(x) = -\frac{\pi^2}{L^2} y_0 \sin \frac{n\pi x}{L}$$

$$\{\varphi(x)\}^2 = y_0^2 \sin^2 \frac{n\pi x}{L}$$

$$\{\varphi''(x)\}^2 = \frac{\pi^4}{L^4} y_0^2 \sin^2 \frac{n\pi x}{L}$$

$$M_e = \int_0^L M \{\varphi(x)\}^2 dx$$

$$K_e = \int_0^L EI \{\varphi''(x)\}^2 dx$$

$$M_e = \int_0^L m y_0^2 \sin^2 \frac{n\pi x}{L} dx$$

$$M_e = m y_0^2 \int_0^L \sin^2 \frac{n\pi x}{L} dx$$

$$M_e = \frac{m * L * y_0^2}{2} = \frac{m_t * y_0^2}{2}$$

$$K_e = \int_0^L EI \frac{\pi^4}{L^4} y_0^2 \sin^2 \frac{n\pi x}{L} dx$$

$$K_e = EI \frac{\pi^4}{L^4} y_0^2 \int_0^L \sin^2 \frac{n\pi x}{L} dx$$

$$K_e = \frac{\pi^4 * EI * y_0^2}{2 * L^3}$$

$$F = \frac{1}{2\pi} \sqrt{\frac{K_e}{M_e}}$$

$$F = \frac{1}{2\pi} \sqrt{\frac{\frac{\pi^4 EI y_0^2}{2 L^3}}{\frac{m_t * y_0^2}{2}}}$$

$$\text{Effective Flexural Rigidity } EI_{\text{Effective}} = \frac{4 * F^2 * L^3 * m_t}{\pi^2}$$

$$\text{Beam Stiffness } K = \frac{48 * EI_{\text{Effective}}}{L^3}$$

$$P = K * \text{Delection Limit}$$

$$DLFA = \frac{\text{acceleration amplitude for a vehicle at high speed}}{\text{acceleration amplitude for a vehicle at low speed}}$$

$$\text{Bridge Capacity} = \frac{P}{DLFA}$$

Appendix F

Collected data and load rating calculations of Ashtabula Bridge

Effective flexural rigidity of Ashtabula Bridge

Truck	Speed (mph)	Sensors			
		1	2	3	4
Empty Truck	10	2.154E+12	2.026E+12	2.154E+12	2.856E+12
	15	2.423E+12	2.564E+12	2.287E+12	2.287E+12
	20	1.294E+12	2.212E+12	2.344E+12	1.196E+12
	25	2.344E+12	1.294E+12	1.5E+12	2.344E+12
Half-loaded Truck	10	2.026E+12	1.236E+12	2.154E+12	2.154E+12
	15	2.212E+12	2.344E+12	2.344E+12	2.344E+12
	20	2.154E+12	2.154E+12	2.154E+12	2.154E+12
	25	1.901E+12	1.901E+12	2.564E+12	1.78E+12
Fully-loaded Truck	10	2.154E+12	1.442E+12	2.423E+12	2.154E+12
	15	2.212E+12	2.212E+12	2.212E+12	2.212E+12
	20	2.154E+12	2.154E+12	1.901E+12	2.026E+12
	25	2.154E+12	2.154E+12	2.154E+12	2.154E+12
Truck	Speed (mph)	Sensors			
		5	6	7	8
Empty Truck	10	2.287E+12	2.287E+12	2.287E+12	1.442E+12
	15	2.423E+12	2.423E+12	3.009E+12	2.287E+12
	20	1.722E+12	1.839E+12	1.294E+12	1.839E+12
	25	7.655E+11	1.294E+12	1.196E+12	1.294E+12
Half-loaded Truck	10	2.154E+12	2.154E+12	2.154E+12	2.154E+12
	15	2.344E+12	2.48E+12	2.344E+12	2.344E+12
	20	2.154E+12	2.154E+12	2.154E+12	2.154E+12
	25	1.901E+12	1.901E+12	2.154E+12	2.026E+12
Fully-loaded Truck	10	1.337E+12	1.78E+12	2.154E+12	2.423E+12
	15	2.212E+12	2.212E+12	2.212E+12	2.212E+12
	20	1.551E+12	2.026E+12	1.78E+12	2.154E+12
	25	2.154E+12	2.154E+12	2.154E+12	2.154E+12

Effective stiffness of Ashtabula Bridge

Truck	Speed (mph)	Sensors			
		1	2	3	4
Empty Truck	10	2.154E+12	2.026E+12	2.154E+12	2.856E+12
	15	2.423E+12	2.564E+12	2.287E+12	2.287E+12
	20	1.294E+12	2.212E+12	2.344E+12	1.196E+12
	25	2.344E+12	1.294E+12	1.5E+12	2.344E+12
Half-loaded Truck	10	2.026E+12	1.236E+12	2.154E+12	2.154E+12
	15	2.212E+12	2.344E+12	2.344E+12	2.344E+12
	20	2.154E+12	2.154E+12	2.154E+12	2.154E+12
	25	1.901E+12	1.901E+12	2.564E+12	1.78E+12
Fully-loaded Truck	10	2.154E+12	1.442E+12	2.423E+12	2.154E+12
	15	2.212E+12	2.212E+12	2.212E+12	2.212E+12
	20	2.154E+12	2.154E+12	1.901E+12	2.026E+12
	25	2.154E+12	2.154E+12	2.154E+12	2.154E+12
Truck	Speed (mph)	Sensors			
		5	6	7	8
Empty Truck	10	2.287E+12	2.287E+12	2.287E+12	1.442E+12
	15	2.423E+12	2.423E+12	3.009E+12	2.287E+12
	20	1.722E+12	1.839E+12	1.294E+12	1.839E+12
	25	7.655E+11	1.294E+12	1.196E+12	1.294E+12
Half-loaded Truck	10	2.154E+12	2.154E+12	2.154E+12	2.154E+12
	15	2.344E+12	2.48E+12	2.344E+12	2.344E+12
	20	2.154E+12	2.154E+12	2.154E+12	2.154E+12
	25	1.901E+12	1.901E+12	2.154E+12	2.026E+12
Fully-loaded Truck	10	1.337E+12	1.78E+12	2.154E+12	2.423E+12
	15	2.212E+12	2.212E+12	2.212E+12	2.212E+12
	20	1.551E+12	2.026E+12	1.78E+12	2.154E+12
	25	2.154E+12	2.154E+12	2.154E+12	2.154E+12

Dynamic load factor of acceleration (DLFA)

Truck	Sensors			
	1	2	3	4
Empty Truck	1.33	1.3432161	1.33	1.33
Half-loaded Truck	1.33	1.6302834	2.4381396	1.6579661
Fully-loaded Truck	3.0678407	4.4716457	3.9922631	2.7970285
Truck	Sensors			
	5	6	7	8
Empty Truck	1.33	1.33	1.33	1.7022613
Half-loaded Truck	1.33	1.8731069	2.183615	2.2350217
Fully-loaded Truck	4.1414451	4.177086	3.459431	3.4670745

Load bearing capacity of Ashtabula Bridge

Truck	Speed (mph)	Sensors			
		1	2	3	4
Empty Truck	10	186.81116	173.92899	186.81116	247.70503
	15	210.13727	220.13328	198.30833	198.30833
	20	112.18977	189.96769	203.31162	103.73042
	25	203.31162	111.08592	130.12125	203.31162
Half-loaded Truck	10	175.65731	87.469089	101.90509	149.85762
	15	191.85538	165.86346	110.90606	163.09408
	20	186.81116	152.40224	101.90509	149.85762
	25	164.85696	134.49181	121.27548	123.84927
Fully-loaded Truck	10	80.988185	37.195186	70.006052	88.829572
	15	83.175001	57.063477	63.915541	91.228119
	20	80.988185	55.563178	54.921171	83.525861
	25	80.988185	55.563178	62.235089	88.829572
Truck	Speed (mph)	Sensors			
		5	6	7	8
Empty Truck	10	198.30833	198.30833	198.30833	97.707497
	15	210.13727	210.13727	260.91807	154.941
	20	149.3718	159.48987	112.18977	124.61161
	25	66.387468	112.18977	103.73042	87.655397
Half-loaded Truck	10	186.81116	132.64531	113.78326	111.16619
	15	203.31162	152.72357	123.83339	120.98516
	20	186.81116	132.64531	113.78326	111.16619
	25	164.85696	117.05673	113.78326	104.52884
Fully-loaded Truck	10	37.240087	49.158167	71.820727	80.61049
	15	61.613192	61.087478	73.760007	73.597395
	20	43.191737	55.929951	59.355973	71.662391
	25	59.993274	59.481382	71.820727	71.662391

Appendix G

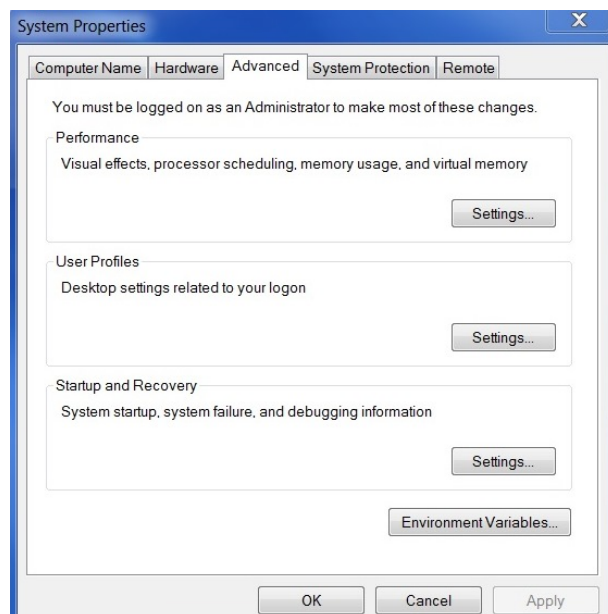
User's Manual for Bridge Rating Software

Section 1: Setting up Laptop Computers for Wireless Sensor Networks

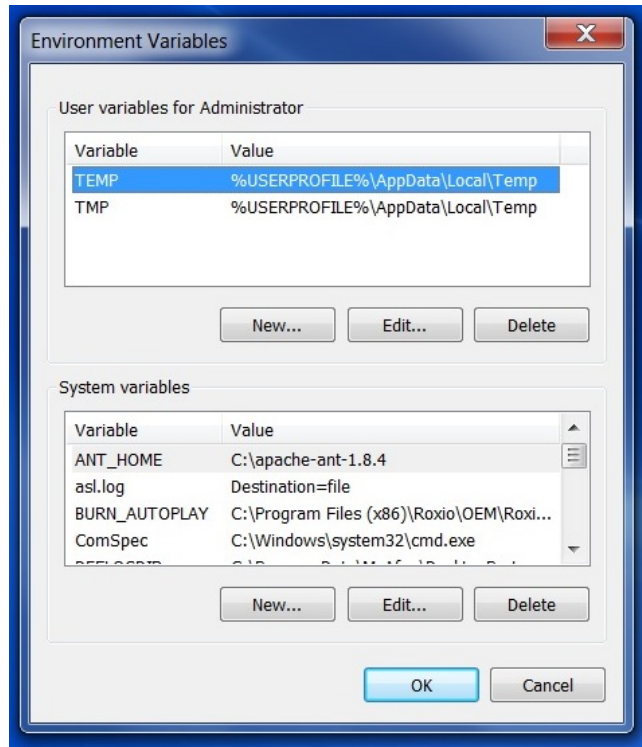
Note: The software packages require full administrative right and 64-bit Windows 7 operating system.

I. Install Java Runtime Environment:

1. Install Java Runtime Environment (64-bit). Click on “jre-7u40-windows-x64.exe” provided in the CD. Follow instructions to install. Remove all other versions of Java from the laptop.
2. Click on “jdk-7u40-nb-7_3_1-windows-x64.exe” provided in the CD and install Java Development Kit and Netbeans IDE. Follow default prompt settings and instructions. After the installation is complete, right click on netBeans IDE 7.3.1, click on “properties”, then on “Compatibility” tab, check “Run this program as an administrator”. Click apply and then hit OK.
3. Copy and save ‘apache-ant-1.9.2’ (provided in the CD) directly in the ‘C:’ drive.
4. Right click on “Computer” on your desktop and click “Properties”. Click “Advanced system settings”. In “System Properties” window, go to ‘Advanced’ tab and click ‘Environment variables’ as shown in the picture below.



5. Click “Environment Variables” button,



6. Click “New...” and add “ANT_HOME” system variable, and enter home directory of apache-ant “C:\apache-ant-1.9.2” as the variable value. Click OK.
7. Click “New...” again, and add “JAVA_HOME” with value “C:\Program Files\Java\jdk1.7.0_40” (depends on the JDK version).
8. Modify the “PATH” system variable to include, “C:\apache-ant-1.9.2\bin”, “C:\Program Files\Java\jdk1.7.0_40\bin”, and “%JAVA_HOME%\bin; %ANT_HOME%\bin;”
9. Restart the laptop computer.
10. Start Windows Command Prompt. Type “ant –version”, and verify that “Apache Ant (TM) version 1.9.2 compiled on July 8, 2013” is installed. Also check the Java version by typing “java –version”.
11. Follow Steps 1 to 10 and prepare the other laptop computer.

II. Install SunSPOT Manager program on laptop computers:

1. Run Internet Explorer (64-bit) as administrator. Go to web address: <http://www.sunspotworld.com/SPOTManager/>, follow the instructions to install Sun Spot Manager.
2. Right-click on the Shortcut for the Sun SPOT Manager Application.
3. Select 'Properties' from the pop-up menu.
4. Select the 'Compatibility' Tab.
5. Make sure that "Run this program as an administrator" is selected.
6. Start the Sun SPOT Manager and proceed with the installation.
7. Restart the laptop computer.
8. Follow Steps 1 to 7 and prepare the other laptop computer.

III. Install Wireless SunSPOT Basestation:

1. Connect the basestation through USB cable to the laptop computer.
2. Start the SunSPOT Manager program. Click the "Refresh" button. The MAC address of the device should be shown in the drop down list.



3. Click SDKs tab, then click on "SDK (Currently Active)" and verify the Version Datestamp is "yellow-101117-1".
4. Upgrade the base station by clicking on the Upgrade button. Wait until the upgrade is complete, click "Basestation" button and choose "Start Basestation". Choose "Start Shared Basestation". When "click the reset button" message appears, click the reset button on the Basestation once and continue with the upgrade.
5. Repeat the same steps for the other Basestation. The two Basestations are ready for deployment with the wireless sensor networks.

IV. Troubleshooting:

If SunSPOT Manager does not run, perform the following:

- a. Right click SunSPOT Manager icon on the laptop, go to "Shortcut" tab, and under Target, write "C:\Program Files\Java\jre7\bin\javaws.exe" at the beginning, if it is not already there.
- b. Double click "Control Panel", type "Java" in the search box, Java button will show up. Double click Java button, go to the "Security" tab, click "Edit Site List" and add "http://www.sunspotworld.com" and click OK.

V. Install Wireless SunSPOT sensor nodes:

1. Connect one SunSPOT sensor through USB cable to the laptop computer
2. Start the SunSPOT Manager program. Click the "Refresh" button. The MAC address of the device should be shown in the drop down list.

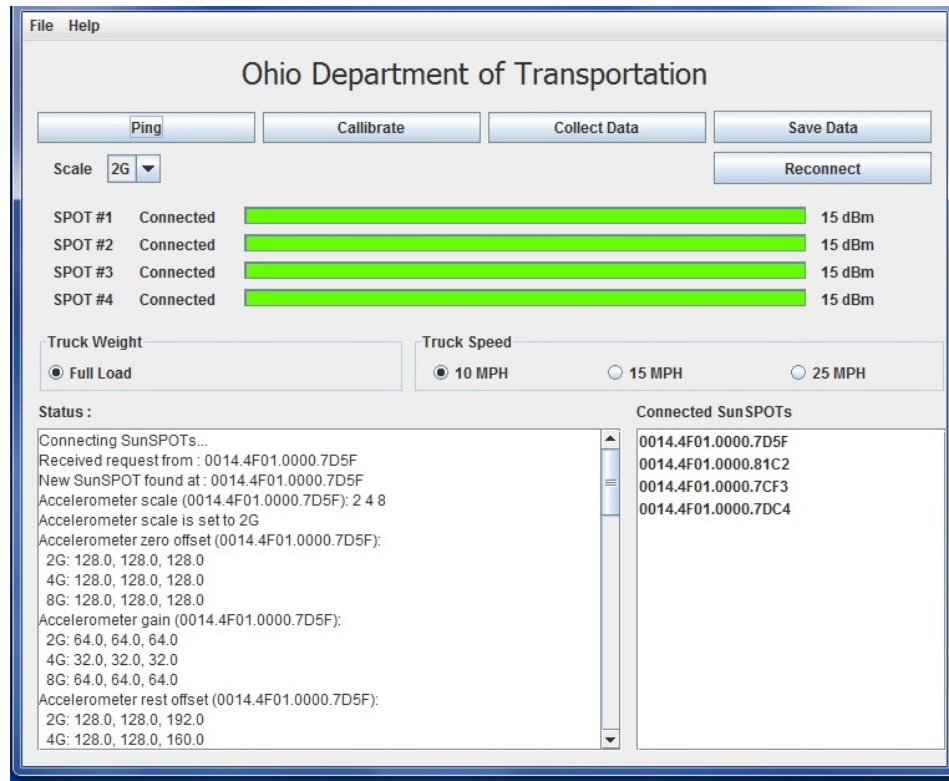


3. Click SDKs tab, then click on "SDK (Currently Active)" and verify the Version Datestamp is "yellow-101117-1".
4. Upgrade the SunSPOT by clicking on the Upgrade button. Wait until the upgrade is complete.

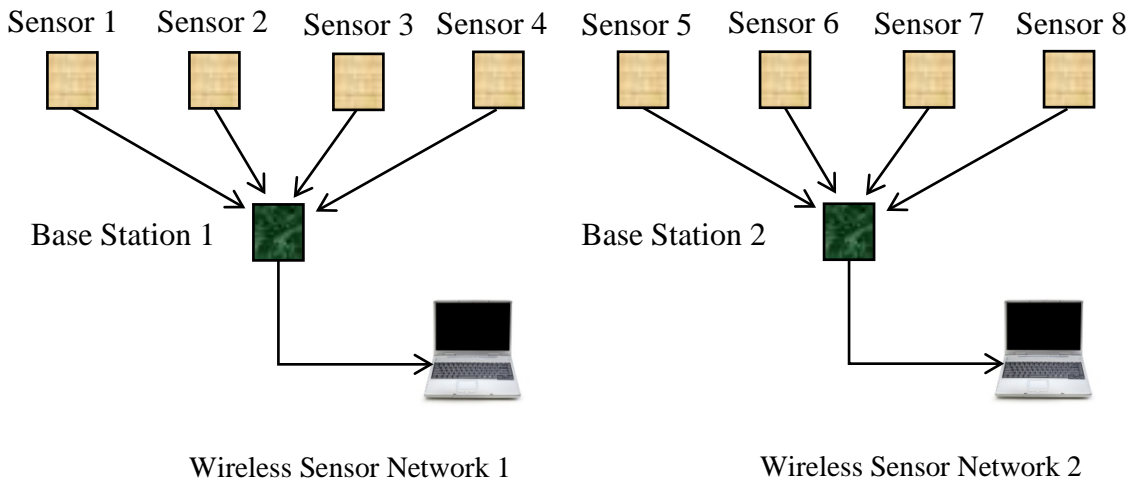
5. When “click the reset button” message appears, click the reset button on the SunSPOT once and continue with the upgrade.
6. Click on the “OTA Command” button and click “Enable OTA Command Server” and finish installation.
7. Follow Steps 1 to 6 to upgrade all SunSPOT.

Section 2: Setting up NetBeans IDE Project

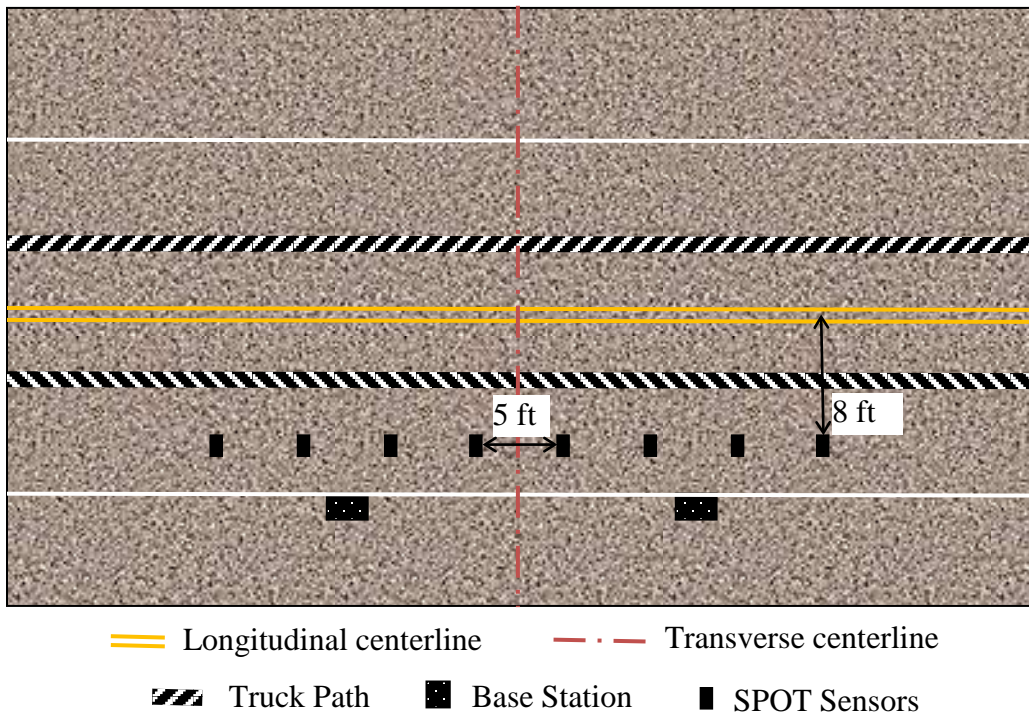
1. Copy “WSN” and ODOTApp” folders from the application software CD to “C:” hard drive of each laptop computer.
2. Click “NetBeans IDE 7.3.1” icon on laptop computer. Open “WSN→WSN1→Basestation1” project. Connect Basestation1 via USB cable to the laptop.
3. Right click on “Basestation1” project icon and click “Clean and Build”. Once complete, right click again on “Basestation1” project icon and click “Run”. “Bridge Monitoring” window should pop up.
4. Connect the external battery to SunSPOT #1 via USB cable and wait to be connected. A green bar should appear full. Connect SunSPOT #2, then SunSPOT #3 and SunSPOT #4 – one at a time and must be in order from 1 to 4. After all four sensors are successfully connected. The window displays four green horizontal bars and MAC addresses of four connected SunSPOT sensors as shown in the following figure.



5. Click “Ping” button. Red and green LEDs on the SunSpot #1 to #4 will blink. Click the “Calibrate” button. If blue LEDs on the SunSpot #1 to #4 blink along with green LEDs, then WSN1 is ready.
6. Prepare Basestation2 and SunSPOT (#5, #6, #7 and #8 in order) for WSN2 following Steps 1 to 4. Both WSN1 and WSN2 are now ready for deployment on a PSBB bridge.



Section 3: Sensor Deployment and Data Collection on a Bridge



1. The SunSPOT sensors are symmetrically placed on the mid-length of the bridge at 5 ft spacing along a line 8 ft from the longitudinal centerline of the bridge, as shown above. The truck has to run over the centerline of the bridge at the designated speed of 10 and 25 mph, and needs to maintain a constant speed during each run.
2. Sensor locations should be marked and cleaned before attaching sensors on the bridge deck using quick-setting epoxy (available in local stores, such as in Home Depot by the brand name “Super Glue: 5 Minute Quick Setting Epoxy”) to prevent absorption of bridge vibration.
3. Glued interfaces between sensors and bridge deck should be stiff enough not to absorb bridge vibration. Wait at least 45 minutes as the glue drying time before running a truck.
4. One heavily loaded truck is necessary to produce sufficient vibration on the bridge. Record axle dimensions and weight of the truck. Run the truck at two different speeds: 10 and 25 mph. The 15 mph button might be useful in future.
5. The “Full Load” and “10 MPH” radio buttons are already pre-selected. Make sure the truck maintains a constant speed of 10 mph. When the truck is approximately 10-15 ft away from the bridge abutment, click “Collect Data” button once. The button caption changes to “Stop Data” and indicates data collection started. Run truck over the bridge at a constant speed of 10 mph. After 15 seconds, click “Stop Data” button. Click the “Save Data” button and save the data in the default format. Do not change the file name during saving. The time-stamped data will be automatically saved with a file name similar to “20131015_115412PM_F10BS#1” on the Basestation1 laptop. Rename the file name to just “F10BS#1”. Do the same on the Basestation2 laptop and rename the file as “F10BS#2”. These data are saved in “.csv” (comma separated value) format.

6. Follow the same procedures in Step 5 to collect data at 25 mph. Rename data as “F25BS#1” in BaseStation1 laptop, and “F25BS#2” in BaseStation2 laptop.
7. Copy all four acceleration files and save in “Data” folder inside “ODOTApp” folder.

Section 4: Bridge Load and Condition Rating using Application Software

1. Double click on the “ODOTApp” folder saved in the C: drive.
2. Double click on the “set up” and install the program. Installation might take a few minutes.
3. Click on the “ODOT_Bridge_YSU” icon on the laptop computer.
4. The “Bridge Condition Assessment and Load Rating” window pops up.

Bridge Condition Assessment and Load Rating

File Help

Input Parameters Bridge Assessment

Box Beam

PSBB Length (in.) 1093.5

Outside Width (in.) 48

Inside Width (in.) 38

Outside Height (in.) 42

Inside Height (in.) 34

Number of Box Beams 11

Number of Diaphragms / Box Beam 5

Diaphragm Thickness (in.) 24

Box Beam End Thickness (in.) 42.25

Concrete

28-day Compressive Strength (psi) 5500

Unit Weight (pcf) 150

Bridge

Pedestrian sidewalks Yes No

End Supports Fixed-Fixed

Wearing Surface Thickness (in.) 6

Truck

Truck #1

Weight (lb) 43100

Speed #1 (mph) 10

Speed #2 (mph) 25

Load Sensor Data

Sensor Data Loaded!

5. The program consists of two tabs: “Input Parameters” and “Bridge Assessment”.
6. Input Parameters: This tab allows one to enter the properties of the bridge and the truck’s weight and speeds. A schematic diagram of bridge geometric parameters is shown in Fig. 4.9.
 - a. Choose “Yes” if the bridge has pedestrian sidewalks.
 - b. Choose “No” if it does not.
 - c. Select the bridge end support condition from the drop-down list. The PSBB bridges usually have ‘fixed-fixed’ support condition.
 - d. Enter the weight of the truck recorded in the field.
 - e. Enter the speeds of the truck. The default is 10 mph.
 - f. Click on the “Load Sensor Data” button and go to “Data” folder where the four files of collected acceleration data from the field were saved.
 - g. Select any one file and click “Open”.

7. Bridge Assessment:

- a. Click on the Bridge Assessment tab. This tab consists of two dialog boxes: “Bridge Load Rating” and “Bridge Condition Rating”, and two buttons: “Start Analysis” and “View Report”.
- b. Click the “Start Analysis” button and wait until analysis is completed.
- c. The window displays the bridge load rating and condition rating.
- d. “Bridge Assessment Report” and “TempData” files are saved automatically in ODOTApp folder.
- e. Click the “View Report” button to see the report. The TempData file contains all acceleration and FFT data.
- f. The input data can be saved by clicking “File → Save Input”.

